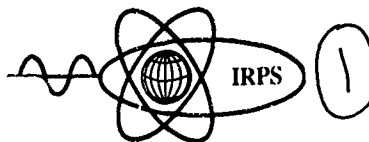


R & D 6559-PH-02  
DATA 45-91-M-0043.

ISRP-5  
Dubrovnik  
1991



AD-A241 257



# 5th International Symposium on Radiation Physics

SUMMARY TRANSACTIONS

**DISTRIBUTION STATEMENT A**

Approved for public release;  
Distribution Unlimited

June 10-14, 1991,  
Dubrovnik Croatia,  
Yugoslavia



RUDJER BOSKOVIC INSTITUTE

Accession For	
Year	1961
Date Recd	
Unit	1000
Subclassification	

7/10/68  
1/10/68  
1/10/68  
1/10/68  
1/10/68

A-1	<del>SECRET</del>
-----	-------------------



Organized by the  
Ruđer Bošković Institute  
Zagreb, Croatia, Yugoslavia

91 9 26 067

## FOREWORD

The 5th International Symposium on Radiation Physics (ISRP-5) follows the symposia in Calcutta (1974), Penang (1982), Ferrara (1985) and Sao Paulo (1988). The objective of this series of symposia is to encourage communication between scientists throughout the world, from universities, research centers, industries, hospitals and other institutions working in the field of science which deals with the physical aspects of interaction of radiation, electromagnetic and particulate, with matter. On such gathering of the physics radiation community the most recent achievements and advances in this broad interdisciplinary area of science could be revealed and discussed.

The response of the scientific community was very satisfactory. Twenty three invited and more than 200 contributed papers were accepted for presentation on the Symposium. Abstracts of all invited and contributed papers are included in this book. Most of them were photocopied as received. However, some of the received texts had to be retyped, due to their very poor quality. We apologize for the reproduction of some abstracts for which we did not have time for retyping before photocopying. Invited papers in full size will be published in the separate volume of the Nucl. Instr. Meth. Phys. Res. as Proceedings of the Symposium. Contributed papers for poster sessions will be refereed and published in one of the subsequent regular volumes of the same journal.

The Organizing Committee made an effort to raise some funds to subsidize the Symposium. The Ministry for Science, Technology and Informatics of the Republic of Croatia was very generous in supporting this event and we are very grateful for this gesture. The Symposium was organized by the Ruder Bošković Institute in Zagreb, Croatia; the financial, administrative and technical support of the Institute is deeply acknowledged. We are also grateful to the European Research Office for their contribution in organizing this Symposium.

The Organizing Committee wants to thank to Mrs Zdenka Kuzmić, administrative secretary, who helped extensively in the making of this book and in all other activities concerning the organization of this Symposium.

The Organizing Committee welcomes all the participants of this Symposium and wishes them a pleasant stay in Dubrovnik.

Organizing Committee

## INTERNATIONAL ADVISORY BOARD

Berenyi D., Hungary  
Derado I., Germany  
Fleming R.F., USA  
Ghose A.M., India  
Haensel R., France  
Hart M., United Kingdom  
Hubbell J.H., USA  
Inokuti M., USA  
Iyengar P.K., India  
Jackson D.F., United Kingdom  
Nascimento I.C., Brazil

Nelson W.R., USA  
Pisk K., Yugoslavia  
Pomansky A.A., USSR  
Povh B., Germany  
Povinec P., Czecho-Slovakia  
Ricci R.A., Italy  
Senjanović G., Yugoslavia  
Shimizu S., Japan  
Whittingham I.B., Australia  
M. Zifferero, IAEA

## INTERNATIONAL PROGRAMME COMMITTEE

Cooper M.J., (Chairman), Coventry, UK  
Berrada M., Rabat, Morocco  
Creagh D.C., Campbell, Australia  
Csikai J., Debrecen, Hungary  
Isabelle D.B., Orléans, France  
Isozumi Y., Kyoto, Japan

Ljubičić A., Zagreb, Yugoslavia  
Logan B.A., Ottawa, Canada  
Paic G., Zagreb, Yugoslavia  
Paschoa A.S., Rio de Janeiro, Brazil  
Pratt R.H., Pittsburgh, USA  
Roy S.C., Calcutta, India

Bradley D.A., (Editorial Secretary),  
Kuala Lumpur, Malaysia

## LOCAL ORGANIZING COMMITTEE

Ljubičić A., Zagreb, Chairman  
Miljanić Đ., Zagreb, Scientific Sec.  
Aničin I., Beograd  
Krešmar M., Zagreb  
Kregar M., Ljubljana

Picek I., Zagreb  
Rendić D., Zagreb  
Srdoč D., Zagreb  
Valković V., Zagreb  
Zovko N., Zagreb

## INVITED PAPERS

## Polarizational Radiation or "Atomic" Bremsstrahlung

Amusia M. Ya<sup>1</sup>

Institut für Theoretische Physik, Universität Frankfurt, Germany

It is demonstrated that a new kind of continuum spectrum radiation exists, where the mechanism of formation is quite different from that for ordinary bremsstrahlung (OB). The latter originates due to slowing down of the changed projectile in the target field, while the former, called polarizational radiation or "atomic" bremsstrahlung (AB), is a result of radiation either of the target or projectile particles dipolarly polarized during the collision process. A number of features are specific for AB: it is almost independent on the mass of the projectile, on its total charge, just as that of the target and is entirely determined by the polarizability of colliding particles. The AB intensity is proportional to the square of the polarizabilities, of the target and projectile particles, while AB spectrum is completely determined by the frequency dependence of the polarizabilities. For heavy particles AB is in fact the only effective source of radiation.

It is demonstrated that in a broad frequency region AB without simultaneous excitation or ionization of colliding particles is parametrically more important than AB accompanied by these processes.

Not only general formulae, but also results of concrete calculations for electron-atom, atom-atom and ion-atom colliding pairs are presented. The specific features of the case when the incoming particles are relativistic are discussed at length: it is shown that in this case the radiation's angular distribution is quite peculiar, there exists dipole radiation in case of collision of two identical particles and the radiation emitted by projectile and target particles can be easily distinguished.

The AB is very important in radiative cooling of gas volumes and in formation of ordered atoms motion under the action of light. It is demonstrated that the mechanism of AB formation is universal in the sense that AB is created whenever colliding particles have internal structure, if their constituents are charged.

A number of examples of colliding pairs are considered, for which AB is quite essential - namely a bare nucleus and an atom, pair of atoms at least one of which is excited, electron, or atom interacting with a molecule. The same mechanism is essential also in formation of radiation in nuclear and elementary particle collisions.

<sup>1</sup>On leave of absence from A. F. Ioffe Physical-Technical Institute, Leningrad K-21, USSR. 194021.

## COMPTON SCATTERING FROM BOUND ELECTRONS

T. SURIĆ

RUĐER BOŠKOVIĆ INSTITUTE, ZAGREB, YUGOSLAVIA

There has been much recent interest in the study of Compton scattering from bound electrons. Experiments have been conducted with tunable, newly available synchrotron sources of high photon flux permitting studies of the process in the resonant regime and with polarized sources<sup>1</sup>. The analysis of experiments conducted with conventional nuclear photon sources has been refined, giving the most accurate measured cross sections to date. These experiments have included attempts to observe the predicted infrared rise of the cross section for soft final photons<sup>2</sup>. Concurrently, the availability of higher speed, large memory computers has facilitated advances in theory. Most recently, an accurate relativistic second order S-matrix code has been developed and tested<sup>3</sup> at energies ranging from a few tens of eVs to hundreds of keV. Validity of simpler approaches<sup>4</sup> is discussed by comparison with the results obtained using this new code. Comparisons with the recent experiments in the resonant scattering regime, at intermediate energy and intermediate momentum transfer regime and at relativistic energies will be given. /

1. See, for example, V. Marchetti and C. Franck, Phys. Rev. Lett. 59, 1557 (1987). and

A. Simionovici, J.P. Briand, P. Indelicato and P. Chevallier, Phys. Rev. A41, 3707 (1990).

2. See for example W. Wolff, H. E. Wolff, L. F. S. Coelho, S. de Barros, and J. Eichler, Phys. Rev. A 40, 4378 (1989).; Saharsha M. Lad, G Basavaraju, and P. P. Kane, Phys. Rev. A42, (1267) 1990.

3. T. Surić, P. M. Bergstrom Jr., K. Pisk and R. H. Pratt (submitted for publication).

4. See, for example, M. Gavrilă, Phys. Rev. A 6 1348 (1972).; ibid. 6 1360 (1972).;

P. Eisenberger and P. M. Platzman, Phys. Rev. A 2, 415 (1970)

A REPORT OF SOME RECENT DOUBLE-BETA DECAY EXPERIMENTS

F.T. Avignone, III, J.I. Collar, and C.K. Guerard

Department of Physics and Astronomy, University of South Carolina 29208  
USA

R.L. Brodzinski, H.S. Miley, and J.H. Reeves

Pacific Northwest Laboratory, Richland, WA 99352, USA

An update of experiments searching for  $2\nu$  and  $0\nu$   $\beta\beta$ -decay will be given. Observations of  $2\nu$   $\beta\beta$ -decay of  $^{82}\text{Se}$ ,  $^{76}\text{Ge}$ ,  $^{100}\text{Mo}$  have thusfar been reported. New efforts involving kilogram quantities of Ge, isotopically enriched to 86% in  $^{76}\text{Ge}$  will also be discussed. New results from the search of  $2\nu$   $\beta\beta$ -decay of  $^{100}\text{Mo}$ , to the first excited  $\text{O}^+$  state in  $^{100}\text{Ru}$  will also be reported. A  $\approx 3\sigma$  positive effect has been observed in this experiment. The meaning of these results in the context of nuclear structure theory will also be reviewed. The methods of radioactive background reduction used by the PNL/USC group will also be presented.



## X-RAY STANDING-WAVES TECHNIQUE: APPLICATION TO THE STUDY OF SURFACES AND INTERFACES

C. Malgrange

Laboratoire de Minéralogie-Christallographie, Universités  
Paris 6 e Paris 7, tour 16, 75252 Paris Cedex 05.

X-ray Bragg diffraction on perfect crystals gives rise to a diffracted beam which is coherent with the incident beam. The superposition of the incident and diffracted waves creates a standing-wave for the electric field which is periodic with the same periodicity as the crystalline lattice planes. For a given position of the crystal inside the reflection domain, the nodes (and antinodes) of the standing-wave are fixed; when the crystal is scanned throughout the whole rocking curve, their position is progressively shifted from the reflecting planes to a position half between the reflecting planes. If the incident radiation is such that it can excite the fluorescence of one given species of atom, the fluorescence signal is proportional to the electric field on the fluorescent atom. Then the relative position of the fluorescence yield curve and the rocking curve depends on the position of the fluorescent atom with respect to the reflecting planes. Consequently, their comparison permits to determine the position of the fluorescent atom within the crystalline lattice.

We will describe the experimental set-up and present some typical results which have been obtained in the study of

- i) adsorbate structures on crystals,
- ii) interfaces between thin epitaxial layers and substrates.

We will end with a few words about the possible extension of this technique to less perfect substrates.

## STATE OF THE ART IN DETECTOR TECHNOLOGY

Glenn F. Knoll  
University of Michigan, Ann Arbor, Michigan, USA

A number of interesting developments over the past several years have the potential to influence the directions in which instruments for the measurement of ionizing radiation evolve in the future. In this paper, a subset of these developments are reviewed that are of particular interest in the detection of low- and medium-energy ( $<20$  MeV) radiations. Topics that are included are:

- a) *Newly-discovered inorganic scintillators.* The search for scintillation materials that combine a high atomic number constituent and fast decay time has yielded several new candidates.
- b) *Fiber scintillators.* A variety of plastic and glass scintillators are now available in the form of optical fibers that permit their use in innovative detector designs.
- c) *Scintillator-photodiode assemblies.* In particular, the superior light yield of CsI(Tl) when combined with the extended spectral response of photodiodes produces a very useful compact detector.
- d) *Enhanced ionization track detectors.* By applying a pulsed RF field, particle tracks in a gas can be visualized through secondary ionization.
- e) *New semiconductor materials.* Use of GaAs,  $\text{HgI}_2$ , and amorphous silicon as materials for direct radiation detectors or photodiodes shows increasing promise.
- f) *Semiconductor drift detectors.* Large-area devices with small capacitance are possible by creating structures in which electrons are drifted parallel to the semiconductor wafer surface.
- g) *Detector-transistor integrated structures.* Very interesting readout capabilities have been demonstrated by combining drift configurations and surface transistor structures on a single chip.
- h) *Superconducting phonon detectors and cryogenic bolometers.* Devices operated near absolute zero temperature have unique capability to measure radiations through processes that are fundamentally new.

In each case, the physical characteristics are reviewed in the context of typical applications in radiation measurements.

## RING IMAGING CHERENKOV DETECTORS

D. Vranić

Ruđer Bošković Institute, POB 1016, 41001 Zagreb, Croatia, Yugoslavia

The concept for a ring imaging Cherenkov detector for particle identification is presented. A  $50 \times 50$  cm<sup>2</sup> test prototype for identification of pions, kaons and protons in heavy ion collisions in the midrapidity range is described. The detector consists of a liquid freon radiator, a multistep avalanche chamber and an optical imaging system. The gas mixture inside the chamber consists of 95% helium and 5% ethane, with an admixture of TMAE vapor at 45-50°C as UV photon sensitive compound. The image is read out by a CCD camera, equipped with a two-stage image intensifier. Some preliminary results of tests are presented.

## LOW ENERGY ANTIPROTON BEAMS

R. Klapisch  
CERN, Geneva, Switzerland

It was the invention of stochastic cooling by S. Van Meer that has allowed antiprotons beams to become a powerful tool for the physicist. As a by-product of the high energy proton-antiproton collider, a versatile low-energy facility, LEAR has been operating at CERN since 1984. The facility and its characteristics will be described as well as example of its use for studying fundamental properties of the antiproton and for topics in Atomic, Nuclear and Particle Physics.

## DEVELOPMENTS IN SUPERCONDUCTING TUNNEL JUNCTION DETECTORS

M. Kurakado

*R & D Laboratories -I, Nippon Steel Corporation,  
1618 Ida, Nakahara-ku, Kawasaki-shi, Kanagawa 211, Japan*

The energy resolution of a radiation detector is essentially limited by the statistical fluctuation ( $\Delta N$ ) of the number ( $N$ ) of electrons excited by a radiation of energy ( $E$ ). The statistical limit of energy resolution  $\Delta E$  is given as  $\Delta E/E = \Delta N/\langle N \rangle \propto (E/E)^{1/2}$ , where  $\langle N \rangle$  is the mean value of  $N$ , and  $E$  ( $= E/\langle N \rangle$ ) is the mean energy required to excite one electron in the detector. Thus, a detector with smaller  $E$  has the potential of higher energy-resolution.

For the case of semiconductor detectors, it is known that  $E$  is empirically given by  $E \approx 2.8 E_g + (0.5 - 1.0) \text{ eV}$ , where  $E_g$  is the gap energy of the semiconductor. The  $(0.5 - 1.0) \text{ eV}$  term arises from the phonon loss; phonons emitted from the electrons excited by a radiation do not contribute to excite other electrons beyond the energy gap. Typical  $E$  values are 3.6 eV for Si and 2.8 eV for Ge. For the case of superconductor detectors,  $\hbar\omega_D$  ( $\omega_D$ : Debye frequency) is usually much larger than  $E_g$  ( $=2\Delta$ ) so that phonons can break Cooper-pairs and excite electrons (quasiparticles). According to a numerical simulation of the cascade excitation process of quasiparticles and phonons in a bulk Sn at 0 K,  $E$  is 1.7 $\Delta$  ( $\approx 1 \text{ meV}$ ) which is about three orders smaller than the case of semiconductors.

Therefore, ultra-high resolution detectors become feasible with superconducting tunnel junctions (STJs) if the excess quasiparticles efficiently pass through the tunnel barrier and contribute to a signal charge. In fact, Sn/SnOx/Sn junctions as x-ray detectors have already shown about three times higher energy resolution than Si semiconductor detectors. Recently, in addition to Sn junctions, other types of STJs such as Nb/Al-AlOx/Nb junctions, which are resistant to thermal cycling, are in progress as radiation detectors.

Electrons in the superconducting state are efficiently excited by non-thermal phonons of energy larger than  $2\Delta$ . Since a single crystal of a semiconductor or an insulator can convert the energy of a radiation into ballistic phonons, such phonons can be sensed by STJs on the surfaces of the crystal. The area and volume of this type of detectors can be much larger compared with a single STJ for direct detection of radiations.

Researches of STJ detectors will be reviewed, including our recent studies on Nb/Al-AlOx/Nb junctions with a single crystal Nb film and on series-connected STJ detectors.

IP-III-1

RECENT PROGRESS IN THE UNDERSTANDING OF THE  
NEUTRON-NUCLEUS INTERACTION

D. Seeliger  
Section of Physics, Technical University, 8027 Dresden, Germany

# FIRST EXPERIMENTS AT THE HEAVY-ION STORAGE RING ESR, DARMSTADT

F. Bosch

Gesellschaft für Schwerionenforschung, Postach 11 05 52, Darmstadt,  
Germany

## ABSTRACT

The heavy-ion storage ring ESR at Darmstadt, in operation since April 1990, is designed for storing, accumulating and cooling both stable and unstable highly-charged ions up to bare uranium ( $U^{92+}$ ). Cooling of bare Ar- and Kr-ions of  $\approx 200$  MeV/u energy by means of a collinear electron beam has been achieved meanwhile, and longitudinal relative momentum spreads  $(\Delta p/p)_L < 10^{-5}$  could be obtained. Capture of cooler-electrons into vacant states of the ions (radiative electron capture) provides a large number of photons, the energy of which renders a precise determination of electron binding energies (1s, 2s ...) in heavy, hydrogen-like atoms. Moreover, those stored and cooled ion beams open the door for doing many other fascinating experiments in the fields of atomic, nuclear, and weak interaction physics.

ELECTRON HOLOGRAPHY AND THE AHARONOV-BOHM EFFECT

AKIRA TONOMURA

Advanced Research Lab., Hitachi, Ltd.,

&

Electron Wavefront Project.

Research Development Corporation of Japan

Hatoyama, Saitama 350-03, Japan

Electron holography<sup>1)</sup> is a two-step imaging method employing both electron and light beams. Once the electron wavefront is faithfully transformed into a light wavefront through the holography process, versatile optical techniques can be utilized. Gabor's original objective of inventing holography in 1949 was to break through the resolution limit of electron microscopes by optically compensating for the inevitable aberrations in the electron lens. However, the intrinsic value had not been not recognized until the advent of a coherent laser in 1960, when laser holography was developed. The situation is similar to electron holography: The advent of our coherent electron beam in 1978 moved electron holography into a practical stage of use.<sup>2)</sup>

This technique opens a new way to investigate the fundamental features of quantum mechanics, as well as to observe and measure the microscopic world, hitherto invisible, by detecting the relative phase distribution of an electron beam transmitted through an object.

The former example is to establish the physical reality of gauge fields by a definitive experiment of the Aharonov-Bohm effect.<sup>3)</sup> The latter example is to observe individual flux lines penetrating a superconductor.<sup>4)</sup>

1) D. Gabor: Proc. R. Soc. London A197 (1949) 454. See also

A. Tonomura: Rev. Mod. Phys. 59 (1987) 637.

2) A. Tonomura et al.: J. Electron Microsc. 28 (1979) 1.

3) A. Tonomura et al.: Phys. Rev. Lett. 56 (1986) 792. See also

M. Peshkin and A. Tonomura: "The Aharonov-Bohm Effect" Lecture Notes in Physics, Vol. 340. (Springer Verlag, 1989)

4) T. Matsuda et al.: Phys. Rev. Lett. 62 (1989) 2519.



SCHWINGER SCATTERING OF NEUTRONS IN THE STUDY OF CONDENSED MATTER

J B Forsyth, ISIS Science Division, Rutherford Appleton Laboratory,  
Chilton Oxon OX11 0QX UK and P J Brown, Institut Laue Langevin, BP  
156, 38042 Grenoble CEDEX, France.

ABSTRACT. In a non-centrosymmetric crystal, the angular velocity of a neutron relative to the electric charges of the atoms gives rise to a small polarisation dependent term in the scattering cross-section (Schwinger scattering). The Schwinger scattering is proportional to the difference between the nuclear charge and the X-ray scattering factor and hence, at low angles, to just those electrons which take part in bonding. The lack of a centre of symmetry in the zinc blende structure, adopted by the important III-V semiconductors, has been exploited to obtain information about bonding electron density in a number of these compounds: GaAs, GaSb, GaP, InAs, InSb and InP. The results obtained for the polarisation dependence of the neutron cross-section for the 111, 311 and 331 reflections are generally lower than those calculated using neutral free atom form factors. The result for the 222 reflection, which is zero for a spherical atom model, is highly significant for GaAs and of the same order in all the measured compounds; it can be attributed to tetrahedral distortion of the atomic charge distributions brought about by bonding. These results are compared to previous estimates obtained by X-ray, gamma-ray and electron scattering.

## **RADON IN SOIL, AIR AND IN GROUNDWATER RELATED TO MAJOR GEOPHYSICAL EVENTS: RECENT ADVANCES.**

Dr. Michel M. MONNIN Centre National de la Recherche Scientifique Laboratoire  
d'Hydrogéologie.

URA-CNRS-1359, Place Eugène Bataillon, F-34095 MONTPELLIER CEDEX 5 - FRANCE

Since the first evidence (1975) that there may exist a correlation between radon concentration variations and earthquake, lots of effort has gone into the assessment of the fact. Several additional evidences have been gathered and it is now considered as an established fact that major geophysical events (earthquakes and volcanic eruption) can be preceded by noticeable precursory signals. A general survey of these investigations is presented

More recently, a particular emphasis has been put on experimental and field analysis of raw data obtained using advanced technology based equipment. In terms of forecasting capability the usefulness of the method depends indeed upon the understanding of the underlying phenomena.

The strict analysis of well documented cases of important geophysical events is presented. Those include earthquakes having occurred in Mexico, Ecuador, and Italy, and eruptions at the Krafla and Piton de la Fournaise volcanoes. Minor events are also reported. In the case of seisms, it is shown that definite and beyond doubt radon anomalies were generated even at rather large distances from the epicenter. Both positive and negative anomalies were found. The influence of ground water and fault networks is strongly suggested by the findings. In the case of volcanoes, a similar behaviour is observed together with other signals related to environmental data, independently of the volcanic activity.

Regarding radon in soil-air, investigations using an additional radon source voluntarily implanted at experimental sites showed that near-surface radon anomalies are primarily due if not exclusively to deeper fluid motion acting as transport vectors. Such behaviour is likely to support the pore collapse (PC) model.

Considering only depth related radon concentration curves, one does expect only moderate amplitude for radon anomalies, which is found different in the Nature. A theoretical model devised on the basis of the analysis of transient states is described. It shows that large amounts of radon are expected to appear during a short duration prior an earthquake or an eruption.

Comparing laboratory experimental data and field measurements in different areas, the influence of meteoric water and temperature on the local radon output has been assessed. It has been shown particularly that short term variations are induced in direct correlation with rainfall and large term variations are induced in counter correlation with rainfall. Finally laboratory experiments cross-checked with deep-well experiments have been carried out regarding radon transport in groundwater as a function of depth. The most striking results are reported.

## PRESENT BASIS OF RADIATION PROTECTION

D.J. Beninson

Comision Nacional de Energia Atomica, Buenos Aires, Argentina

The paper presents the radiobiological and epidemiological bases of the ICRP recommendations and the implications of the linear-non threshold relation for protection. It includes discussions of applications of the system of protection to "practices" and to "intervention". The reasons for changing the dose limits are analysed together with the concept of "detriment" and examination of criteria to judge exposure consequences. The paper also outlines the reason for the quantities recommended.

## COMPETING MICROPROBE METHODS IN MINERALOGY

J.L. Campbell

Guelph-Waterloo Program for Graduate Work in Physics,  
University of Guelph, Guelph, Ontario N1G 2W1, Canada

The electron microprobe has long been a mainstay of mineralogy and geochemistry, providing via X-ray spectroscopy both quantitative spot elemental analysis of individual grains and a scanning capability that maps the distribution of major and minor elements. Nonetheless many problems require better detection limits as they demand true trace element analysis and the ability to map trace element distributions. New non-destructive X-ray techniques such as SXRF and micro-PIXE provide detection limits that can approach the ppm level and thus open new horizons for investigation. Examples of their application both in economic mineralogy and fundamental geochemistry will be given. These examples include trace element fingerprinting of grains, zoning studies, solid and fluid sub-surface inclusions, geothermometry, precious metal assay, and analysis of grain boundary regions. The two methods compete with SIMS and with AMS, although only the former is at present a true microprobe technique. The relative strengths of the various techniques will be discussed, and the merit of using combinations demonstrated.

RADIATION HARDNESS ASSURANCE OF SPACE ELECTRONICS.

Leonard Adams. ESA-ESTEC. Noordwijk. Netherlands.

**Abstract.**

The space radiation environment is both complex and dynamic. The earth's magnetic field serves to 'trap' charged particles and the earth is surrounded by 'belts' of these particles, known as the Van Allen belts. Furthermore the magnetosphere and outer space are subjected to a flux of solar particles comprising all types of charged particles. This flux is a function of solar activity and may rise sharply by several orders of magnitude during a solar flare. Galactic Cosmic Rays originating from outside the solar system pervade space and are composed of highly energetic (GeV range) heavy ions which can be extremely damaging.

Radiation causes significant damage to electronic components and the performance of any spacecraft is governed by the performance of the various electronic systems such as scientific instruments, data handling and communications.

Instruments for space research employ highly complex electronics and there is an increasing emphasis on imaging instruments which require large amounts of memory and powerful advanced data processing. Scientific payloads are heavily constrained in terms of mass, volume and power which requires the electronic designer to use low power technologies with a high level of integration. Such technologies are generally very sensitive to radiation effects.

This paper discusses the hardening of space electronics against radiation effects and, in particular, the discipline of 'Hardness Assurance' covering test, analysis and countermeasures at electronic system and component level.

POSITRON ANNIHILATION IN THE STUDY OF MATERIAL DAMAGE

Prasanta Sen  
Saha Institute of Nuclear Physics  
1/AF, Bidhannagar, Calcutta-700064 (India).

A brief introduction to the subject of positron annihilation techniques (PAT) will be presented. The application of the PAT to the characterisation of radiation induced defects in metals and to investigate the defect kinetics during post irradiation isochronal annealing are discussed. Typical examples are given showing the processes of positron trapping, detrapping, helium-vacancy complex formation, vacancy-impurity interaction, bubble characterisation and positronium formation in radiation induced defect rich metals. Some recent results of PAT indicating the presence of vacancy-like defects in quasicrystals of Al-Mn, Al-Mn-Si and Al-Cu-Fe will be presented. The use of the positron micro probe for the studies of micro defects is also discussed.

INDUSTRIAL APPLICATIONS OF SYNCHROTRON RADIATION

by

Paul Barnes

Dept. Crystallography, Birkbeck College, Malet Street,  
London WC1E 7HX, U.K.

and

Daresbury Laboratory, Warrington WA4 4AD.

ABSTRACT

Synchrotron radiation has many applications in materials science. The academic world has increasingly recognised this over the last decade, but industry also now finds that it must be prepared to pay the high costs of synchrotron - based research. While traditionally this industrial use has been primarily in the EXAFS spectroscopy area, the techniques of Powder Diffraction, Protein Crystallography and Small Angle Scattering are becoming industrially more attractive. Purchasing of synchrotron beam time however can also come from quite unexpected areas such as micro-machining and space research! Examples will be given, covering these and other areas, to show how the synchrotron use can aid problem solving, particularly with respect to materials synthesis and simulation of in-service performance.

SMALL ANGLE SCATTERING STUDIES OF IRRADIATED MATERIALS

G. Albertini<sup>1</sup> and R. Coppola<sup>2</sup>

- 1) Dipartimento di Scienze dei Materiali e della Terra,  
Facoltà di Ingegneria, Università degli Studi, Via  
Brecce Bianche, 60131 Ancona (I).
- 2) ENEA, CRE-Casaccia, C.P. 2400, 00100 Roma (I).

The study of microstructural radiation damage in metallic materials is of utmost importance in a large variety of technical fields relating to energy production plants; more specifically the availability of radiation resistant alloys is at present considered as a key issue for the development of commercial fusion reactors.

Since its earliest applications, Small-Angle Neutron Scattering (SANS) has provided an effective investigation tool to characterize in a non-destructive way the presence and the evolution of microstructural defects associated to radiation damage in pure metals and technical alloys, thus contributing to the development of these latter ones.

The present contribution will review the main SANS studies in this domain including the most recent results of a research programme concerning the characterization of He-bubble growth in a martensitic steel developed as structural material for fusion reactors (MANET).



## STUDY OF COSMIC RADIATION BY UNDERGROUND DETECTORS

C. de Marzo

Physics Department, Università di Bari and INFN,  
Sezione di Bari, Italy

The study of cosmic radiation by underground detectors has undergone remarkable progresses in the last ten years. Today several big underground laboratories are taking data on general issue of particle astrophysics, around the world.

Among the many specific goals of these facilities the study of the physics content of the mu-signal is reviewed, paying a special attention to the recent results obtained by means of MACRO detector at the Gran Sasso Laboratory, which is the largest apparatus at present devoted to this research field.

The most recent results on:

- Muon astronomy
  - Muon bundles and primary cosmic ray chemical composition
  - High energy neutrinos
- are reported in the present talk.

## Sudbury Neutrino Observatory

G.T. Ewan, Queen's University

on behalf of the SNO Collaboration<sup>†</sup>

### Abstract

The Sudbury Neutrino Observatory (SNO) detector is a 1000 tonne heavy water ( $D_2O$ ) Čerenkov detector designed to study neutrinos from the sun and other astrophysical sources. The use of heavy water allows both electron neutrinos and all types of neutrinos to be observed by three complementary reactions. The detector will be sensitive to the electron neutrino flux and energy spectrum shape and to the total neutrino flux irrespective of neutrino type. These measurements will provide information on both vacuum neutrino oscillations and matter enhanced oscillations, the MSW effect. In the event of a supernova it will be very sensitive to muon and tau neutrinos as well as the electron neutrinos emitted in the initial burst enabling sensitive mass measurements as well as providing details of the physics of stellar collapse.

---

<sup>†</sup> The Sudbury Neutrino Collaboration: H.C. Evans, G.T. Ewan, H.W. Lee, J.R. Leslie, J.D. MacArthur, H.-B. Mak, A.B. McDonald, W. McLatchie, B.C. Robertson, B. Sur, P. Skensved (Queen's University); C.K. Hargrove, H. Mes, W.F. Davidson, D. Sinclair (Centre for Research in Particle Physics); E.D. Earle, G.M. Milton, E. Bonvin, (Chalk River Laboratories); P. Jagam, J. Law, J.-X. Wang, J.J. Simpson (University of Guelph); E.D. Hallman, R.U. Haq (Laurentian University); A.L. Carter, D. Kessler, B.R. Hollebone (Carleton University); R. Schubank, C.E. Waltham (University of British Columbia); R.T. Kouzes, M.M. Lowry, R.M. Key (Princeton University); E.W. Beier, W. Frati, M. Newcomer, R. Van Berg (University of Pennsylvania); T.J. Bowles, B.T. Cleveland, P.J. Doe, S.R. Elliott, M.M. Fowler, R.G.H. Robertson, D.J. Vieira, D.L. Wark, J.B. Wilhelm, J.F. Wilkerson, J.M. Wouters (Los Alamos National Laboratory); E. Norman, K. Lesko, A. Smith, R. Fulton (Lawrence Berkeley Laboratory); N.W. Tanner, N. Jelley, P. Tient, J. Barton (University of Oxford).

DARK MATTER IN THE UNIVERSE

B.V.Pritvchenko

117312, Institute for Nuclear Research of the  
Academy of Sciences of the USSR, 60th October  
Anniversary Prospect, 7a, Moscow, USSR

The problem of dark matter in the Universe is considered in view of possible existence of weak interacting massive particles (WIMP's). Classification of these particles is given, their interaction with matter, methods for registration and methods for identification of useful events are considered. The estimations of interaction of WIMP's with various media are made. The review of experiments carried out and planned is given.

## NEUTRINO RADIATION FROM SUPERNOVAE

J.A. Grifols

Grup de Física Teòrica, Universitat Autònoma de Barcelona  
08193 Bellaterra, Spain

In a supernova event about  $10^{53}$  erg gravitational binding energy are released. The bulk of it is carried off by neutrinos. The neutrino burst detected on February 1987 recorded the supernova explosion that took place in the Large Magellanic Cloud some 50 Kpc away from Earth and confirmed the basics of models of stellar collapse. Indeed, the neutrino luminosity inferred from observation agrees with the luminosity predicted by detailed model calculations of neutrino transport. However, there is some room (within the uncertainties of both theory and observation) for extra exotic sources of energy drain. Current completions of Particle Physics predict a plethora of new states. Among them, there are Right-Handed neutrinos, which appear in almost any extension of the minimal Standard Model of electroweak interactions. In particular, if neutrinos are massive Dirac particles, the right-handed degrees of freedom should be copiously emitted in a supernova collapse. Using SN1987A data one can place bounds on neutrino masses or on the magnetic moment of the neutrino. Furthermore, independently of the energetics of stellar dynamics, the actual detection of neutrinos at IBM and Kamioka has led to relevant limits on neutrino mass, neutrino lifetime, and neutrino charge.

## CONTRIBUTED PAPERS

Session I

FUNDAMENTAL PROCESSES IN RADIATION PHYSICS

## THE ELECTROMAGNETIC RADIATION IN NEUTRON-ATOM COLLISIONS

M.Ya.Amusia<sup>1</sup>, A.S.Baltenkov<sup>++</sup>, A.V.Korol<sup>+++</sup>, A.V.Solov'yov<sup>1</sup>

<sup>+</sup> Institut für Theoretische Physik der Universität Frankfurt am Main, Germany

<sup>++</sup> Institute of Electronics of the Academy of Sciences of the USSR, Tashkent

<sup>+++</sup> Leningrad State Maritime University, Leningrad, USSR

The radiation spectrum is calculated, which is generated in a collision of a neutron with an atom or an ion. The important role of atomic electrons in the formation of radiation spectrum is demonstrated. It appeared that the main source of the radiation in the region of the characteristic atomic frequencies is the induced during the collision process the time-dependent atomic dipole moment. It is produced both by the recoil of nucleus when the neutron collides with it, and by the direct interaction of the neutron's magnetic moment with the atomic electrons. In the atomic frequencies region the intensity of radiation, emitted in the direct neutron-nucleus collision proved to be less, than that of atomic electrons, virtually excited either by neutron magnetic moment or due to nucleus recoil.

The process has been considered for the low and high neutron collision velocities. The zero-range potential  $U(\vec{R}) = -4\pi f/M \cdot \delta(\vec{R})$  ( $f$  is the singlet or triplet proton-neutron scattering amplitude;  $M$  is the nucleon mass) has been used for the description of the slow neutrons scattering on the atomic nucleus. The interaction of the fast neutrons with the nucleus has been treated as a rapid perturbation acting on the atom. That permits to express the considered process cross section in the most general form:

$$d\sigma = d\sigma_{nN}(\vec{q}) \cdot dW(\vec{q}/M_N)$$

Here  $d\sigma_{nN}(\vec{q})$  is the differential scattering cross-section of the neutron on the nucleus,  $\vec{q} = \vec{p} - \vec{p}'$  is the transferred momentum,  $M_N$  is the nucleus mass. For light and intermediate nuclei the presence of neutron magnetic moment is negligible. The exact expression for the  $dW(\vec{q}/M_N)$  is presented in our work [1]. The obtained cross section contains information on the neutron-nucleus scattering and the atomic structure. For very heavy nucleus the recoil is negligible, while the atomic electron cloud is polarized due to interaction with the neutron magnetic moment.

## References

- [1] M.Ya.Amusia and et al, Sov.Phys.JETP, vol.66(5), p.377 (1987)

<sup>1</sup>Permanent address. A.F.Ioffe Physico-Technical Institute of the Academy of Sciences of the USSR, Leningrad, 194021

Work supported in part by Alexander von Humboldt Stiftung

# A NOVEL ANALYSIS OF NUCLEAR EXCITATION IN AN ELECTRON TRANSITION

A. Ljubičić, D. Kekez

Ruđer Bošković Institute, POB 1016, 41001 Zagreb, Croatia, Yugoslavia

B.A. Logan

Ottawa-Carleton Institute of Physics, University of Ottawa,

Ottawa K1N 6N5, Canada

The mechanism for nuclear excitation in an electron transition (NEET) has been reanalyzed. In contrast to other calculations our analysis shows that the NEET process probability does not depend on the details of the nuclear transition but rather on the properties of the electron states. For the NEET probability  $P$  we obtained the expression:

$$P \approx \frac{g_N}{2\pi} \frac{\Gamma_R(n'l'm' \rightarrow nlm) \Gamma_T(nlm)}{[\epsilon_{n'l'm'} - B_{nlm} - \omega_N]^2 + [\Gamma_T(nlm)/2]^2}$$

where the nuclear statistical factor  $g_N = (2I^* + 1)/(2I_0 + 1)$  where  $I^*$  and  $I_0$  are respective total spins of the excited and ground states, and  $\Gamma_T(nlm)$  and  $\Gamma_R(n'l'm' \rightarrow nlm)$  are the total width of the initial electron state and the radiative width for the transition between the two electron states, respectively, with binding energies  $B_{n'l'm'}$  and  $B_{nlm}$ ;  $\omega_N$  is the energy of the nuclear state.

Our predictions are in very good agreement with the available experimental data.



## SINGLE-SCATTER MONTE CARLO COMPARED TO CONDENSED HISTORY RESULTS FOR LOW ENERGY ELECTRONS

Clinton T. Ballinger, Dermott E. Cullen, Sterret T. Perkins, and James A. Rathkopf  
Lawrence Livermore National Laboratory  
University of California  
P.O. Box 808, L-95  
Livermore, CA 94550

and

William R. Martin and Scott J. Wilderman  
University of Michigan  
Department of Nuclear Engineering  
Ann Arbor, MI 48109

It is widely acknowledged that the condensed history methodology is inadequate for low energy electron transport problems, especially in materials of high atomic number. A Monte Carlo code which simulates individual electron interactions has been written and the results compared to those of condensed history to determine when condensed history transport is valid. Condensed history requires a number of restrictive assumptions about the scattering characteristics in order to predict the electron state (energy, direction, and position) after several collisions. These assumptions, which are valid at high energies, fail with decreasing energy and increasing atomic number. Comparison of single-scatter and condensed history results indicate the range of condensed history validity. This report discusses development of the single-scatter Monte Carlo code and shows comparisons with experimental and condensed history results for keV-range electrons. The multi-scattering distributions in energy and angle used in the condensed history method are compared directly with analogous distributions generated via the single-scatter code. In addition, through judicious replacement of components in the condensed history method with the more accurate single-scatter treatment, the sources of failure have been identified. Substituting distributions generated by single-scatter Monte Carlo for condensed history distributions was inspired by the response history Monte Carlo (RHMC) method which is an alternative approach for solving electron transport problems. The excellent agreement between the RHMC results and those from single-scatter Monte Carlo amplifies the need for improvements in the condensed history method. The material dependent energy where the condensed history method fails and the reasons for the failure are discussed.

## LYOLUMINESCENCE AND A WORKING MODEL TO EXPLAIN ITS BEHAVIOUR

B. K. Chatterjee, S. C. Roy and T. Sur  
Dept. of Physics, Bose Institute, Calcutta - 700 009, INDIA

Lyoluminescence, the luminous reaction upon dissolution of irradiated organic compounds in specific solvents, pose as an excellent candidate to be used as a dosimeter of ionizing radiations. The mechanism of lyoluminescence is however extremely complex depending on the mass (grain size) and nature of the sample, temperature of the solvent, pH of the solvent, dissolved oxygen and other compounds (scavengers, quenchers and other phosphorescent compounds like luminol), oxygen originally present in the compounds, storage time, heat treatment etc. Various theoretical models are proposed, but due to the complexity of the process a single satisfactory treatment explaining the entire process is lacking. We present here a rate kinetic model based on the Russel-Vassil'ev scheme, utilizing a postulate by Ettinger and Puite<sup>1</sup>(EP), to explain the general behaviour of the process (pH of the solvent, presence of other compounds and the effect of the oxygen dissolved in the solvent has not been considered). The model explains the observed dependences of the radical concentration and light yield on the irradiation dosage. It also supports the EP postulate as a possible mechanism of lyoluminescence. Comparison of our model with experimental observations will be presented.

---

1. K. V. Ettinger and K.J. Puite, Int. J. Appl. Radiat. Isot. 33, 1115 (1982)

SINGLE QUANTUM ANNIHILATION  
OF POSITRONS AROUND 1 MeV

I-5

B.V.Bhat<sup>+</sup>, K.M.Varier and

J.C.Palathingal<sup>\*</sup>

Department of Physics, Calicut University,  
Kerala - 673635, India

Abstract

Differential cross sections for the single-quantum annihilation of positrons have been measured in gold and lead. The monoenergetic positron beam was obtained by means of double-lens intermediate image beta ray spectrometer using a  $\text{Ge}^{68}$  source. Two thin foils of lead and gold and a thick foil of lead was used as targets, mounted at the focal plane of the spectrometer. Single quantum annihilation photons were measured using high resolution HPGe detector. Annihilation from K- and L-shell electrons with the incident positrons was identified. Angular distribution of the annihilation gamma photons has been attempted and it has been found to be in agreement with the results of Johnson. Average total cross section in thick target of lead has also been measured and was found to agree with the value of Johnson.

---

<sup>+</sup> Present address: Department of Physics,  
Sri.J.C.B.M.College, Sringeri,  
Karnataka - 577 139, India.

<sup>\*</sup> Present address: Department of Physics,  
University of Puerto Rico, Mayaguez,  
Puerto Rico, 000708, USA.

## MEASUREMENT OF DOUBLE PHOTON COMPTON SCATTERING

B.S. Ghuman, Bhajan Singh and B.S. Sandhu  
 Physics Department, Punjabi University,  
 Patiala-147002, India.

In a collision between a photon and a free electron, quantum electrodynamics predicts some higher order processes in addition to normal or single photon Compton effect. The most significant of these is double photon Compton scattering which is a third order process and involves the emission of one recoil electron and two degraded photons. An exact expression for double photon Compton scattering has been derived by Mandl and Skyrme using relativistic quantum electrodynamics and can be regarded as a double Compton analog of Klein-Nishina formula for the single photon Compton scattering. The double photon differential Compton cross-section formula involves five independent variables and is a complicated function of energies and scattering angles, which makes it difficult to study the features of this phenomena. The probability for occurrence of double photon Compton scattering increases with increase of incident photon energy and this process contributes significantly to the total scattering coefficients at high incident energies. To understand the features of this process we have carried out some calculations at 662 keV incident energy. These calculations indicate an increase in cross-section with the decrease in scattering angle and energy of one of the emitted photon.

In view of scanty and fragmentary experimental data on double photon Compton scattering we have measured the intensity and energy distribution of double photon Compton scattering of 662 keV gamma rays for aluminium scatterer of thickness 40 mg/cm<sup>2</sup>. 662 keV gamma rays are obtained from Cs-137 radioactive source of strength 8.0 Ci. Two NaI(Tl) detectors working in coincidence are used for the detection of two simultaneously emitted photons. Various parameters which are involved in the determination of the cross-section are either determined experimentally or obtained from the available literature. The coincidence spectra of one of the emitted photons is recorded by fixing the energy window of the second photon and is corrected for chance and false coincidences. The measured values of intensity and energy distribution of double photon Compton scattering are found to be in agreement with the theoretical data of Mandl and Skyrme.

## MEASUREMENT OF COMPTON SCATTERING FROM BOUND ELECTRONS

Bhajan Singh and B.S.Ghumman  
Physics Department, Punjabi University,  
Patiala-147002, India.

The study of Compton scattering from bound electrons is essential to understand the behaviour of the electron in the shell and attenuation of low energy radiations in different media. Various non-relativistic and relativistic theories based upon different atomic models are available to understand the binding effects of inner shell electrons in the atom. The general predictions of these theories are, small value of cross-section at small scattering angles, broadening of K-shell Compton peak, shift of K-shell Compton peak from the free electron Compton peak, presence of infra-red divergence and high energy tail. Several measurements are available at various energies and for different elements but these are often in disagreement with each other and available theoretical data. In the present experiment we have carried out measurements at scattering angles ranging from 30° to 150° for different elements at 662, 279 and 145 keV incident energies. Measurements have been made using two NaI(Tl) scintillation detectors to detect scattering gamma rays in coincidence with K-shell fluorescent X-rays that follow this process. Scatterers of various thicknesses ranging from 12 mg/cm<sup>2</sup> to 50 mg/cm<sup>2</sup> are used and thickness dependence of K-shell Compton cross-section is studied experimentally. Our results on intensity distribution of gamma rays from K-shell electrons show small cross-section value at small scattering angles and increases to a maximum followed by a broad minima at large scattering angles. Energy distribution of K-shell Compton scattered gamma rays shows a broadened peak but this broadening is much smaller than that predicted by various theories. Negligible shift of K-shell Compton peak from the free electron Compton peak is observed in the measured spectra. No infra-red divergence is in the experimental spectra.

PRESENT STATE OF EXPERIMENTAL RESEARCH ON SECONDARY ELECTRON  
FIELDS IN MATTER UNDER THE INFLUENCE OF  $\gamma$ -RADIATION

M. Ya. Grudskii, V. V. Smirnov

The process of forming of secondary electron radiation fields is the basis for interpretation and qualitative estimation of the effects induced in the medium by  $\gamma$ -radiation. The accurate calculation of the spatial-energy distribution and the number of electrons emerging from irradiated target of thickness approximately equal to electron range in given medium is highly tedious task because the mathematical description of the electron multiple scattering is too complicated.

In this report we present series of experimental data on yields (electrons per incident photon) and spatial-energy distributions obtained at V. G. Khlopin Radium Institute during last 15 years. Measurements were made for monoenergetic collimated photon beams with  $E_\gamma = 30 \text{ keV} + 3 \text{ MeV}$  incident on flat targets produced on the basis of pure materials with the atomic number  $Z$  from 13 to 82. In the case of normal incidence angular distributions possess azimuthal symmetry, and space current vector in the space above (or under) emitting target is normal to the target surface. In the case of oblique incidence there exists a component of the space current tangential to the surface as well as normal to the surface. The ratio of these components characterizes the degree of two-dimensional angular distribution asymmetry. It grows with increasing of  $E_\gamma$  and with decreasing of  $Z$ .

Analysis of the presented results allowed us to establish some regularities of secondary electron radiation field formation, and their comparison with theoretical predictions - to make clear what are the possible sources of systematic errors inherent to different methods and initial data applied to calculation of secondary electron field characteristics.

## INCOHERENT SCATTERING AT LOW MOMENTUM TRANSFERS

D.A. Bradley\*, C.S. Chong, A.A. Tajuddin, A. Shukri and A.M. Ghose\*\*  
 School of Physics, University of Science of Malaysia, 11800 USM Penang  
 \* Dept. of Radiology, National University of Malaysia, 50300 K. Lumpur  
 \*\*Variable Energy Cyclotron Centre, Calcutta 700 029, India.

We compare (Table 1) results of experiment and predicted values<sup>1</sup> of the incoherent-scattering function  $S(x, Z)$  for atoms exhibiting large relativistic effects. Allowance is made for target attenuation by appeal to an extrapolation technique<sup>2</sup> modified to current needs. Also included in Table 1 are measured values of total-scatter cross-sections, combining incoherent and counterpart coherent-scattering intensities<sup>2</sup>. We accord with tabulated  $S(x, Z)$  value and the results of a number of other groups (see, for instance, ref. 3). We find no evidence for systematic over-estimate in the non-relativistic-wavefunction  $S(x, Z)$  values<sup>1</sup> as reported by Kane et al.<sup>4</sup>

TABLE 1

$E_{\text{photon}} = 661.6 \text{ keV}$

Scattering angle (deg)	$x(\text{\AA}^{-1})$	$[S(x, Z)/Z]_{\text{ex}}$	$[(d\sigma/d\Omega)_{\text{ex}}]$ (b $\text{Sr}^{-1}$ )	$[S(x, Z)/Z]_{\text{th}}$	$[(d\sigma/d\Omega)_{\text{th}}]$ (b $\text{Sr}^{-1}$ )
6.4	2.978	0.850 (0.867)	4.89 $\pm$ 0.49 (4.96)	0.830 (0.806)	13.62 $\pm$ 1.40 (12.83)
8.2	3.815	0.940 (0.909)	4.70 $\pm$ 0.47 (4.53)	0.892 (0.855)	9.23 $\pm$ 0.92 (9.02)
10.4	4.836	0.961 (0.940)	4.09 $\pm$ 0.41 (3.99)	0.945 (0.924)	7.78 $\pm$ 0.78 (7.54)
12.3	5.716	0.983 (0.955)	3.85 $\pm$ 0.39 (3.77)	0.949 (0.919)	6.89 $\pm$ 0.69 (6.80)
15.1	7.010	1.026 (0.989)	3.74 $\pm$ 0.37 (3.54)	0.953 (0.945)	6.29 $\pm$ 0.63 (6.26)

$E_{\text{photon}} = 279.2 \text{ keV}$

Scattering angle (deg)	$x(\text{\AA}^{-1})$	$[S(x, Z)/Z]_{\text{ex}}$	$[(d\sigma/d\Omega)_{\text{ex}}]$
8.2	1.610	0.623 (0.810)	3.73 $\pm$ 0.27 (3.63)
10.4	2.040	0.697 (0.861)	3.01 $\pm$ 0.22 (2.85)
12.3	2.412	0.843 (0.894)	2.42 $\pm$ 0.19 (2.50)
15.1	2.958	0.960 (0.923)	2.34 $\pm$ 0.21 (2.25)

Values in parentheses refer to the corresponding predicted values.

## REFERENCES:

1. J.H. Hubbell, Wm. J. Veigle, E.A. Briggs, R.T. Brown, D.T. Cromer and R.J. Howerton, J. Phys. Chem. Ref. Data 4 471 (1975).
2. D.A. Bradley, C.S. Chong, A.A. Tajuddin, A. Shukri and A.M. Ghose, Phys. Rev. A41 5974 (1990).
3. J.C. Dow, J.P. Lestone, R.B. Taylor and I.B. Whittingham, J. Phys. B21 2425 (1988).
4. P.P. Kane, J. Mahajani, G. Basavaraaju and A.K. Priyadarsini, Phys. Rev. A28 1509 (1983).

## THE NATURE OF ELECTROMAGNETIC RADIATION

M. Simhony

Physics 5, The Hebrew University, Jerusalem, Israel

\*\*\*

Even with the now achievable million MeV energies it is impossible to create or destroy a single electron ( $e^-$ ) or positron ( $e^+$ ). Therefore, 1.02 MeV is not the creation energy of an  $e^-$  and  $e^+$  but the energy of their binding in the electromagnetic (EM) field. All observed quantum effects prove that our EM field is an  $e^-e^+$  lattice (epola) with per particle (or per  $l_0^3$  unit cube) binding energy  $bE=0.51$  MeV, mass  $m_e=9.1\cdot 10^{-31}$  kg, and lattice constant  $l_0=(4.4 \pm 0.5)$  fm.<sup>1</sup> The electron radius is  $R_e \leq 0.1$  fm, so that only a  $10^{-3}$  part of the volume of our EM field is filled by particles. Thus, the nuclei and electrons of atomic bodies can move through the essentially empty EM field (epola), causing no winds but de Broglie waves in it. The velocity of bulk deformation (BD) waves in the epola is  $v_d=(bE/m_e)^{1/2}=300$  Mm/s  $\approx c$ . Therefore, EM waves are the detectible result (and cause) of BD waves in the epola. A BD wave consists of half-wave ( $\lambda/2$ ) BD clusters (HWC), each containing  $\pm \delta N$  excess bound particles, held in an  $l_0$ -thin monolayer on its surface. Hence, the HWC energy is  $E_{cl} \propto \delta N \propto (\lambda/2)^2$ , while the number of particles is  $N_{cl} \propto (\lambda/2)^3$ . The photon energy  $E_p$  is transferred from particle to particle in the wave, therefore  $E_p=E_{cl}/N_{cl} \propto \lambda^{-1}$  (Planck's postulate). An EM wave of  $E_p=m_e c^2=bE$  (Compton wave) has  $\lambda=2426$  fm= $\lambda_c$ ,  $N_{cl}=1.1\cdot 10^7=N_c$ ,  $\delta N=1$ , and the number of photons is  $N_p=1$ . For EM waves of  $\lambda > \lambda_c$ , we have  $E_p=m_e c^2(\lambda_c/\lambda)=1.24$  eV $\cdot\mu m/\lambda$ ;  $N_{cl}=N_c(\lambda/\lambda_c)^3$ ;  $\delta N=(\lambda/\lambda_c)^2$ ;  $E_{cl}=m_e c^2\delta N$ ;  $N_p=E_{cl}/E_p=(\lambda/\lambda_c)^3$ . In EM waves of  $\lambda < \lambda_c$  (epola impact waves) the HWC is always invaded by a single excess particle,  $\delta N=N_p=1$ , and  $E_{cl}=E_p=m_e c^2(\lambda_c/\lambda)=hf$ . The shortest epola wave has  $\lambda=2l_0=280$   $\lambda_c$  and energy 140 MeV. At such energies, the "wave" is just a free  $e^-e^+$  pair of velocity  $v=c$ . The physics behind particle-wave duality, transverseness of EM waves, a.o. problems of EM radiation will be presented.

1. M.Simhony: The Electron Positron Lattice Space, Jerusalem 1990 (160 pp). Particle Creation in the Electromagnetic Field, invited presentation at Workshop XVI of PANIC 12, MIT, Cambridge 1990; to appear in Proceedings. Physical Nature of Phonons and Photons, in S. Hunklinger et al (Eds.), Phonons 89, World Scientific, Singapore 1990, pp.175-177.



COMPARISON OF THE SPENCER-FANO EQUATION WITH THE CONTINUOUS-SLOWING-DOWN APPROXIMATION CORRECTED FOR ELECTRON GENERATION\*

Michael A. Dillon, Mituo Inokuti, and Mineo Kimura  
Argonne National Laboratory, Argonne, IL 60439 U.S.A.

The time-dependent Spencer-Fano equation<sup>1</sup> for electron degradation in a single-component system may be written as

$$v^{-1} \frac{\partial z(T, t)}{\partial t} = n K_T z(T, t), \quad (1)$$

where  $z(T, t)$ ,  $v$ ,  $T$ , and  $n$  are respectively the electron degradation spectrum, electron velocity, electron kinetic energy, and molecular density. The cross section operator  $K_T$  is given by

$$K_T = K'_T + \sum_{\alpha} \int_{2T+I_{\alpha}}^{T_0} dT' \frac{d\sigma_{I\alpha}(T', T+I_{\alpha})}{dE} z(T', t) dT', \quad (2)$$

where  $d\sigma_{I\alpha}/dE$  is the differential ionization cross section of the  $\alpha$ th shell with ionization potential  $I$  for production of electrons with kinetic energy  $T$ . The continuous-slowing-down approximation with full accounting of electron production<sup>2</sup> is obtained by approximating  $K'_T$  with

$$K'_T \equiv \frac{\partial s(T) z(T, t)}{\partial T}, \quad (3)$$

where  $s$  is the stopping cross section.

In the present study we compare the results obtained from the numerical integration of Eq. (1) with results employing  $K'_T$  of Eq. (3). Special attention is focused on the time-dependent yields of ions and excited states produced by electron degradation in argon.

#### References

1. M. Inokuti, M. Kimura, and M. A. Dillon, Phys. Rev. A **38**, 1217 (1988).
2. K. Kowen, Phys. Rev. A **41**, 2500 (1990).

\*Work supported in part by the U.S. Department of Energy, Assistant Secretary for Energy Research, Office of Health and Environmental Research, under Contract W-31-109-Eng-38, and by the U.S./Yugoslavia Cooperative Research Program of the National Science Foundation.

# TRANSITION RADIATION IN A THIN SINGLE CRYSTAL ON CAPTURE INTO THE CHANNELING REGIME

N.P. Kalashnikov (a) and V.M. Ristić (b)

(a) *Engineering College at the I.A. Likhachev Automobile Plant, Moscow;*

(b) *Faculty of Natural Science, University "S. Marković", Kragujevac.*

On entry of a charged-particle beam into a crystal at a small angle to a crystallographic axis or plane, channeling is observed. Capture of a particle into the channeling regime is determined in this case by the relation between the energy of the transverse motion and the height of the potential barrier created by the atoms of the plane. The scattering process can be accompanied by radiation of a certain number of photons and in the case  $\omega < E^2/m$  ( $\hbar = c = 1$ ), using the general rules of diagram technique, the probability of radiation  $dw_{\text{rad}}$  could be simply related to  $dw_{\text{el}}$ , the probability of scattering of charged particles at the crystal boundary.

The result is

$$dw_{\text{rad}} = (e^2/\pi^2) \sum (d^3k/2\omega) [(p_1 e)/(p_1 k) - (p_2 e)/(p_2 k)]^2 dw_{\text{el}}(p_1 \rightarrow p_2),$$

where  $p_1$  and  $p_2$  are the 4-momenta of the electron before and after scattering, and  $e$  is the 4-vector of the polarization of the radiation.

In order to obtain  $dw_{\text{el}}$  we are approximating the potential by Kronig-Penney model potential. Substituting  $dw_{\text{el}}$  into above relation, summing over the polarizations of the photon, and integrating over the solid angle of the radiation and over frequency we can estimate the probability of radiation per electron, which is a quantity of the order  $Ze^2(R_0/a)^2 \approx 2 \cdot 10^{-8}$ ,  $R_0$  being the effective radius of the potential.

In summary, the rearrangement of the wave function of a charged particle on crossing a crystal boundary is accompanied by electromagnetic radiation which does not depend on the thickness of the crystal.

# VUV emission of rare gases at ns-threshold exciting photon energy.

V.L.Sukhorukov, B.M.Lagutin, I.D.Petrov  
Rostov Railway Engineers Institute, 344007 Rostov-on-Don USSR

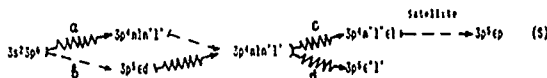
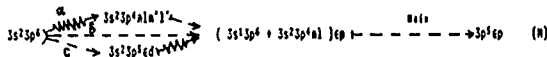
H.Schmoranzner, A.Ehresmann, M.Wildberger  
Dept. of Physics, University of Kaiserslautern, D-6750 Kaiserslautern FRG

It was shown [1,2], that the shape of VUV emission spectra of rare gases, excited by photons with near ns-threshold energies, strongly depends on the exciting photon energy. In the same work the dependence mentioned above was correlated with the energy positions of doubly-excited states  $3s^23p^4nl^2$  (here and below electron configurations of Ar are taken as an example).

In the present work an attempt was made to improve our understanding of the physical processes giving rise to VUV emission of rare gases. To solve this problem we used some measured integral characteristics of Ar and Kr VUV spectra and made the estimations of the qualitative changes of these values from Ar to Kr.

From the experimental spectra we got the ratio of emission intensities of all satellite lines to the main line  $^1I/^1I$  in the exciting photon energy region 32-34 eV for Ar and 28-32 eV for Kr. The ratio of satellite intensities connected with transitions from quartet  $^4I$  and doublet  $^2I$  states in configurations  $3s^23p^4nl(2^4I)$ ,  $(^4I+^2I: ^1I)$ , has also been obtained. These values are  $(^1I/^1I)_{Ar}=0.196$ ,  $(^1I/^1I)_{Kr}=0.820$ ,  $(^4I/^2I)_{Ar}=1.31$  and  $(^4I/^2I)_{Kr}=5.35$ , i.e. the integral intensity of satellites increased by 4.18 and the integral intensity of quartet satellites by 4.00 from Ar to Kr.

To understand the origin of these changes we made estimations of integral intensities of lines, radiating due to the following processes:



Here  $\rightarrow$  and  $\xrightarrow{\text{A}}$  mean dipole electric and Coulomb interaction respectively. Summation (integration) over all intermediate states has been performed. The estimations mentioned above showed a great importance of the following two effects:

1.  $3p$  spin-orbit interaction. This interaction in S(a,b) processes permits transitions into quartet  $3p^4nl(^4I)nl^2$  states forbidden in LS coupling. It has to be pointed out that the increase of spin-orbit interaction from Ar to Kr influences the S(a) process due to the increase of the spin-orbit constant by 3.52. This seems to be one of the reasons for the increasing ratios  $^4I/^2I$  and  $^1I/^1I$  from Ar to Kr.

2. Autoionization decay of doubly excited states (process S(c) and S(d)). Doubly excited states decay due to both S(c) and S(d) channels. It has to be pointed out that the states which decay by S(d) channel give no contribution to VUV emission. Our calculation also showed that the relative probability of S(c) decay increases from Ar to Kr due to the localization of  $nl$ -orbitals. This fact is an additional reason for the increase of  $^1I/^1I$  ratio from Ar to Kr.

## References:

1. K.-H. Scharfner, P. Lentz, B. Möbus, H. Schmoranzner and M. Wildberger, Phys. Lett. A 128 (1986) 374.
2. H. Schmoranzner, M. Wildberger, K.-H. Scharfner, B. Möbus and H. Nagel, Phys. Lett. A 150 (1990) 201.

DETERMINATION OF TL PARAMETERS OF  $\text{LiF:Mg,Cu,P}$  PRODUCED AT  
ININ-MEXICO.

Juan Azorín, Alicia Gutiérrez and Pedro González.  
Instituto Nacional de Investigaciones Nucleares (ININ)  
Carretera México-Toluca, Km. 36.5 Salazar, México.

Three important parameters to be determined in a thermoluminescence study are the activation energy ( $E$ ), the frequency factor ( $s$ ) and the kinetics order. Results of experiments made with  $\text{LiF:Mg,Cu,P}$  prepared at the Instituto Nacional de Investigaciones Nucleares (ININ) are presented in this paper. These results have been obtained using glow curve shape methods and the deconvolution method. The main peaks in the glow curve obey first order kinetics.

The values of the kinetic parameters obtained by different methods are in good agreement among them.

## SMALL ANGLE ELASTIC SCATTERING OF 122 AND 245 keV $\gamma$ RAYS.

Leanne P Guy, Raymond B Taylor and Ian B Whittingham  
Physics Department  
James Cook University  
Townsville, Australia 4811

### Abstract

The elastic scattering of 122 and 245 keV  $\gamma$  rays from a source containing  $^{152}\text{Eu}$  and  $^{154}\text{Eu}$  has been measured for scattering through  $5^\circ$ ,  $7^\circ$  and  $10^\circ$  by targets of Al, Cu, Mo, Sn, Ta and Pb. The experimental cross sections have been normalized to theoretical cross sections for carbon. The results for 245 keV  $\gamma$  rays have been obtained using a least-squares fit of the overlapping elastic and Compton peaks whereas the results for 122 keV  $\gamma$  rays have been obtained by a subtraction method using theoretical Compton cross sections. The experimental elastic cross sections are in very good agreement (to better than 5%) with the theoretical calculations of Kane et al and provide strong support for the calculational scheme of Kissell and Pratt for the evaluation of total atom Rayleigh scattering in the regime where there are significant contributions from outer electron shells.

## INCOHERENT SCATTERING FUNCTION AT SMALL MOMENTUM TRANSFERS

Leanne P Guy, Raymond B Taylor and Ian B Whittingham

Physics Department  
James Cook University  
Townsville, Australia 4811

### Abstract

The energy spectra have been measured for the scattering of 245 keV  $\gamma$ -rays through  $5^\circ$ ,  $7^\circ$  and  $10^\circ$  by targets of Al, Cu, Mo, Ta and Pb. The overlapping Compton and elastic peaks were extracted using a least-squares analysis in which the Compton lineshape was fitted to a convolution of an instrumental lineshape and a theoretical  $Z$ -dependent relativistic impulse approximation (RIA) atomic lineshape. For the small momentum transfers of this investigation, the integrated RIA energy spectra differ significantly from those obtained using Waller-Hartree incoherent scattering functions. In contrast to previous investigations at higher momentum transfers, where the experimental and theoretical results for the incoherent scattering function all agreed to within experimental error, the present experimental results for the smallest momentum transfers and lightest elements are significantly lower than both sets of theoretical calculations. This suggests that these theoretical approaches to total-atom Compton scattering may be inadequate at small momentum transfers for light elements.

Evaluation of the enhancement ratio of characteristic K X-rays produced by 59.54 keV in monoelemental thick targets.

E. Casnati, C. Baraldi and A. Tartari

Dipartimento di Fisica dell'Università. I-44100 Ferrara, Italy

In experiments involving the characteristic K radiation emitted by thick targets, in addition to direct X-ray emission which depends on the K photoeffect cross section, fluorescence yield, target self attenuation and geometric parameters, the detector is reached by an additional K radiation coming from the explored volume owing to three indirect, non-negligible effects.

Firstly, each elementary volume elastically scatters the K radiation produced elsewhere. Secondly, the K X-rays generated in the volume by incident radiation are accompanied by X-rays stimulated by radiation which is elastically or inelastically scattered in all the other volumes of the target. Obviously inelastic scattering is only possible if the energy of the incident radiation is greater than that of the K edge by an amount exceeding that of the Compton shift.

The authors have worked out a model and an analytic procedure which permit evaluation of the enhancement ratio of the measured radiation density flux as a function of the targets thickness and the irradiated area dimensions. Accurate experimental checks carried out on monoelemental Mo, Cd and Sn targets by 59.54 keV incident photons confirm the validity of the model. The results obtained show that the X-ray enhancement ratio can reach values as high as 5 to 9% under the examined conditions, even for thicknesses not exceeding one mean free path of the incident radiation when the irradiated area is several mean free paths wide.

**CALCULATIONAL METHODS FOR SECONDARY ELECTRON  
EMISSION YIELDS FROM SOLIDS UNDER GAMMA-RAY  
AND CHARGED PARTICLE IRRADIATION**

A. Akkerman\*, A. Breskin, R. Chechik and A. Gibrakhterman\*

Physics Department

Weizmann Institute of Science, Rehovot, 76100, Israel.

The secondary electron emission (SEE) from solids, induced by charged particles and gamma rays, has a vast field of applications such as in instrumentation for material probing, dosimetry and design of radiation detectors. The high energy tail of the SEE spectrum ( $E_e > 100$  eV) initiates processes of generation and slowing down of secondary electrons, well described theoretically. Hence, it is possible to obtain with high accuracy the main characteristics of such processes using computer simulation techniques. The interpretation of the slow energy tail ( $E_e < 100$  eV) of the SEE spectrum is complicated by the necessity to consider some solid state effects (excitation and decay of plasmons, creation and annihilation of phonons etc.) for which there is a lack of exact theory. There exist only a few models to describe SEE processes and the computer simulations may now be used to verify some of them by comparison with experimental results.

In this review we briefly discuss models used and calculational methods developed for SEE simulations. We present also the results of calculations for differential (energy spectra, angular distributions) integral (yields, mean values) obtained for a wide range of materials irradiated by charged particles and gamma-rays over a broad energy spectrum.

The SEE data may be used for various practical applications in particular for developing a new class of high flux X-ray imaging radiation detectors. The method will be discussed.

---

\* Visiting Scientists from the Alma-Ata High Energy Physics Institute, Kasakh, SSR.



Equipartition, Planck's Radiation Law and Quanta

CHRISTOPHER G. JESUDASON  
Department of Chemistry  
University of Malaya  
59100 Kuala Lumpur, MALAYSIA

By extending the concept of equipartition, it is possible to derive a non-quantum version of Planck's radiation law, without ad hoc assumptions such as zero-point, zero temperature random radiation [Phys. Rev. 186(5), 1304 (1969), Phys. Rev. A. 42(12), 7006 (1990)] which violate classical thermodynamical principles. The meaning of the Planck constant is discussed together with the quantum hypothesis. A coarse-averaged description, which may be refined to any order is employed throughout.

KEYWORDS: Planck Radiation Law, Equipartition Theorem,  
Quantum Theory

THE EXCITATION OF THE 279.2 keV LEVEL IN THE DECAY OF  $^{137}\text{Cs}$ 

A.H.Kukoč, M.M.Marković and I.V.Aničin

The Boris Kidrič Institute, Vinča, Belgrade, Yugoslavia

In  $^{137}\text{Ba}$  it is well established from many reaction studies that there exists the  $1/2^+$  level at 279.2 keV. It is potentially fed by the  $Q=895$  keV,  $\Delta I=3$ ,  $\Delta\pi=\text{no}$   $\beta$ -transition from the  $7/2^+$  ground state of  $^{137}\text{Cs}$ , which is followed by the emission of the  $M1/E2$ ,  $\alpha_{\text{tot}}=0.04$ , 279.2 keV radiation. We decided to make use of the convenient circumstance that in another long-lived calibration gamma-ray source,  $^{133}\text{Ba}$ , there exists the 276.4 keV (7.09%) radiation offering the possibility to determine the intensity of the 279.2 keV transition with an error which will practically not exceed the combined errors of the activities of the two sources involved, what in our case amounts to the final 6%. We used the  $E=14\%$ ,  $R=1.7$  keV germanium detector with the measured peak/Compton of 47.5:1, in the 10 to 15 cm lead shielding (though the integral background rate in the range of 20 to 2900 keV was only 0.63 cps still all the low-energy background lines were observed superimposed on the final  $^{137}\text{Cs}$  spectrum!). No coincidence measurements were done and no anti-Compton suppression was used. The source-to-detector distance was 15 cm and the 5 cm long, 1 cm hole, lead collimator was used throughout. The activities of the sources were in the 100 kBq range. The total detection efficiency for the 279 keV gamma-ray was found to be  $1.42(6)\text{E-3}$ . After the exposure time of 540 ks the intensity of the 279 keV line, integrated channel-by-channel, was  $(-1.9 \pm 1.8)\text{E+3}$ . According to Ref.1 the corresponding limiting intensity at the  $99.73\%$  CL, converted into absolute intensity, is  $I_{\text{lim}}=2.27(13)\text{E-5}$ . For the presumably allowed  $\beta$ -transition this leads to  $\log ft > 14.94(2)$  (ref.2). This is already well within the region of the second-forbidden unique transitions (ref.3). Any feeding by the branching from the 661.6 keV isomeric state will only further increase this value.

Comparing this with the value of  $\log ft > 13.3$  for the  $Q=665$  keV,  $\Delta I=3$ ,  $\Delta\pi=\text{no}$  transition in the third of the ubiquitous triad of the long-lived calibration isotopes,  $^{60}\text{Co}$  (ref.4), one might think of the difference being not only due to the difference in detection sensitivities but also due to the nuclear structure effects - the decay of  $^{137}\text{Cs}$  destroying and the decay of  $^{60}\text{Co}$  completing a closed shell ( $N=82$  and  $Z=28$  respectively).

1. I.V.Aničin and C.T.Yap, NIM A259(1987)525
2. R.I.Verrall et al. NIM 42(1966)258
3. S.Raman and N.B.Gove, Phys.Rev. C7(1973)1995
4. C.Lederer, V.Shirley, "Table of Isotopes", Wiley 1978

ADJOINT CALCULATIONS FOR MULTIPLE SCATTERING OF COMPTON AND  
RAYLEIGH EFFECTS

J.E. Fernández\* and M. Sumini  
Laboratorio di Ingegneria Nucleare di Montecuccolino  
University of Bologna  
via dei Colli 16, 40136 Bologna, Italy

As it is well known, the experimental determination of the Compton profile requires a particular geometry with a scattering angle close to  $\pi$ . That situation involves a narrow multiple scattering spectrum that overlaps the Compton peak making it difficult to analyze the different contributions to the profile.

We show how the solution of the adjoint problem can help in devising the more useful experimental configuration, giving, through its classical "importance" meaning, a formally clear picture of the whole problem.

---

\*Fellow of CONICET, Buenos Aires, Argentina. On leave from the Faculty of Mathematics, Astronomy and Physics, University of Córdoba, Argentina.

INFLUENCE OF THE TILT OF THE PLANE OF PROPAGATION TO CANCEL  
THE MULTIPLE SCATTERING EMISSION

J.E. Fernández\*

Laboratorio di Ingegneria Nucleare di Montecuccolino  
University of Bologna  
via dei Colli 16, 40136 Bologna, Italy

In some recent papers we have stressed the importance of the tilt of the plane of propagation (the plane containing the collimated incidence and take-off directions) to cancel higher-order of XRF emission. In this work we show that such an influence can be extended to all the prevailing interactions that occur in the X-ray regime: the photoelectric, the Rayleigh and the Compton effects, i.e. the multiple scattering interactions involving these effects vanish when the tilt angle approaches to  $\pi/2$ . Regarding the scattering processes, the tilt of the plane of propagation does not affect the scattering angle, so this technique provides a tool to isolate the scattering peaks from the disturbing background due to multiple scattering. The influence on the multiple scattering intensities is proved by recourse to analytical expressions deduced with the transport theory in previous papers.

---

\*Fellow of CONICET, Buenos Aires, Argentina. On leave from the Faculty of Mathematics, Astronomy and Physics, University of Córdoba, Argentina.

DIFFUSION OF POLARIZED PHOTONS IN THE FRAME OF THE TRANSPORT  
THEORY

J.E. Fernández\* and V.G. Molinari  
Laboratorio di Ingegneria Nucleare di Montecuccolino  
University of Bologna  
via dei Colli 16, 40136 Bologna, Italy

In the frame of the multiple applications of Synchrotron Radiation X-Ray Spectrometry (SRXRS), a detailed description of the transport of polarized photons under several boundary conditions in condensed media is of utmost importance. The account for polarization requires four parameters to describe the X-ray beam. Further, the state of polarization, and hence these four parameters, change when the photon undergoes every scattering event. Accordingly, a proper description of photon transport including polarization effects involves four coupled equations of transfer. In this work we deduce the transport equations including polarization effects for an homogeneous target of infinite thickness irradiated with a collimated and monochromatic beam of X-rays. Exact iterative solutions for such equations are reported, which are universally valid with all types of interactions. An example is given for the diffusion of natural light (unpolarized) in an homogeneous condensed medium.

---

\* Fellow of CONICET, Buenos Aires, Argentina. On leave from the Faculty of Mathematics, Astronomy and Physics, University of Córdoba, Argentina.

HIGH-ORDER MULTIPLE SCATTERING CONTRIBUTIONS IN X-RAY  
SPECTROMETRY

R. Sartori\* and J.E. Fernández\*\*  
Laboratorio di Ingegneria Nucleare di Montecuccolino  
University of Bologna  
via dei Colli 16, 40136 Bologna, Italy.

Multiple scattering contributes important parts of the emission spectrum from thick targets excited with X-ray photons. Both the continuous and discrete parts of the spectrum receive enhancement by multiple scattering. Recently, some expressions were deduced allowing the computation of the second-order chains of the Compton and Rayleigh effects. In this work we extend those calculations to the third- and the fourth-orders of multiple scattering by means of Monte Carlo simulation. MC results are computed using full expressions for the interaction angular coefficients (i.e. scattering coefficients including atomic form factors). The second-order result is compared to the computation by deterministic means, showing close agreement except in the extreme of the Compton-Compton spectrum. Higher-orders are important in low Z elements but can be safely neglected in the medium Z range.

---

\*Fellowship of CONICOR, Córdoba, Argentina.  
\*\*Fellow of CONICET, Buenos Aires, Argentina. On leave from the Faculty of Mathematics Astronomy and Physics, University of Córdoba, Argentina.

CORRECTION FOR MULTIPLE SCATTERING IN ATTENUATION COEFFICIENT  
MEASUREMENTS

R. Sartori\* and J.E. Fernández\*\*  
Laboratorio di Ingegneria Nucleare di Montecuccolino  
University of Bologna  
via dei Colli 16, 40136 Bologna, Italy.

Calculations of the diffusion of photons in thin thickness targets have been performed with recourse to the transport theory. An order-of-interactions solution of the Boltzmann transport equation for photons is used to describe the multiple scattering terms due to the prevailing effects in the X-ray regime. We found that the main corrections are due to the influence of the pure Rayleigh effect. First- and second-order chains of the photoelectric, the Rayleigh and the Compton effects have been considered as possible sources of overlapping contributions to the transmitted intensity.

An analytical expression for the correction factor to the attenuation coefficient is given in terms of the direction and energy of the emitted radiation. Some examples are given for pure element targets.

---

\*Fellowship of CONICOR, Córdoba, Argentina.

\*\*Fellow of CONICET, Buenos Aires, Argentina. On leave from the Faculty of Mathematics, Astronomy and Physics, University of Córdoba, Argentina.

X-RAY FLUORESCENT ANALYSIS OF SAMPLES WITH ELEMENTS HAVING  
OVERLAPPED CHARACTERISTIC LINES.

Raul A. Barrea and Raul T. Mainardi\*.

Facultad de Matematica, Astronomia y Fisica. Universidad  
Nacional de Cordoba. - Laprida 854 - Cordoba - Argentina.

A procedure to determine the concentration of elements having overlapped lines was developed. It is based on the successive modification of the experimental arrangement method. To test its feasibility we performed extensive calculations with a simulation program supposing monochromatic excitation of binary samples composed of lead and arsenic in various relative concentrations.

The Lachance and Trail formalism proved to be suitable, for our case, to relate intensities with concentration.

\* Member of the National Research Council of Argentina (CONICET).



MEASUREMENT OF THE X-RAY ABSORPTION EDGE AMPLITUDE OF  
ERBIUM BY ATTENUATION OF A COMPTON PROFILE.

Alejandro P. Ayala and Raul T. Mainardi\*.

Facultad de Matematica, Astronomia y Fisica. Universidad  
Nacional de Cordoba. - Laprida 854 - Cordoba - Argentina.

The x-ray absorption edge of Erbium was measured by detection of the Compton profile of aluminum, at several different angles, by a high resolution intrinsic germanium detector.

The primary x-ray beam from an Americium 241 radioactive source, scattered in an aluminum target has a wide spectrum in energies spanning both sides of the absorption edge of Erbium. This beam is then attenuated by a carefully weighted Erbium foil and energy analyzed by a germanium detector.

The data analysis consists, among other features, of a careful numerical deconvolution where special techniques, needed when discontinuities or sudden variations are present, have been applied.

Our results have been compared with calculated results from tables and they show agreement with greater precision than of existent data.

\* Member of the National Research Council of Argentina (CONICET).

NUCLEAR EXCITATION BY GAMMA-RAY SCATTERING AT GIANT DIPOLE  
RESONANCE

L. Lakosi, J. Sáfár, A. Veres

Institute of Isotopes of the Hungarian Academy of Sciences,  
Budapest, Hungary and

T. Sekine, H. Kaji and K. Yoshihara

Department of Chemistry, Faculty of Science, Tohoku  
University, Sendai, Japan

The  $(\gamma, \gamma')$  reaction has long been considered to have a double-humped excitation function in the giant dipole resonance region. The first (sharp) peak takes place at the neutron emission threshold, whereas a comparable second (broader) one appeared in earlier experimental results at about the resonance maximum. Most favourable opportunities for the experimental study of this phenomenon are provided by excitation of long-lived isomers of stable nuclei. 4.5 h half-life  $^{115m}\text{In}$  and 56 min half-life  $^{103m}\text{Rh}$  isomers were excited by bremsstrahlung of the Tohoku LINAC in the 14 to 50 MeV region. The integrated isomer production cross section as a function of the endpoint energy remained nearly constant as  $9.3 \times 10^{-27}$  and  $22.6 \times 10^{-27} \text{ cm}^2/\text{MeV}$ , respectively, in the whole energy region. This corresponds to the lack of the existence of a comparable second peak, in contrast with earlier experiments.

Statistical cascade model calculations were performed to follow the energy dependence of the isomer production and inelastic gamma-ray scattering. The preequilibrium correction was determined in a fully spin dependent formulation of the exciton model. The calculation provided one peak at the neutron separation energy. Beyond the threshold the inelastic scattering abruptly reduces and a little second peak of about two orders of magnitude smaller seems to appear.

Our calculated results compare favourably with the experimental isomer production cross sections.

THE TOTAL MASS ATTENUATION COEFFICIENT OF 145.4 keV  
GAMMA RAYS IN BROAD BEAM GEOMETRY SET UP

H.A.JAHAGIRDAR, B.HAMUMAIHAH AND S.R.THONTADARYA,

DEPARTMENT OF PHYSICS, KARNATAK UNIVERSITY,  
DHARWAD - 580 003, INDIA.

Abstract

The total mass attenuation coefficient,  $\mu_m$ , of 145.4 keV gamma rays, emitted from  $^{141}\text{Ce}$  radioisotope in Pb;  $(\text{CH}_3\text{COO})_2\text{Pb} \cdot 3\text{H}_2\text{O}$ ;  $\text{Pb}(\text{NO}_3)_2$ ;  $\text{PbO}_2$ ;  $\text{PbO}$ ;  $\text{Na}_2\text{WO}_4 \cdot 2\text{H}_2\text{O}$  and  $\text{BiPO}_4$  materials has been measured for the first time using broad beam geometrical configuration, employing a 2" x 1" NaI (Tl) detector spectrometer system coupled to a 1k Multichannel Analyser. The measured  $\mu_m$  values, in  $\text{cm}^2/\text{g}$  for the above materials in the transmission range  $0.5 \geq T \geq 0.2$ , respectively are  $2.12 \pm 0.02$  (2.2);  $1.25 \pm 0.03$  (1.27);  $1.40 \pm 0.01$  (1.43);  $1.78 \pm 0.06$  (1.92);  $1.96 \pm 0.03$  (2.05);  $0.97 \pm 0.02$  (1.04) and  $1.52 \pm 0.03$  (1.6). The corresponding theoretical values estimated from mixture rule using tabulated values of Hubbell (Hubbell J.H. Int. J. Appl. Radiat. Isot, 33, 1268, 1982) are given in paranthesis. In this measurement the thickness of the absorbers are so chosen that it is equal to one mean free path of the incident gamma rays in that medium. The measured values were found to be 1.5% to 7% less than the theoretical values in the said transmission range. This may be attributed to the contribution of the scattered photons to the transmitted intensity. The measurement of  $\mu_m$  in broad beam geometry set up is important because of its practical applications in variety of fields like medicine, biology, industry, forestry etc. (Hubbell J.H. NIST J. Research - a private communication).

MEASUREMENT OF X-RAY MASS ATTENUATION COEFFICIENTS USING MIXED  
RADIATION EMITTERS.

B.R.KERUR, S.R.THONTADARYA AND B.HANUMAIAH

DEPARTMENT OF PHYSICS, KARNATAK UNIVERSITY,  
DHARWAD - 580 003, INDIA.

Abstract

A new and accurate method has been developed by us (B.R.Kerur et. al. 1991, accepted for publication in Appl. Radiat.Isot.) to determine the mass attenuation coefficient,  $\mu_m$ , of low energy pure X-rays in aluminum by employing a proportional counter spectrometer system coupled to a 1k Multichannel Analyser. The present report is an extension to verify the suitability of this method by employing  $^{57}\text{Co}$  and  $^{65}\text{Zn}$  radioisotopes which emit mixed radiations in addition to 6.460 keV and 8.118 keV X-rays. The mass attenuation coefficients of these X-rays in aluminum, copper, tantalum, nylon, teflon and lucite materials have been measured after applying various corrections to eliminate the contributions due to other radiations. The different methods of applying these corrections to extract accurate value of  $\mu_m$  for all the above materials have been discussed in detail. The measured values of  $\mu_m$  were compared with the corresponding theoretical values of Saloman et. al. (E.B.Saloman et. al. Atomic data and Nuclear data tables 38(1), 1, 1988) and a good agreement between them is obtained which confirms the extension of our earlier method to mixed radiation emitters.

NOTE ON NUCLEAR EXCITATION BY POSITRON  
ANNIHILATION WITH K-SHELL ELECTRONS

Toshifumi Saigusa

Department of Natural Sciences, Ryukoku University,  
Kyoto 612, Japan

and

Sakae Shimizu

Institute for Chemical Research, Kyoto University,  
Kyoto 606, Japan

Experimental data of nuclear excitation of  $^{115}\text{In}$  by positron annihilation with K-shell electrons are examined on the effective number of positrons from the source used.

The nuclear excitation by annihilation of fast positrons with a K-electron of an atom was first discussed by Present and Chen. The process was established experimentally by Shimizu's group and others, and the nearly same cross sections of the excitation of the isomer level of  $^{115}\text{In}$  were obtained from the experiments. From these results the similar cross sections were given for nuclear excitation of the 1078-keV excited level. But subsequent theoretical studies of the nuclear excitation all gave smaller cross sections than the experimental values. The discrepancy between experimental and theoretical values spreads 2 or 7 order of magnitude.

In the present work the result of reevaluation of the number of positrons concerning the nuclear excitation of the excited level is discussed.

MEASUREMENTS OF EXPERIMENTAL INCOHERENT SCATTERING FUNCTIONS:  
AN ANALYSIS OF THE DERIVED COHERENT AND INCOHERENT SCATTERING  
CROSS-SECTIONS IN SOME RARE EARTH ELEMENTS AT LOW PHOTON ENERGIES

DONEPUDI V RAO

DEPT. OF PHYSICS, SIR C R R AUTONOMOUS COLLEGE, ELURU-534.006  
ANDHRA PRADESH: INDIA

A B S T R A C T

Incoherent scattering functions have been experimentally determined for photon energies 84.4, 123.6, 145 and 320 keV. in the angular range  $10-130^\circ$  for the elements Sc, Y, La, Ce, Gd, Dy, Er, Yb, W, Pt and Pb with the use of Aluminium difference technique. For scattering angles of  $40^\circ$  or more the coherent scattering of photons were clearly separated from the incoherently scattered photons. On the other hand  $\theta < 40^\circ$  the incoherently and coherently scattered photons were not resolved. Theoretical differential coherent scattering cross-sections at low angles were calculated using relativistic  $F(X, Z)$  values tabulated by Hubbell and Øverø based on SCF Hartree-Fock wave functions. The incoherent contribution has been estimated by subtracting the theoretical coherent scattering cross-section from the observed total spectrum. The experimental values have been compared with those estimated on the basis of Non-relativistic Hartree-Fock wave functions to assess the influence of electron binding. The experimental  $S(X, Z)$  values are employed to deduce the differential incoherent scattering cross-sections in conjunction with the Klein-Nishina free electron values. The results show a clear deviation from the K-N values at low angles, the deviations are also seen to increase with increasing  $Z$ . As a by-product, coherent scattering cross-sections have been evaluated for Sc, Y, La, Ce, Pt and Pb. A comparison with the data of Hubbell et al reveals a good correspondence between theory and experiment for the non-relativistic incoherent scattering function but not for the non-relativistic atomic form factor.

Acknowledgements:- The experimental part of this work was completed at the Physics Department of IIT, Khargapur, India. I am grateful to Prof. Dr. John H Hubbell, NITS, Gaithersburg, MD USA, Prof. V.V. Rao, Department of Physics, Nuclear Physics Laboratory, IIT, Khargapur and Prof. S.C. Roy, Bose Institute, Calcutta for their interest and encouragement in the present work.

HEAVY NEUTRINO EMISSION IN THE EC DECAY OF  $^{71}\text{Ge}$ 

I. Žlimen, A. Ljubičić, S. Kaučić, T. Tustonić  
Ruđer Bošković Institute, P.O. Box 1016, 41000 Zagreb  
Croatia, Yugoslavia

B.A. Logan  
Ottawa Carleton Institute of Physics, University of Ottawa,  
Ottawa, Ontario K1N6N5, Canada

Several laboratories reported<sup>1-4</sup> the evidence for the existence of heavy 17 keV neutrino with the mixing probabilities in the range 0.8-1.6%. In our previous work<sup>4</sup> we have investigated the possibility of the existence of heavy neutrinos with masses in the range 10-40 keV. In this work the possibility of neutrinos having masses in the range of 40-100 keV was investigated by studying internal bremsstrahlung emitted by a  $^{71}\text{Ge}$  source. We have used HPGc detector and careful measurements of detector's efficiency and response function have been made. Results of the analyses of the data from this experiment will be presented.

## References

1. J.J. Simpson, Phys. Rev. Lett. 54 (1985) 1891.
2. A. Hime and J.J. Simpson, Phys. Rev. 39D (1989) 1837.
3. I. Žlimen et al., in: International Symposium on Solar Neutrino Detection with  $^{205}\text{Tl}$ , October 9-12, 1990. Dubrovnik, Croatia, Yugoslavia.
4. E.B. Norman et al., in: 14<sup>th</sup> Europhysics Conference on Nuclear Physics, Rare Nuclear Decays and Fundamental Processes, October 20-26, 1990. Bratislava, Czecho-Slovakia.

EFFECT OF C-K TRANSFER OF VACANCIES ON THE PRODUCTION OF  
L-SHELL FLUORESCENT X-RAYS

N. SINGH, R. MITTAL and K.L. ALLAWADHI  
Department of Physics, Punjabi University, Patiala-147002, India

The effect of the transfer of photon induced L-subshell vacancies due to Coster-Kronig transitions on the production of L-shell X-rays have been investigated. For this purpose, a computer program with its own database has been made to generate  $L_I$ ,  $L_{II}$ ,  $L_{III}$  and  $L_{IV}$  X-ray production cross-section for elements with  $Z \leq 40$ . The program outputs the cross section both by including and excluding the effect of the C-K transfer of vacancies among L-subshells. The database for L-subshell decay rates is based on the calculated values of Scofield [1]. For L-subshell fluorescence yields and Coster-Kronig transition probabilities, the values of both Krause [2] and Chen et al [3] have been included in the database and the choice between the two can be exercised. However, the data for L-subshell photo-ionization cross-sections have to be entered externally in the interactive mode either directly through the computer keyboard or through the prepared input file. The results of the calculations show that  $L_{IV}$  group of X-rays is the least affected while  $L_I$  and  $L_{II}$  groups of X-rays are the most affected by the C-K transfer of vacancies. The effect is found to vary from nearly 20% to 35% with the increase of Z number from 60 to 92.

REFERENCES

- 1 J.H. Scofield, At.Data Nucl. Data Tables, 14(1974)121.
- 2 M.O. Krause, J.Phys.Chem. Ref.data, 8(1979)307.
- 3 M.H. Chen, B. Crazemann and H. Mark, Phys.Rev. A24(1981)177.



K X-RAY SATELLITE SPECTRUM OF Ca EXCITED BY PHOTONS

V. RADHA KRISHNA MURTY

Department of Physics  
University of Botswana  
Private Bag 0022  
GABORONE  
Botswana

K. PARTHASARADHI

Department of Nuclear Physics  
Andhra University  
VISAKHAPATNAM 530 003, INDIA

N. V. R. MURTI and K. S. RAO

Centre for Studies in Resources Engineering  
Indian Institute of Technology  
BOMBAY 400 076, INDIA

ABSTRACT: K X-ray satellite spectrum of Ca excited by photons is studied using LiF(200) Plane Crystal Spectrometer. The satellite energies and their relative intensities are examined in the light of theoretical data and experimental data available by electron and proton excitations. The energies are found to be in general agreement with the available data. However,  $KL^1/KL^0$  intensity ratio is found to be in general agreement with that of electron excitation than that with proton excitation.

ORIENTATION PHENOMENA IN THE STOPPING  
POWER OF HEAVY CHARGED PARTICLES  
N.P.KALASHNIKOV. MOSCOW AUTOMOBILE-CONSTRUCTIVE INSTITUTE  
(THE ZIL FACTORY INSTITUTE)

Using the quantum-mechanical treatment we have developed the theory of the heavy charged particles stopping power due to the excitation and the ionization of the target atoms. For the inelastic amplitude we use the Glauber-Franco approximation. This approach permits to take into account simultaneously the elastic interaction of the projectiles with the potential of the target nucleus and inelastic interaction of the projectiles with the atomic electrons. The simultaneous treatment of the elastic and inelastic interactions leads to decrease the stopping power. This decreasing can be called the dynamic shadow effect. For very fast charged particles the shadow area becomes small and the inelastic scattering process is unaffected by the atomic nucleus. The developed theory of the energy dissipation permits to account for the experimentally observed violation of the Bragg additivity rule. The chemical binding in molecules leads to the spacial redistribution of the electron density. The abovementioned dynamic shadow effect on the inelastic interactions results in orientational phenomena in the stopping power. As an illustration we consider the energy dissipation of protons by the two-atomic molecule  $H_2$ . The orientational dependence of the stopping power is due to the covalent binding in the molecule  $H_2$ . If the two-atomic molecule axis is parallel to the velocity vector of the incident heavy charged particle, the mutual dynamic shadow effect leads to the additional decrease of the stopping power unlike the case of the perpendicular axis orientation with respect to the projectile velocity. Averaging the stopping power over the all axis orientations of  $H_2$  we obtain the 5% decreasing of the stopping power in respect of the Bragg rule.

DWBA CALCULATIONS OF THE PAIR PRODUCTION CROSS SECTION  
FOR 6.0 MeV PHOTONS

K. K. Sud

Department of Physics, University of Jodhpur,  
Jodhpur, India

C. W. Soto Vargas

Escuela de Fisica, Universidad de Costa Rica,  
San Jose, Costa Rica.

We present in this communication the results of the DWBA calculations of the electron-pair-production cross section by using the technique of Wright et al<sup>1</sup> and Sud and Sharma<sup>2</sup> for 6.0 MeV photon on  $Z = 1, 30, 50, 68, 82$  and  $92$ . The results are compared with the available semi-empirical formulas which are obtained by interpolating the low energy DWBA results and high energy approximate results as well as with the interpolated experimental data.

References:

1. L. E. Wright, K. K. Sud and D. W. Kosik  
Phys. Rev. C38 , 562 - 572 (1987 ).
2. K. K. Sud and D. K. Sharma  
Nucl. Inst. and Methods A255, 90 - 95 (1987).

## SOLID STATE EFFECTS ON X-RAY ATTENUATION CROSS SECTIONS MEASUREMENTS

By C. CUSATIS, Depto. de Física, UFPR, Brazil.

It is not a simple task to avoid, when possible, or to account for solid state effects like diffraction on good precision x-ray absorption cross-sections determination.

A method is proposed to avoid Bragg diffraction on x-ray attenuation measurements in perfect single crystals.

The method was used in measurements of attenuation cross sections for silicon and for six characteristic x-ray line wavelengths, with precision of approx. 0.1%. For those energies the absorption cross-sections and the imaginary parts of the atomic scattering factors were determined with the same precision.

Results will be presented and comments will be made to demonstrate the importance of solid state effects on x-ray interaction cross-sections measurements.

ELASTIC SCATTERING OF PHOTONS  
- LIMITS FOR THE FREE ATOM APPROXIMATION -

O.D.Gonçalves<sup>†</sup>, R.C.de Farias<sup>†</sup>, W.M.dos Santos<sup>†</sup>, J.Eichler<sup>‡</sup>

<sup>†</sup> Instituto de Física da UFRJ, P.B. 68528, 21941, Rio de Janeiro, Brazil

<sup>‡</sup> Technische Fachhochschule Berlin, Physiklabor, 1000 Berlin 65, Germany

We have measured elastic scattering cross sections of photons for momentum transfer in the range  $0.1\text{\AA}^{-1} \leq x \leq 2.2\text{\AA}^{-1}$  with  $E\gamma = 59.5$  and  $316$  Kev, in order to test the limits of momentum for which the scattering can be considered as being due to free atoms (Rayleigh Scattering). Polycrystal, liquid, perfect crystals and crystal powder samples were used as scatterers. The measurements with  $E\gamma = 316$  Kev were done in an angular range from  $0.5^\circ$  to  $10^\circ$  with an geometrical resolution of  $0.1^\circ$ . The measurements with  $E\gamma = 59.5$  Kev were performed between  $2^\circ$  and  $20^\circ$  and resolution of about  $1^\circ$ . Until now, most of the precise experimental data on elastic photon scattering have been done using similar molecular structures as scatterers. The present results allow the conclusion that high precise data ( $\Delta d\sigma/d\Omega \leq 2\%$ ) on elastic scattering of photons can be compared with Rayleigh scattering theories only for  $x > 1.\text{\AA}^{-1}$ .

# ELECTRON DEGRADATION AND YIELDS OF INITIAL PRODUCTS: SUBEXCITATION ELECTRONS IN H<sub>2</sub> AND D<sub>2</sub> GASES\*

Mineo Kimura, I. Krajcar-Bronić,<sup>‡</sup> and Mitio Inokuti  
Argonne National Laboratory, Argonne, IL 60439 U.S.A.  
<sup>‡</sup>Ruder Bošković Institute, Zagreb, Yugoslavia

The present study treats subexcitation electrons<sup>1</sup> in molecular hydrogen and focuses on isotope effects, i.e., differences between H<sub>2</sub> and D<sub>2</sub>. An elementary notion is the stopping cross section  $s(T)$ , the mean energy loss of an electron of kinetic energy  $T$  per unit pathlength in a medium of unit molecular density. This quantity is evaluated as  $s(T) = \sum_j E_j \sigma_j(T)$ , where  $\sigma_j(T)$  is the cross section for electron collisions of kind  $j$  that results in energy transfer  $E_j$ . For subexcitation electrons,  $j$  refers to elastic scattering, rotational excitation, or vibrational excitation. According to the Born approximation, the stopping cross sections for vibrational and rotational excitations in D<sub>2</sub> are half of their counterparts. The contribution of elastic scattering in D<sub>2</sub> is also nearly half of that in H<sub>2</sub>. Hence, over the entire contribution to  $s(T)$ , one could expect the isotope effect to be about a factor of two for various physical quantities relevant to electron degradation.

We have conducted a comparative study of subexcitation electrons in H<sub>2</sub> and D<sub>2</sub> below 8 eV by using the Spencer-Fano (SF) theory<sup>1</sup> and its simplified version, the continuous-slowing-down approximation (CSDA).<sup>1</sup>

Our detailed analysis shows that the isotope effect is 1.7 at energies where no significant differences occur in the cross sections for the two gases. The cross sections become increasingly different at very low energies. Hence, the isotope effect is very pronounced below 0.1 eV.

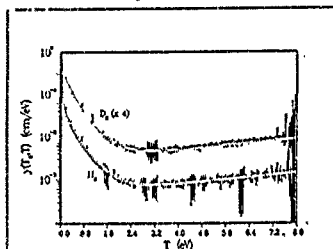


Figure 1. Degradation spectra obtained from the SF and CSDA for both H<sub>2</sub> and D<sub>2</sub> gases with initial electron energy 8 eV.

The submitted manuscript has been authored by a contractor of the U.S. Government under contract no. W-31-109-ENG-38. Accordingly, the U.S. Government retains a nonexclusive, royalty-free license to publish or reproduce the published form of this contribution, or allow others to do so, for U.S. Government purposes.

## Reference

1. M. Kimura and M. Inokuti, Comments At. Mol. Phys. 24, 269 (1990).

\*Work supported in part by the U.S. Department of Energy, Assistant Secretary for Energy Research, Office of Health and Environmental Research, under Contract W-31-109-Eng-38, and by the U.S./Yugoslavia Cooperative Research Program of the National Science Foundation.

RADIATIVE ORBITAL ELECTRON CAPTURE IN  $^{113}\text{Sn}$ 

Sr. Little Flower, B.R.S. Babu and K. Neelakandan,  
Department of Physics, University of Calicut, Calicut, India.

AND

R.N.Mukherjee and B.B.Baliga,  
Saha Institute of Nuclear Physics, Calcutta, India.

## ABSTRACT

Innerbremsstrahlung (IB) accompanying the orbital electron capture transition in  $^{113}\text{Sn}$  was measured using a HPGe detector. Correction for the Pileup due to the source dependent 392keV gamma was applied. The measured pulse height distribution of IB photons was corrected for detector response following the procedure of Liden and Starfelt. The decay energy of  $^{113}\text{Sn}$  is determined to be  $(642.9 \pm 5.0)\text{keV}$  which is in good agreement with the latest mass table value<sup>1</sup>.

The experimental distribution closely agrees with the theoretical 1S-intensity distribution obtained using Intemann<sup>2</sup> theory. Morrison Schiff<sup>3</sup> (MS) theory does not consider the effect of the Coulomb field of the nucleus. Most of experimental transition energy determinations have been made by constructing a Jauch<sup>4</sup> plot. The accuracy of this procedure entirely depends on how closely the investigated spectrum is approximated by MS theory. Eventhough for transitions  $k \gg Z\alpha$ , Jauch plot is expected to give sufficiently accurate results, IB intensities are expected to experience significant reduction in the medium and heavy Z nuclei<sup>5</sup>. Our results in the present investigation precisely display this characteristic. Also our results show that the contribution from 2S, 2P and 3P capture intensities is negligible. The results will be discussed.

## References:

1. A.H. Wapstra and G. Audi, Nucl. Phys. A432, 44 (1985)
2. R.L.Intemann, Phys. Rev. C3, 1 (1971)
3. P.Morrison and L.I.Schiff, Phys. Rev. 58, 24 (1940)
4. J.M.Jauch, ORNL Report No.ORNL-1102 (1951)
5. W. Bambynek et al., Rev. Mod. Phys. 49, 77 (1977)

# THERMOLUMINESCENT PROPERTIES AND DEFECT STABILITY IN SILVER DOPED CRYSTALS

A M Mdebuka

Department of Physics, University of Port Hare, Alice, South Africa

Thermoluminescence in room temperature X-irradiated  $\text{KCl} : \text{Ag}$  (14 ppm) crystals has been examined.  $\text{KCl} : \text{Harshaw}$  (nominal pure) crystals are also used for comparison. Stability of defects and kinetics of recombination processes occurring during thermoluminescence are investigated with a closer look at impurity effects. X-irradiations were performed at increasing doses (25 kV and 20 mA, 35 kV and 30 mA, 45 kV and 40 mA) for 5 hours at each setting. Results indicate that the stability of defects in Ag-doped samples increases with dose. General-order kinetics methods indicate that recombination processes follow the first-order kinetics since the probability of retrapping (0.01) is far less than that of recombination (0.99). Using several first-order kinetics methods, the frequency factor seem to be in the region associated with escape frequency of electrons ( $10^9 - 10^{12} \text{ s}^{-1}$ ).



## THEORETICAL UPPER AND LOWER LIMITS TO EXPERIMENTAL PHOTOEFFECT CROSS SECTIONS OF ATOMS

L. Gerward

Laboratory of Applied Physics, Technical University of Denmark, DK-2800 Lyngby,  
Denmark

Rigorous calculations of photoeffect cross sections have been reported, among others, by Scofield<sup>1</sup>, who uses the Hartree-Slater atomic model, but provides factors for individual subshells to renormalise his results to the Hartree-Fock model. The renormalisation procedure has been assumed to improve the results for atoms with atomic number less than 55. Recently, Saloman and Hubbell<sup>2</sup> have suggested that the Scofield values without renormalisation are in better agreement with experiment than the renormalised values in the photon energy range 0.1-1 keV.

In the present work, photoeffect cross sections in the X-ray range 5-25 keV have been derived from experimental mass attenuation coefficients, measured by the author and others. The data are compared with theoretical cross sections calculated by Scofield. Systematic trends suggest that the Scofield values with and without the Hartree-Slater to Hartree-Fock renormalisation can be used as lower and upper limits to the experimental photoeffect cross sections. In other words, the renormalised and unrenormalised Scofield cross sections seem to satisfy the inequality

$$\sigma_{\text{Sc,renorm}} < \sigma_{\text{experiment}} < \sigma_{\text{Sc,unrenorm}}$$

The need for accurate experimental values of photoeffect cross sections is stressed in order to make meaningful comparisons between theory and experiment.

### References

1. J.H. Scofield, Lawrence Livermore Nat. Laboratory Report UCRL 51326 (1973).
2. E.B. Saloman and J.H. Hubbell, Nucl. Instrum. Methods A 255 (1987) 38.

DOUBLE  $\beta^+$ -DECAY,  $e^-e^+$  CONVERSION AND DOUBLE  $e^-$  CAPTURE  
PROCESSES: UPDATE STATUS OF THE THEORY AND EXPERIMENT

V.M. Novikov

Institute for Nuclear Research of the USSR Academy of Sciences,  
Moscow, USSR

Many experiments on search for double beta decay ( $\beta\beta$ ) were performed. Alternative processes of double  $\beta^+$ -decay ( $\beta^+\beta^+$ ),  $e^-e^+$  conversion and double electron capture (double EC) are supposed to have much longer predicted lifetimes. However, in contrast with  $\beta\beta$  events,  $\beta^+\beta^+$  and  $e^-e^+$  ones have more intricate structure, and therefore, much better background suppression is achievable. For some cases experimental sensitivity is quite competitive with that one in  $\beta\beta$  experiments.

The present paper reviews present experimental and theoretical situation in this field. All update known experimental results and theoretical predictions of lifetimes for different isotopes are listed. The  $^{78}\text{Kr}$  experiment started this year is discussed rather in detail. Some new possibilities for different isotopes are considered.

# THEORETICAL STUDY OF INNER SHELL PHOTOABSORPTION SPECTRA OF HCl AND HF.

V.A.Yavna, B.M.Lagutin, V.A.Popov, S.A.Yavna

Rostov Railway Engineers Institute, Rostov-on-Don, 344017,  
USSR.

Influence of multi-electron correlations and nuclear oscillations on cross sections redistribution in  $L_{2,3}$  - photoabsorption spectrum of HCl and K-spectra of HF and HCl has been studied. The following correlations have been taken into account: monopole rearrangement of electron shells /1/, correlation rarefication of outer electron shells' density /2/, vacuum correlations /3/. In calculation of photoionization cross sections and oscillator strengths, dependence of vertical dipole transition operator matrix element on nuclear coordinate has been considered. In Fig.1 theoretical HCl K-photoabsorption spectrum is compared with the experiment.

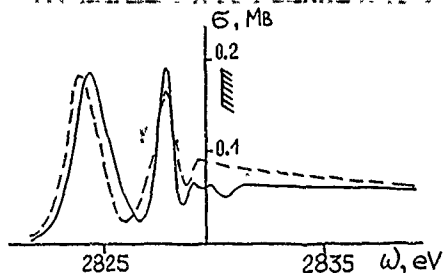


Fig.1. (---)-ex-  
periment /4/;  
(—)- theory.  
The absolute val-  
ues of cross sec-  
tions are theoret-  
ical ones.

## References

- /1/ Sukhorukov V.L. e.a.// Opt.Spectr. (USSR)-1979,v.47
- /2/ Yavna V.A. e.a.//Opt.Spectr.(USSR)-1985,v.61,p.922.
- /3/ Hopersky A.N. e.a.//Opt.Spectr.(USSR)-1987,v.63,p.204.
- /4/ Bodeur S. e.a.// 15-th int. conf. on X-Ray and Inner-  
Shell Proc.,Knoxville,USA,July,1990,p.CO3

# INFLUENCE OF AUTOIONIZATION TYPE CORRELATIONS ON NEAR EDGE INNER SHELL ATOMIC PHOTOABSORPTION

A.N.Hopersky, V.A.Yavna

Rostov Railway Engineers Institute, Chair of Physics  
344017 Rostov-on-Don, USSR

Within a multi-configurational approximation, a method to include the effect of autoionization (AI) type correlations on inner shell atomic near edge photoabsorption has been developed. The corresponding SCF equation for the photoelectron /1/ differs formally from that of Hartree-Fock approximation by presence of the additional potential  $D(\omega; r)$  dependent on the photon's energy  $\omega$  and AI channel's structure.

This work's theory has been applied to calculate the cross section of giant  $M_{23}$ -photoabsorption resonance in atomic Mn /2/. Inclusion of  $D(\omega; r)$  has led to the increase of the excited 3d-state's mean radius (the effect of correlation pressing out of 3d state by a "slow" 2f-electron of  $3d^4(1S)2f, 6P$ -AI channel) and, therefore to the increase of theoretical value of photoabsorption resonance energy (Fig.1).

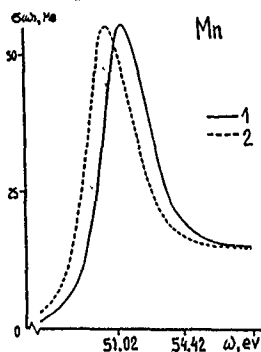


Fig.1. Mn  $M_{23}$ -photoabsorption cross section 1 -including and 2 - not including the potential  $D(\omega; r)$ .

3p level's spin-orbital split is neglected.

$$\Gamma_{3p} = 3,0 \text{ eV} / 2/.$$

## REFERENCES:

- /1/ Hopersky A.N., Yavna V.A. //Opt.Spectr.(USSR), 1990, V.69, No 3, P.523-526.
- /2/ Bruhn R., Sonntag B., Wolff H.W. //Phys.Lett., 1978, V. 69A, No 1, P.9-11.

## XANES OF HEAVY ATOMS' INNER SHELLS:

 $\text{KN}_{23}$  -PHOTOABSORPTION OF Kr

A.N.Hopersky, V.L.Sukhorukov, I.D.Petrov

Rostov Railway Engineers Institute, Chair of Physics  
344017 Rostov-on-Don, USSR

This paper's aim is to generalize the theory and method of calculating XANES developed earlier for light atoms /1/ ( $\text{KL}_{23}$  -Ne,  $\text{KM}_1$  -Na,  $\text{KN}_{23}$  -Ar), for the case of heavy atoms. As an example, the  $\text{KN}_{23}$  -photoabsorption spectrum of the atomic Kr has been calculated within the K-shell threshold region (Fig.1).

The main multi-electron effects, which being included, give 20% agreement with the experiment /2/ are: monopole rearrangement of electron shells in the field of K- and N-vacancies; multiplet splitting of the configurations  $1s^{-1}4p^{-1}n_1pn_2p-n_3s(d)n_4d$  excitations; opening of channels of  $1s4p$ -np $\mathcal{E}$ p single and  $1s4p$ - $\mathcal{E}p\mathcal{E}p$  double ionizations.

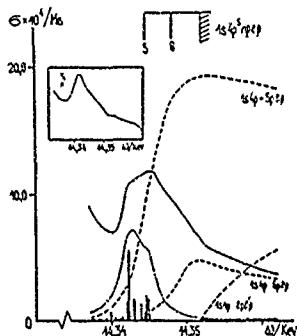


Fig.1. K -XANES of atomic Kr:

— this work's theory;  
 --- double photoexcitation spectrum;  
 - - - - excitation/ionization and double ionization channels.

Inserted is the experiment of ref. /2/.  $\omega$  is the absorbed photon's energy. The width  $\Gamma_{1s}^{\text{Kr}} = 2,69$  eV.

## REFERENCES:

- /1/ Sukhorukov V.L., Hopersky A.N., Petrov I.D., Yavna V.A., Demokhin V.F. // J. Physique. - 1987, V.48, No 10, P.1677-1683.  
 /2/ Bernieri E., Burattini E. // Phys. Rev. A. - 1987, V.35, No 8, P.3322-3326.

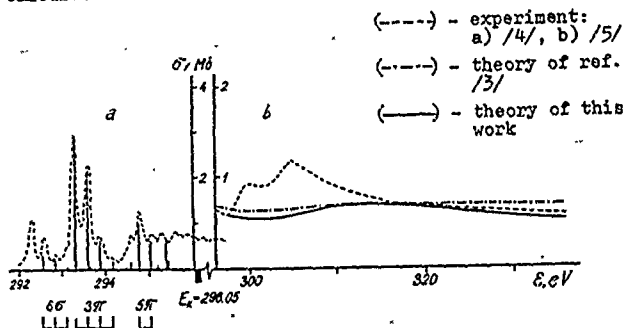
## MULTI-ELECTRON EFFECTS IN XANES OF SIMPLE MOLECULES

V.A.Yavna, A.M.Nadolinsky, V.F.Demekhin

Rostov Railway Engineers Institute, Chair of Physics  
344017 Rostov-on-Don, USSR

The spectra of  $16\sigma$  shell photoabsorption in CO and  $N_2$  and that of  $26\sigma$  shell in CO have been calculated considering monopole rearrangement of electron shells in the field of a vacancy, correlational rarefaction of valence shell density of final state /1/ and vacuum correlations /2/.

Calculated  $26\sigma$  CO spectrum is presented in the fig.



In the pre-edge region the amplitudes of Lorentzian curves are presented. To make the comparison with the experiment easier, the  $26\sigma - 3\pi$ ,  $6\sigma$  lines are presented with vibronic series with the intensities taken from the experiment /6/.

## References

- /1/ Yavna V.A. et al //Opt. & Spectr.(USSR)-1985, V.61, P.922.
- /2/ Hopersky A.N. et al //Opt. & Spectr.(USSR)-1987, V.63, P.204.
- /3/ Yavna V.A. et al //Opt. & Spectr.(USSR)-1990, V.69, P.1278.
- /4/ Show D.A. et al //J.Phys.B - 1984, V.17, P.2091.
- /5/ Kay R.E. et al //J.Phys.B - 1977, V.10, P.2513.
- /6/ Tronc M. et al //J.Phys.B - 1979, V.12, P.137.

I-49

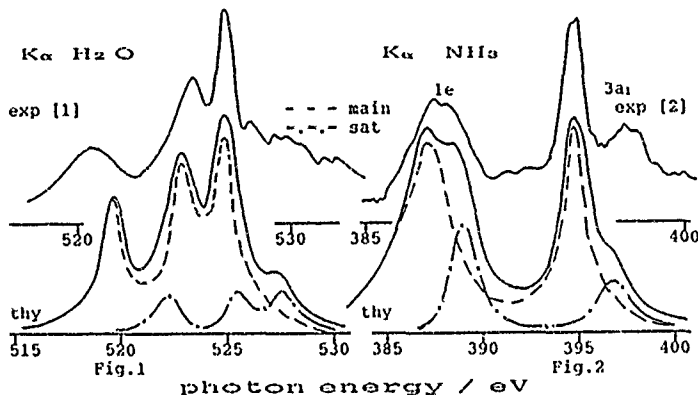
# Theoretical study of K $\alpha$ -omission in hydride molecules of the second row atoms.

Lagutin B.M., Vasilieva M.E., Sukhorukov V.L., Demekhina L.A.  
Rostov Railway Engineers Institute, 344017 Rostov-on-Don, USSR

K $\alpha$ -spectra of Ne-like molecules CH $_4$ , NH $_3$ , H $_2$ O, HF are calculated. In calculation both single-centre and MO LCAO methods have been used. Electric dipole is-MO transitions of both main configuration and that with an additional outer MO vacancy were considered. The probability of the appearance of additional vacancy was calculated within a sudden excitation theory.

A good agreement of the results of the two methods is obtained when extended MO LCAO basis and multi-channel self consistent single-centre method were used.

It is obtained that taking the multiple ionization satellites into account allows one to explain several features and to obtain generally good agreement of theory and experiment (fig.1). However, in case of NH $_3$  molecule (fig.2) there is still a disagreement of theory and experiment which is that  $(I_e/I_{3a_1})_{\text{theor}} = 1.7$  while  $(I_e/I_{3a_1})_{\text{exper}} = 1.1$ . There is also some disagreement in the shape of spectral lines (experimental width of 1e line is twice as great as that of 3a $_1$  line). It is possible that this discrepancy is caused by the neglect of vibronic effects. This supposition is based on the estimation of vibronic effects influence on the K $\alpha$ -spectrum of CH $_4$ .



## References:

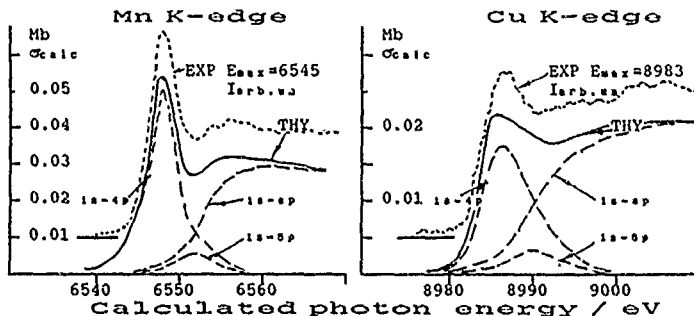
1. J.Nordgren J.Phys.Colloque, suppl., No.12, 1987, tome 48.
2. J.Nordgren e.a. J.Phys.B: At.Mol.Phys., v.9, No.2,1976, p.295.

# Theoretical study of near edge K-photoabsorption of Mn and Cu atoms.

Sukhorukov V.L., Hopersky A.N., Petrov I.D. and Lagutin B.M.  
Rostov Railway Engineers Institute, 344017 Rostov-on-Don, USSR

Effects of multielectron and relativistic phenomena on near edge K-photoabsorption spectra of Mn and Cu is studied. Calculated absolute values of multiplet component energies, their intensities for the transitions  $1s-np$  in  $Mn([Ar]3d^5 4s^2)$  and  $Cu([Ar]3d^1 4s^1)$ , and photoabsorption cross sections (Fig.1) are predicted.

It has been obtained that the main effect affecting the theoretical values of components intensities is a monopole rearrangement of electron shells (MRES). Calculating multiplets centres of gravities and ionization thresholds, one has to include both MRES and relativistic effects. Small value of  $3d-np$  Coulomb interaction as compared with that for  $4s-np$  account for the fact that the first white line in the experimental Mn K-spectrum [1] is splitted less then it is in Cu K-spectrum. Taking into account the spin orbital splitting of  $3d(Mn)$ - and  $4p(Mn,Cu)$ -electrons leads to insignificant changes in the spectra.



## References:

1. U.Arpa, G.Materlik, M.Meyer and B.Sonntag, 1990.  
Materials of International XAFSVI Conference (private communication)



# Near edge subvalence shells photoionization of atoms and simple molecules.

Sukhorukov V.L., Petrov I.D., Lavrent'ev S.V. and Lagutin B.M.  
Rostov Railway Engineers Institute, 344017 Rostov-on-Don, USSR

We review of the modern state of the theory of photon absorption by subvalence atomic and simple molecules' shells. For the first time the anomalous behaviour of cross section dependence near subvalence shells photoionization thresholds was predicted theoretically in ref [1]. The prediction was based on calculation of Ar 3s-shell photoionization taking into account the inter-shell correlations, described by mixing of 3s- $\epsilon p$  and 3p- $\epsilon d$  ionization channels by 3p $\epsilon p$ -3s $\epsilon d$  excitations. Later this prediction was supported experimentally [2].

The accuratization of the theory was made in ref.[3] where by calculating Xe 5s-photoionization it had been shown that it is important to include both inter-shell correlations and dipole polarization of 5p-shell when 5s-vacancy appears, the latter being described by 5p $\epsilon p$ -5s $\epsilon d$  excitations. Taking these excitations into account allows one not only to calculate os. photoionization cross section dependence on energy more accurately, but also it accounts for the complex structure of X-ray photoelectron spectrum of 5s-shell and its dependence on the energy of the exciting radiation. One should note that the calculation considering atomic ionization through np- $\epsilon d$  channel followed by excitations of 3p $\epsilon d$ -nln' $\epsilon$  type in Ar predicted that 3p $\epsilon$ nln' $\epsilon$ 1' states photoionization cross sections are comparable with those of single ionizations. Direct measurements of the mentioned processes' cross sections are absent up to now, however, several experiments [4,5] showed that 3p $\epsilon$ nln' $\epsilon$ 1' states' excitation cross sections can be quite large. There is no calculations yet on these states' excitation cross sections.

## References:

1. Amusia M.Ya., Ivanov V.K., Cherepkov N.A. and Chernysheva L.V. Phys.Lett., 1972, v.A40, p.361-362.
2. Samson J.A.R. and Gardner J.L. Phys.Rev.Lett., 1974, v.33, p.671-673.
3. Sukhorukov V.L., Petrov I.D. and Demekhin V.F. Opt.Spectr.(Sov.), 1985, v.58, p.1365-1366.
4. Hall R.I., Avaldi L., Dawber G., Rutter P.M., MacDonald M.A. and King J.C. J.Phys.B, 1989, v.22, p.3205-3216.
5. K.-H. Scharfner, P.Lenz, B.Mobus, H.Schmoranzner and M.Wildberger Phys.Lett.A, 1988, v.128, No.6,7, p.374-377.

## MOLECULAR SHADOW LEVELS PHOTOIONIZATION CROSS

## SECTIONS

S.V.Lavrentiev, I.D.Petrov, V.L.Sukhorukov

Rostov Railway Engineers Institute,  
Rostov-on-Don, 344017, USSR

It was shown in ref.[1] that during the appearance of a subvalence shell vacancy in atoms and  $AH_n$ -type molecules (A are the 3rd row atoms), the many electron interaction called in ref. [3] a dynamical dipole polarization of electron shells (DPES) gives rise to a complex multiplet structure containing both main level corresponding to a certain subvalence AO or MO and so called shadow levels.

On the other hand, in photoionization of atomic and molecular outer shells essential are the correlations included in RPAE [2].

In this work in calculation of main and shadow levels photoionization cross sections in  $SiH_4$ ,  $PH_3$ ,  $H_2S$  and  $HCl$  near ionization thresholds both intra- and intershell RPAE correlations were taken into account.

It is shown that DPES effect on photoionization of molecules is stronger than it is on that of an isoelectronic Ar atom because of multi-atomic potential. Shadow levels cross sections values are, at certain energies, greater than the main levels values. This must be most clearly observed in molecular photoelectron spectra.

## References:

1. V.L.Sukhorukov, V.F.Demekhin-Coord.Chem. (USSR), 9(1983)158
2. M.Ya.Amusia, N.A.Cherepkov-Czech Stud.in Atom.Phys., 5(1975)47
3. V.L.Sukhorukov, I.D.Petrov-Izv.Acad.Sci.USSR., 49(1985)1463

## Monte Carlo Simulation of the Scattering Contributions to the XRF Line

Héctor Jorge Sánchez \* and Renzo Sartori \*

Facultad de Matemática, Astronomía y Física,  
Universidad Nacional de Córdoba,  
Laprida 854 CP 5000 Córdoba  
ARGENTINA

### Abstract

A Monte Carlo program to simulate the scattering contributions to the fluorescent line was developed.

Simulations were carried out on three samples ( $Z=14, 28, 40$ ) in several geometrical situations (incident and take off directions of the photons). The results show that the scattering effects do not exceed the 4 % for the analyzed elements. A good agreement between normal-incidence simulations and theoretical results was found.

The vanishing of multiple interactions inside the sample, when the propagation plane approximates to  $\pi/2$ , was also verified.

---

\*Fellowship of CONICOR, Córdoba, ARGENTINA

THE ROLE OF CORRELATION EFFECT IN PROCESSES WITH  
PARTICIPATION OF EXCITATIONS OF SOLID'S ELECTRON SUBSYSTEM.

Boris V. Andreev

*Institute of Physical Chemistry of the Academy of Sciences  
of the USSR, Leninsky prospekt 31, Moscow 117915, USSR.*

In the report there are considered processes which proceed via (are stimulated by) excitations of electron subsystem under radiation (photo-) influence on solid. As it is known, introduction of effective interaction between excitations diminishes essentially their lifetime, what should affect processes with the participation of excitations. Under conditions of such an effective interaction strong dependence of excitations' lifetime upon their concentration is revealed as a specific dose-rate effect. The so-called high correlated solids (HCS) are predisposed to manifestation of such dependences under radiation (photo-) influence on them.

The specific dose-rate effect in HCS is discussed in the report on the example of soft-mode crystals [1], Mott dielectrics [2] and systems with local electron pairs [3].

1. B.V.Andreev et al. *J.Phys.:Condens.Matter*, 1 (1989) 3359
2. B.V.Andreev *Conf. on Quantum Chemistry of Solids*, 26th - 30th Nov. 1990, Riga, Abstr.book, P.287.
3. B.V.Andreev et al. *Phys.Lett.*, 152A (1991) 293.

## SCATTERING OF RADIATION BY ELECTRONS IN THE COULOMB FIELD

Viorica Florescu

Faculty of Physics, University of Bucharest, P.O.Box MG-11  
R-76900, Bucharest - Măgurele, ROMANIA

We study the process of radiation scattering by electrons which evolve in the presence of a Coulomb field. The radiation field is described by a monochromatic plane wave of frequency  $\omega$  and polarization  $\vec{s}$ . We use perturbation theory for the field-electron interaction, but describe the electrons by appropriate Coulomb waves of given energies and asymptotic momenta. The analytic equations we use are similar to those describing two-photon absorption by free electrons or two-photon bremsstrahlung<sup>1,2</sup>.

In the nonrelativistic description adopted here, the inelastic scattering ( $\omega' \neq \omega$ ,  $\omega'$  the frequency of the scattered photon), like multiple absorption or emission, is possible only due to the presence of the Coulomb field. If  $\omega' > \omega$ , and  $h\omega' > E$ , resonances appear at frequencies satisfying  $h\omega' = E + |E_n|$ , where  $E$  is the incident electron energy and  $E_n$  a Bohr energy.

As remarked before<sup>3</sup>, in the elastic limit ( $\omega' = \omega$ ) the existing equations present some difficulties that we are able to handle.

We intend to present our results for the scattering cross-sections and compare with existing results obtained in nonperturbative treatments<sup>4,5</sup>.

1. H. Gavrilă, A. Maquet and V. Vénard, Phys. Rev. A 32, 2537 (1985); and Phys. Rev. A 42, 236 (1990).
2. V. Florescu and V. Džamo, Phys. Lett. A 112, 73 (1986).
3. A. Florescu and V. Florescu, Abstracts of ICOMP V, p. 133, Paris, 1990.
4. L. Dimou and F. H. M. Faisal, Phys. Rev. Lett. 59, 872 (1987).
5. A. Franz, H. Klar, J. T. Broad and J. S. Briggs, J. Opt. Am. Soc. B 7, 545 (1990).

## RELATIVISTIC S-MATRIX CALCULATIONS OF WHOLE ATOM COMPTON SCATTERING

P. M. Bergstrom, Jr.,<sup>1</sup> T. Suric,<sup>1,2</sup> K. Pisk,<sup>2</sup> and R. H. Pratt<sup>1</sup>

<sup>1</sup>Department of Physics and Astronomy, University of Pittsburgh,  
Pittsburgh, PA 15260 USA

<sup>2</sup>Ruder Boskovic Institute, 41000 Zagreb, Yugoslavia

We have recently reported development of a computer code to calculate inelastic (Compton) scattering of photons by bound atomic electrons in second order external field quantum electrodynamics.<sup>1</sup> Some results obtained for scattering from inner shell electrons have been presented at this meeting.<sup>2</sup> We report here exploratory cases of calculations for the scattering of photons from whole atoms (all shells) above the K shell binding energy.

Traditional theoretical treatments of Compton scattering from bound atomic electrons start from the nonrelativistic Hamiltonian

$$H_{\text{int}} = \frac{1}{2} e^2 A^2 - e \vec{p} \cdot \vec{A}$$

Most commonly used approximations only use the first or 'A<sup>2</sup>' term. Among these approximations are the form factor<sup>3</sup> and impulse<sup>4</sup> approximations, for the doubly differential cross section, and the incoherent scattering function,<sup>5</sup> for the cross section differential in scattered photon angle. Simple expressions for Compton profiles in terms of the doubly differential cross section follow in the impulse approximation. The second ( $\vec{p} \cdot \vec{A}$ ) term has been explored by Gavrilu and coworkers<sup>6</sup> for K and L shell electrons of hydrogen-like systems at low energy. Interesting spectral features resulting from this term include the infrared divergence, which is a general aspect of the process, and resonances, which occur in scattering from most many electron atoms.

We present results by subshell for the doubly differential cross section for the scattering of photons from carbon and aluminum. We compare with approximate theories.<sup>3,4,6</sup> We sum over electrons to obtain whole atom profiles. We select an appropriate cutoff and integrate over scattered photon energies, comparing with the incoherent scattering function.

1. T. Suric, P. M. Bergstrom, Jr., K. Pisk, R. H. Pratt, University of Pittsburgh Report 421, submitted for publication (1991).

2. T. Suric, Invited talk at this meeting.

3. F. Schnaidt, *Ann. Phys.* 21, 89 (1934).

4. P. Eisenberger and P. M. Platzmann, *Phys. Rev.* A2, 415 (1970).

5. J. H. Hubbell, Wm. J. Veigele, E. A. Briggs, R. T. Brown, D. T. Cromer and R. J. Howerton, *J. Phys. and Chem. Ref. Data* 4, 471 (1975).

6. See for example M. Gavrilu, *Phys. Rev.* A6, 1348, 1360 (1972).

A LIMIT ON ELECTRON-ANTINEUTRINO REST MASS FROM AN  
EXPERIMENTAL STUDY OF EXTERNAL BREMSSTRAHLUNG  
OF TRITIUM BETA RAYS

K. Kovačević

Ruder Bošković Institute, Zagreb, Croatia, Yugoslavia

I. Sorić and J. Tudorić-Ghemo

University of Split, Split, Croatia, Yugoslavia

The dependence of the ratio of theoretical predictions to the measured yields in the bremsstrahlung spectrum from tritium decay on the electron-antineutrino rest mass has been analyzed. The external bremsstrahlung spectrum from  $\beta$ -decay of  $^3\text{H}$  absorbed in Ti was measured by a pin-photodiode detector coupled with an improved low-noise preamplifier. The relative detector efficiency and the detector response function were determined by measuring the X-ray spectrum from a  $^{241}\text{Am}$  source. Theoretical prediction for the bremsstrahlung energy spectrum was obtained by a three-fold convolution of the electron energy distribution, the bremsstrahlung energy distribution for monoenergetic incident electrons and the detector response function. A preliminary upper limit of 50 eV for the electron-antineutrino rest mass was derived.

**Session II**  
**RADIATION SOURCES AND DETECTORS**



# ON MECHANISMS OF THE SUBTHRESHOLD DEFECT PRODUCTION IN COVALENT SEMICONDUCTORS

M.S. Yunusov, S. Abdurackmanova, M. Zaikovskaya, B. Oksengendler  
Institute of Nuclear Physics Academie Nauk Uzbekian SSR

Subthreshold effects in p- and n-Si induced by X-irradiation with maximum energy 50 keV in the temperature range 80-400 K have been investigated. The influence of X- flux density ( $I$ ), the position of a Fermi level ( $E_F$ ) and quasi - level ( $E_F^i$ ), the impurity concentration ( $N_{imp}$ ) on the production of close Frenkel pairs (CFP) and their annealing kinetics under minority carrier injection conditions were studied.

The investigated effects give new information on the mechanisms of subthreshold defect production (SDP) and the injection enhancement associated with the participation of CFP, doping impurities, and biography unhomogeneous.

Under low - temperature X- irradiation were generated CFP. CFP are completely annealed with two channels (either of annihilate or of decay) released upon capture of injected minority carriers at the localized level. The annealing cannels depend on  $E_F^i$ . The dependence of CFP concentration ( $N_{CFP}$ ) on  $N_{imp}$  is non-linear ( $N_{CFP} \sim N_{imp}^k$ ,  $k$  can be varied from 0,42 to 0,98) under X - irradiation with flux density from  $5 \cdot 10^{12}$  to  $1,8 \cdot 10^{14}$  quanta. $\text{cm}^{-2}\text{s}^{-1}$ .

The initial mechanism of SDP is "Coulomb explosion" with cross - section  $\sigma_d \approx 10^{-27}$  to  $10^{-26}$   $\text{cm}^2$  in p - Si. The role of an impurity in this effect depends on its electron structure and migration properties. When CFP is generated in the region of the shallow local electronic state orbital this shallow level is shifted and we can see the spectrum of the perturbed local states. The cross - section of the shallow level disappearance is

$$\sigma_{sh} = \sigma_d R_+^3 N_{imp},$$

where  $R_+$  - is the shallow electronic orbital radius. The theoretical evaluation of  $\sigma_{sh}$  in doped p-Si at  $N_{imp} > 10^{17}$   $\text{cm}^{-3}$  gives  $\sigma_{sh} \approx 10^{-24}$   $\text{cm}^2$ .

# EFFECT OF HEAVY ION BOMBARDMENT ON THERMOLUMINESCENCE AND PHOTOTRANSFER THERMOLUMINESCENCE IN NATURAL QUARTZ

M.Fathony<sup>\*1</sup>, S.A Durrani and Y.M Amin<sup>\*\*</sup>

School of Physics and Space Research  
University of Birmingham  
Birmingham B15 2TT  
England

## Abstract

The response and sensitivity of thermoluminescence (TL) and phototransfer thermoluminescence (PTTL) in natural quartz after high-energy-heavy-ion irradiation have been investigated. Natural quartz samples were irradiated by  $^{136}\text{Xe}$  ions of energy 11.56 MeV/nucleon at GSI, Darmstadt, Germany. It was found that the TL response increases linearly with dose between  $10^5$  and  $10^8$  ion per  $\text{cm}^2$ , whereas beyond this point the response seems to be supralinear. PTTL response, carried out with a UV-light source of wavelength 254 nm, was found to be linear with the dose of  $^{136}\text{Xe}$  ions in the range  $10^5$  -  $10^{11}$  ion per  $\text{cm}^2$ . The sensitivity of TL and PTTL in quartz after a small test-dose of  $\beta$  irradiation, after annealing out the ion dose at  $500^\circ\text{C}$ , has also been investigated. The TL sensitivity was found to be enhanced by a factor of  $\sim 9.5$  with a Xe dose of  $10^{11}$  Xe ion per  $\text{cm}^2$ , whereas the PTTL sensitivity was enhanced by a factor of  $\sim 5$  at  $10^{11}$  Xe ion per  $\text{cm}^2$ . Thus quartz sample, pre-dosed by heavy ion irradiation, is seen to display an increase in both its TL and PTTL sensitivity which is a desirable feature for its use as a radiation detector.

---

<sup>1</sup>On leave from:

\*National Atomic Energy Agency of Indonesia (Batan),  
PSPKR Batan, P.O.Box 43 Kby.L., Jakarta Selatan,  
Indonesia.

\*\*Department of Physics, University of Malaya,  
59100 Kuala Lumpur, Malaysia

## EFFECT OF THERMAL-DRAINING TEMPERATURE ON THE BEHAVIOUR OF PHOTOTRANSFER THERMOLUMINESCENCE IN NATURAL QUARTZ

M.Fathony<sup>\*1</sup>, S.A Durrani and C Antipas  
School of Physics and Space Research  
University of Birmingham  
Birmingham B15 2TT  
England

### Abstract

The effect of the thermal-draining temperature on the behaviour of phototransfer thermoluminescence (PTTL) in natural quartz, following irradiation with  $\gamma$ -rays, has been investigated. Powdered quartz samples were irradiated with 1 kGy  $\gamma$ -rays before being thermally drained separately at different temperature; viz. 125, 180, 225, 300, 400, 500, 600 and 700 °C, to remove various thermoluminescence peaks. The PTTL process was carried out by means of two different UV wavelengths: 254 nm and 366 nm. The response, in term of integrated glow area under the 110°C PTTL peak, was found to fall rapidly with the increase of draining temperature between 125°C and 300°C. For drainage at 400°C onward, the PTTL response felt very slowly. The UV illumination time needed for achieving the maximum PTTL response rose with the increase of draining temperature: slowly from 125°C to 400°C, and rapidly from 400°C to 700°C. These observations are interpreted in terms of the transfer of charges from deep to shallow TL traps. The investigation has also proved to be in throwing light on the mechanism of PTTL in natural quartz, which is of importance in radiation dosimetry using TL methods.-

---

<sup>\*1</sup> On leave from:  
National Atomic Energy Agency of Indonesia (Batan),  
PSPKR Batan, P.O.Box 43 Kby.L., Jakarta Selatan,  
Indonesia.

*Photon Backscattering from Cylindrical  
Geometry with Coaxial Cavity*

A. Barna, G. Ochiaiana, M. Oncescu, *Institute of Atomic  
Physics, P.O.B. MG-6, R-76900, Bucharest, Romania*

L. Ochiaiana, *Department of Electrotechnics, Polytechnic  
Institute of Bucharest, Romania*

Using mathematical modelling based on Monte Carlo procedure, the parameters of probability distribution (PD) of exit points of backscattered photons were estimated for cylindrical-shaped material layers with coaxial cavity. This geometry is specific for gamma-gamma gauging, level and density measurements. PD depends on the distance  $h$ , measured on the cylindrical cavity generatrix, between the source-plane and the exit point of the backscattered photon. For PD is proposed a model function given by

$$p(h) = \frac{(w_2 - 2w_1)}{(w_2 - w_1)(2w_2 - 3w_1)} \left(1 + \frac{h}{w_2 - 2w_1}\right) \exp\left(-\frac{h}{w_2 - w_1}\right)$$

The significance of the two parameters:  $w_1$  is the abscissa of the maximum in PD,  $w_2$  is the inflexion point.

The parameters of PD have been estimated for point isotropic sources of  $^{137}\text{Cs}$  and  $^{60}\text{Co}$ , for  $\text{H}_2\text{O}$ ,  $\text{SiO}_2$  and C. The scatterer thickness was chosen as the saturation thickness from the point of view of photon backscattering. In computations, two values of cavity radius were considered: 2 and 5 cm, four values of the photon emission angle:  $20^\circ$ ,  $30^\circ$ ,  $50^\circ$  and  $60^\circ$ .

The assessment of PD is required in radiometric design to determine by calculation the fraction of photons backscattered from the investigated material towards the detector. These quantities allow for an optimal detector location against the radiation source for measurement equipments based on gamma backscattering [1, 2].

[1] C. Popescu and M. Oncescu, *Rev. Roum. Phys.* **28**, 439 (1983)

[2] Gabriela Ochiaiana, C. Popescu and M. Oncescu, *Rev. Roum.*

*Phys* **28**, 489 (1983).

## IRRADIATION-TEMPERATURE EFFECTS IN CHEMICALLY ETCHED SSNTD's

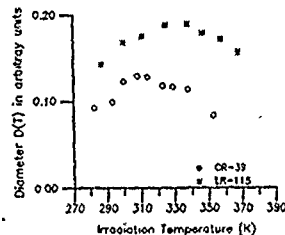
A. Shukri, C.S. Chong, D.A. Bradley\*, A. Ghani Sidek, H. Atan, A.A. Tajuddin and T. Bandyopadhyay  
 School of Physics, University of Science of Malaysia, 11800 USM Penang  
 \* Dept. of Radiology, National University of Malaysia, 50300 K. Lumpur.

LR-115 Type II and CR-39 track-detecting media are subjected to simultaneous heating and normal-incidence  $\alpha$ -irradiation. Trends in variation of the surface opening dimension  $D(T)$  of chemically etched tracks are observed (Graph 1) and the response is modelled on the basis of a quasi-statistical relation<sup>1</sup> of the form:

$$D(T) = \frac{A \exp(-E_o/kT) T^n}{1 + \exp[(T - T_c)/T_o]}$$

A is a proportionality constant.  $E_o$  is interpreted as an activation-energy for formation of point and extended defects and molecular scissions and is included within an exponential probability term with k as Boltzmann's constant. Growth of  $D(T)$  is characterised as  $T^n$ , modelling the temperature dependence of diffusion

mechanisms that involve defects and scissions, with n as an appropriate numerical index. Reduction in  $D(T)$  is modelled by the denominator, representing a tendency for depopulation of defects through recombination and other annealing processes;  $T_c$  is viewed as a critical transition temperature and  $T_o$  as the range of temperature over which there is sensitivity to annealing. Values of the parameters, determined by best-fit to experimental data are found to be:



Detector	n	$E_o$ (eV)	$T_c$ (K)	$T_o$ (K)
LR-115 Type II	0.5	0.112	335	35
CR-39	0.5	0.112	330	21.5

Further work currently proceeds on the response of Lexan, another popular track-detection medium.

## REFERENCES:

1. C.S. Chong, D.A. Bradley & Abdul Ghani Sidek, Appl. Radiat. Isot. Part A, 40, 651 (1989).

## OPTICAL FIBRES AS RADIATION DOSIMETER

H. Henschel, O. Köhn, H. U. Schmidt

Fraunhofer-INT, D-5350 Euskirchen, FRG

## Abstract:

The best known effect of nuclear radiation on optical fibres is an increase of their light attenuation, i.e. the formation of colour centres.

If it is possible to identify fibres where this effect is independent on dose rate as well as on environmental parameters, they can be an interesting alternative to traditional dosimeter mediums, provided they exhibit sufficient sensitivity as well as lifetime of the colour centres.

We found out that graded index fibres that are co-doped with phosphorus (P) are excellent candidates:

- Their response (radiation induced loss) is nearly independent on dose rate within the tremendous range from  $10^{-3}$  rd/s to  $3 \cdot 10^{12}$  rd/s,
- The increase of induced loss with dose is linear up to at least  $10^6$  rd ( $10^4$  Gy),
- The induced loss varies only little with fibre temperature between  $-50$  °C and  $+100$  °C,
- The lifetime of the light absorbing colour centres is extremely long (no "fading"),
- The sensitivity cannot only be preselected by the irradiated fibre length, but also by the wavelength of the conducted light (decrease from about 0.6 dB/10m·krd at 670 nm to about 0.04 dB/10m·krd at 1300 nm).

The availability of highly stable light emitting diodes (LEDs) with wavelengths between about 600 nm and 1300 nm, as well as of cheap, stable receivers enables the construction of inexpensive, compact dose - as well as dose rate meters, especially for higher dose levels.

NEUTRON AND GAMMA DOSES IN FAST NEUTRON FIELDS  
AT THE RB REACTOR AND ITS SURROUNDINGS

Marina Šokčić-Kostić, Milan Pešić, Dragoljub Antić  
The Boris Kidrič Institute of Nuclear Sciences, Vinča  
POB 522, 11001 Belgrade, Yugoslavia

The RB is a bare, zero power nuclear facility with natural and enriched uranium fuel ( 2% and 80% ) and  $D_2O$  as moderator. It is possible to create different configurations of nonreflected and partially reflected critical systems and to make experiments in the field of thermal neutrons. The fields of fast neutrons with "softened" fission spectrum are made by modifying the system ( outside convertor, inside convertors - EFC, CFTS-1, CFTS-2 and HERBE ). According to that it is possible to realise various dosimetry experiments.

During the operation of the RB reactor the doses of neutron and gamma radiation are continuously controlled and registered by measuring the dose rates in determined measuring points. The stationary dosimetry system of the reactor and transferable dosimetry instrumentation are used for these measurements. The neutron spectrum in fast neutron fields is measured by activation technique. The methods of threshold detectors for fast and resonance detectors for intermediate spectrum are used in these measurements. Foil activities are measured using scintillation technique and  $^{41}Ar$  absolute counting method. The neutron spectrum in system HERBE is calculated.

The mean neutron and gamma dose rates in measuring points are analysed. The results of measurements for various operation modes and power values are given. The neutron absorbed doses are determined on the basis of analytical relations using absorbed dose - neutron flux conversion factors for 25 energy groups. The obtained results are analysed.

According to the obtained results in the range between 0,270 and 0,450 Gy/Wh we can conclude that it is possible to use these fields for different dosimetric purposes, irradiation and material studies. There is only one limitation: the realised flux values cannot be larger than  $10^{10}$  n/cm<sup>2</sup>s.

## THE EFFECT OF GAMMA SPECTRUM ON THERMOLUMINESCENT DOSIMETER RESPONSE

Heitor Silva

Institute of Nuclear Sciences and Engineering  
Estrada Nacional N<sup>o</sup> 10, 2685 Sacavém, Portugal

### ABSTRACT

The thermoluminescent dosimetry is a relative method, that is, it is necessary to calibrate previously the dosimeter in a known radiation field. The cobalt-60 sources are, by far, the most used calibration sources, as well as in industrial applications and therapy. In most of practical situations the gamma spectra are different from that of cobalt-60 gamma-rays (1.17 and 1.33 MeV). The reason is the photon absorption and scattering inside the irradiated samples or the utilization of a different source, like in case of nuclear reactors. As the thermoluminescent dosimeters are usually calibrated in a cobalt-60 source, it is necessary to know the effect of gamma spectrum in dosimeter response. In this work the response as a function of energy is analysed quantitatively for the most used thermoluminescent dosimeters (lithium fluoride, lithium tetraborate, calcium fluoride, calcium sulphate and aluminum oxide) for energies ranging from 0.010 to 10 MeV. A calculation method based on Burlin general cavity theory is used. The theoretical results agree with the experimental ones from this work and other authors. The results are applied to obtain the response of thermoluminescent dosimeters under some typical gamma spectra, particularly the case of spectra in 0, 5, 10, 20, 30 and 40 cm in water (or tissue) irradiated by a cobalt-60 source and in the case of a pool research reactor. The results show that, in case of lithium fluoride and lithium tetraborate, the response differs, in every case, by lesser than 1% from the response to cobalt-60 gamma-rays. For the other dosimeters that response differs significantly from the response to cobalt-60 gamma-rays. In these conditions the calcium fluoride, calcium sulphate and aluminum oxide must be used in known spectra or in high energy gamma spectra, where the energy dependence is low.



## DIELECTRIC EFFECT OF PLASMA COLUMN IN SILICON SURFACE BARRIER DETECTOR

Ikuo Kanno

Japan Atomic Energy Research Institute  
Tokai-mura, Naka-gun, Ibaraki 319-11, Japan

The residual defect in a silicon surface barrier detector (SSB) has been recognized as the result of recombinations of electrons and holes of a plasma column. The recombination model, however, failed to explain the dependences of the residual defect on bias voltage and on resistivity of SSB.

Based on the dielectric property of the plasma column, a new candidate for the residual defect is proposed. At the top and bottom of the dielectric plasma column, negative and positive charges are induced by the facing positive and negative electrodes. The induced charges screen the movements of the electrons and holes inside the plasma column from the electrodes. The screened movements do not contribute to the charge induction on the electrodes. The residual defect is ascribed to the screening of the electrons and holes inside the dielectric plasma column from the electrodes.

The model of dielectric effect is presented. The calculated residual defect is shown as functions of depletion layer thickness, bias voltage, SSB resistivity and the plasma column length.

Experimental results on the residual defect are shown for  $^{58}\text{Ni}$  ions and  $^{127}\text{I}$  ions. The incident angle dependence of the residual defect is also studied. The analysis method employing the model of dielectric effect is proposed and applied to the experimental results.

With the model of dielectric effect, the residual defect is clearly explained, especially in its bias voltage and resistivity dependences.

WINDOW SIZE LIMITATIONS FOR THE ENERGY RESOLUTION OF  
NON-FOCUSED GAS PROPORTIONAL SCINTILLATION COUNTER

J.M.F. Dos Santos, A.C.S.M. Bento and C.A.N. Conde  
Physics Department, University of Coimbra  
P-3000 COIMBRA, PORTUGAL

ABSTRACT

The dependence of the energy resolution of an X-ray radiation detector on the entrance window diameter is studied for a given design of non-focused uniform electric field Xenon filled Gas Proportional Scintillation Counter. Energy resolutions of 8.6%, 9.6% and 11% were obtained for 10, 15 and 20mm window diameters, respectively, and for 5.9 keV X-rays.

Pulse amplitude dependence on the radial and azimuthal position of the X-ray interaction point is studied both experimentally and using Monte Carlo simulation method for an ideal detector. In view of these results, the improvement of the detector energy resolution is considered, discussing the photomultiplier performance as well as the detector design for optimum grid parallelism.

Simulation results showed that, as a limit, window diameters of less than 20mm give rise to pulse amplitude fluctuations lower than 3.5% when using 2" diameter photomultipliers.

DETERMINATION OF THE NEUTRON ENERGY SPECTRA  
OF THE Am-Be NEUTRON SOURCE BY SEMICONDUCTOR  $^3\text{He}$  SPECTROMETER

S. Avdic, M. Pesic

The Boris Kidrič Institute of Nuclear Sciences-Vinča

P.O. 522, Beograd, Yugoslavia

ABSTRACT

The neutron spectrum measurements of Am-Be neutron source were performed using ORTEC Model 780 semiconductor neutron detector with  $^3\text{He}$ , in diode coincidence arrangement. The background spectrum was accumulated by using the same spectrometer head filled with  $^4\text{He}$  at the same pressure as the previous case. The neutron spectra have been evaluated from measured pulse-height distribution using developed numerical code HE3 for calculation of detection efficiency in a collimated beam. The numerical code HE3 is based on Monte Carlo method for real spectrometer geometry and angular anisotropy of the reaction products in the center of mass system. The relative efficiency for detection of the reaction products in coincidence was calculated as a function of neutron energy, detector orientation angle and low level discriminator setting. The calculations were performed in the first collision approximation and neglecting the coincidence background response, due to reactions occurring in the silicon of the diodes. After background subtraction, experimental data were smoothed and efficiency corrections were performed. A Good agreement was achieved between the obtained spectrum of Am-Be neutron source and spectra published by other authors.

SIMULATION OF THE ELECTRON TRANSPORT IN MATTER  
IN THE ENERGY RANGE BELOW 50 keV

A. G. Lebedev, A. S. Serebryakov

In the energy range below 50 keV Monte Carlo simulation of the electron transport in matter with standard collision grouping is impossible, and up to now only individual collision model is used in this energy region.

In this report we present results of calculations based on new principle of grouping, which we suggested previously. The main idea is in dividing the electron trajectory in steps containing fixed number ( $n = 16$ ) of elastic collisions. Angular distributions at the end of each step are calculated by folding of single elastic scattering distributions obtained from differential cross sections taken in numerical form, and spatial and energy distributions are constructed on the basis of derived simple empirical expressions.

Application of developed software to several problems (there were calculated spectra of electrons transmitted through barriers and backscattered from bulk targets, shapes of  $\phi(\rho z)$  functions for solving EPMA problems, and spatial distributions of secondary electrons in gases associated with resolution of position-sensitive X-ray detectors) and comparison of calculated and experimental results showed high reliability of the new approach - in all cases the deviation of calculated differential characteristics from experimental data was within 10 - 15 %. In the latter case the initial electron energies were especially low (3 + 5 keV).

The package of software may be useful in on-line solving of analytical problems in EPMA, Auger- and photo-electron spectrometry if the analytical instrument is attached to a computer of PC/AT class. This software provides considerable saving of computer time, while the accuracy of calculations remains of the same order as for individual collision mode. There are no restrictions to apply this software to any problem of low energy electron transport in matter

## RESEARCH REACTOR CORE OPTIMIZATION FOR NEUTRON EXPERIMENTS AND IRRADIATION

M. Ravnik, I Mele, A Trkov  
"J.Stefan" Institute, Ljubljana  
Slovenia, Yugoslavia

Research reactors have been and will remain the most powerful and commonly used sources of neutrons in fundamental and technological research. Utilization of their experimental facilities can be significantly improved by optimizing the reactor core size, shape and loading pattern with respect to the particular requirements. This is especially true for reactors with mixed cores /1/ where two or more types of fuel with different enrichment or uranium content are used at the same time.

Efficient core optimization can be performed only by using reactor calculations in combination with measurements. Development of small and personal computers made reactor calculations, which were entirely in the domain of reactor designers, available also to research reactor users. Presented in this paper is a package of computer codes which was developed at J.Stefan Institute for TRIGA reactor calculations. It consists of unit cell transport code (WIMS, /2/) and several one-two and three-dimensional diffusion codes for global reactor calculations (e.g. TRIGAP, /3/). The codes in the package share an effective cross-section library in which the burn-up and temperature effects are considered. Comparison of calculational results to measurements shows good agreement even in case of complicated mixed cores. All codes are adapted for IBM-PC-AT-386 computer.

The main purpose of the paper is to show some practical results and principles of TRIGA reactor mixed core optimization using reactor calculations. The optimization of neutron spectrum in central and peripheral irradiation channels is described together with power and flux peaking analysis. Optimal core configuration for pulse mode operation is treated with respect to temperature limitations. Core management for long term stationary mode operation is presented, optimizing for fuel costs and beam channel utilization. Results are supported by experimental evidence.

/1/ M.Ravnik, Nuclear Safety Parameters of Mixed TRIGA Cores, Workshop on Reactor Physics Calculations, ICTP, Trieste, 12 Feb - 13 March 1990, Proceedings in press

/2/ J.R. Askew, F.J. Fayers, P.B. Kemshell, A General Description of the Lattice Code WIMS, J. of the British Nucl. Energy Soc., p. 564, Oct. 1966

/3/ I. Mele, M. Ravnik, TRIGAP - A Computer Programme for Research Reactor Calculations, IJS-DP-4238, J. Stefan Institute, Ljubljana 1985

Development of a novel neutron detector based upon Dynamic  
Random Access memories.

D Daranbara, A C Beach, N M Spyrou

Department of Physics, University of Surrey,

Guildford, Surrey, GU2 5XH, UK

Abstract

A novel neutron detector is being developed which functions on the principle of soft error creation in Dynamic Random Access Memories (DRAM). These soft errors are produced by the interaction of charged particles with the memory device itself. Neutron detection is made feasible by the use of  $(n,\alpha)$  reactions in a lithium converter. System design incorporates 48K bytes of dynamic memory which is interfaced to a Zilog Z80A microprocessor. Special consideration is reserved for constraining system dimensions. Initial findings highlight the usefulness of such a device in neutron detection.

## CHANGES IN BACKGROUND DUE TO A COMPTON SUPPRESSION SHIELD IN A LOW-LEVEL $\gamma$ -SPECTROSCOPY SYSTEM

I. Bikit, J. Slivka, M. Vesković, M. Krmar and Lj. Čonkić  
Institute of Physics, Faculty of Science  
University of Novi Sad, Yugoslavia

Introducing a large volume NaI(Tl) crystal with associated photomultipliers and electronics as anticoincidence shield into a low level chamber containing a Ge-detector influences the residual background count rate considerably with anticoincidence active, as well as in passive mode.

The chamber is constructed with a large cavity ( $1 \times 1 \times 1 \text{ m}^3$ ) to keep a large wall-detector distance, with walls of pre- WW-II cast steel 25 cm thick. The Ge-detector of 25% relative efficiency having a peak-to Compton ratio for the 1332 keV Co-60 line of about 60 is located within the chamber together with its dewar. The integral background count rate (30-2000 keV) of this assembly is 1.55 counts/s. The anticoincidence shield is an annulus-with-plug type  $9 \times 9$ " NaI(Tl) crystal with 7 photomultipliers. After inserting it into the chamber it acts both as an additional shield and as a source of  $\gamma$ -emitting nuclei. The integral count rate is not changed, but the changed structure of the continuum and of the lines in the spectrum affect the minimum detectable activity for various radionuclides. This is more pronounced with active anticoincidence, when the integral background drops to 0.62 counts/s. Trying to distinguish between the effects of contributing to background and background screening by the shield, the response of the central detector to the radiation of a circumventing point source was measured. Comparing the detection limits for the simultaneous detection with the Ge and NaI(Tl) detectors it is shown that, despite the inferior resolution, and due to high efficiency, the NaI(Tl) detector can yield in some cases spectral information complementary to that of Ge.

NEUTRON ADMIXTURES IN THE BREMSSTRAHLUNG  
OF THE 15 MeV LINAC

M. Krmar, J. Slivka, Lj. Čonkić, M. Vesković, I. Bikit, Z. Kuzmanović\*

Institute of Physics, Faculty of Science,

\*Institute of Oncology, Faculty of Medical Science,  
University of Novi Sad, Yugoslavia

Medical linacs operated at energies above the threshold for  $(\gamma, n)$  reactions can produce neutrons by interaction of high energy bremsstrahlung photons with the target, flattening filter, collimators and other components of the equipment and the surrounding material. The produced neutron flux is thus dependent on the surrounding of each machine and can not be detected by means of conventional dosimetry. We investigated the neutron flux of the 15 MeV Siemens linac "Mevatron-77" by activation detectors.

For standard conditions (100 cm distance,  $10 \times 10$  cm<sup>2</sup> field size) from the activation of As-75, I-126 and Cd-110 it has been estimated that the neutron flux is  $10^5$  neutrons cm<sup>-2</sup>s<sup>-1</sup>. The results of the flux distribution in the beam and in the treatment room will be presented.

From these data and from the measurement of the epithermal to thermal neutron flux ratio the activity induced by neutron capture in different types of tissue will be estimated.



## PROPORTIONAL COUNTER WITH NATURAL GAS

A. A. da Silva<sup>1</sup>, .. L. Awwal<sup>2</sup>, A. H. de Oliveira<sup>2</sup>.

1 - Pontificia Universidade Católica de Minas Gerais,  
Brasil.

2 - Universidade Federal de Minas Gerais, Brasil.

In nuclear reactions involving neutrons, there is always the occurrence of gamma radiation from the decay of excited nuclear states. Therefore, a mixed field of neutron and gamma radiation is formed. The absorbed dose from this field has the contributions of neutrons and gammas, since the dose from gamma rays can be as much as 20% of that from neutrons.

In all range of energy, the quality factor for neutrons is different from that of gamma, therefore, in determination of dose equivalent it is necessary to know the absorbed dose from neutrons and gamma rays separately.

In this work, the construction and development of a proportional counter sensitive to neutron and gamma rays, which permits to simulate a microscopic region of tissue in order of some microns, is proposed. A spectral distribution in energy from the radiations is obtained from this counter, which treated adequately permits the computation of the absorbed dose, dose equivalent and quality factor in a large range of energy.

DETERMINATION OF  $^{139}\text{La}$  ACTIVITY IN  $\text{La}_2\text{O}_3$  BY COMPARISON WITH KNOWN  $^{137}\text{K}$  ACTIVITY

A.H. Kukoč, M.M. Marković, I.V. Anižin, G.P. Škoro

B. Kidrič Institute, Vinča, Belgrade, Yugoslavia

In our recent paper [1] we have recommended lanthanum compounds  $\text{La}_2\text{O}_3$  and  $\text{La}(\text{NO}_3)_3 \cdot 6\text{H}_2\text{O}$  and their natural radioactive impurity  $^{232}\text{Ac}$  (with daughters) as a "self calibration source" for efficiency determination.

Since the determination of the number of La-atoms (total activity) by weighing of particular La-compound may be misleading [2], we are comparing it with the activity of well behaved p.a. compound KCl.

The results of 3 measurements of homogeneous mixture of 59.72 g BDH p.a.  $\text{La}_2\text{O}_3$  and 9.96 g of p.a. "Merck" KCl with low-background HPGe spectrometer ( $\epsilon_p = 14\%$ , FWHM = 1.7 KeV; integral count rate in the energy range 20-2880 KeV of 0.63 cps), are presented in the Table.

Integral count rate [cps]	Counting time [ks]	Activity $^{139}\text{La}$ $A_1$ [Bq]	Activity $^{137}\text{La}$ $A_2$ [Bq]	Activity $^{232}\text{Ac}$ [Bq]
10.3	165	36.4 (7)	35.7 (7)	116.3 (30)
9.8	165	35.4 (7)	34.5 (7)	112.0 (30)
11.5	165	36.0 (7)	35.4 (7)	118.6 (30)

In the first column different integral count rates reflect the different distribution of the source material inside the air-tight polyethylene vial (the material occupied 60% of the vial's volume).

The activities  $A_1$  are obtained by taking equal efficiencies for the two close energy gamma rays at 1436 KeV ( $^{139}\text{La}$ ) and 1461 KeV ( $^{137}\text{K}$ ). The activities  $A_2$  are the results of the best fit of the efficiency curve ( $\epsilon = a \cdot E^b$  or  $\epsilon = a \cdot b \cdot 1/E$ ) through the lines 788 KeV ( $^{232}\text{Ac}$ ), 1436 KeV ( $^{139}\text{La}$ ) and 1461 KeV with the  $^{139}\text{La}$  activity being a free parameter.

The last column contains  $^{232}\text{Ac}$  activity in the sample determined from its daughter  $^{212}\text{Pb}$ .

[1] A.H. Kukoč, M.M. Marković, I.V. Anižin, P.R. Adžić, Natural Radioactive Impurities in Lanthanum Compounds as Calibration Source for Gamma Spectrometry of Voluminous Samples, to be published in "Radiochimica Acta", 1991.

[2] J. Sato, T. Hirose, Radiochem. & Radioanal. Lett., 46, 145 (1981).

FAST NEUTRON PULSING FACILITY  
AT THE RUĐER BOŠKOVIĆ INSTITUTE

S. Blagus, Đ. Miljanić, D. Rendić, D. Tomić, B. Vojnović and M. Zadro  
Ruđer Bošković Institute, POB 1016, 41001 Zagreb, Croatia, Yugoslavia

Sinusoidal nanosecond chopping and bunching system as well as square wave microsecond and millisecond chopping systems were developed and applied on the post-acceleration beam of the existing 300 kV neutron generator. The bunching by the klystron buncher of the three gap type has been used. All components of the systems were designed for deuteron beam of 160 KeV. Using the sinusoidal system the beam pulses with FWHM of approximately 3 ns, with frequency of 5 MHz have been obtained. Square wave systems can produce pulses with adjustable width and frequency in microsecond and millisecond region.

A MATHEMATICAL MODEL FOR DESCRIPTION  
OF THE RADIATION FIELDS

V. Stanić

"Boris Kidrić" Institute of nuclear sciences  
P.O. box 522, 11001 Beograd, Yugoslavia

In this paper, starting from the model for transport of the radiation field, expressed by the integro-differential equation, an equivalent relation is proposed:

$$\left[ \partial/\partial x + T \right] \Psi(x, \mu) = Q(x, \mu),$$

where  $T$  is the modified transport interaction operator,  $Q$  is the source and  $\Psi$  is the flux density of the radiation field. The semi group  $\exp(-Tx)$  is determined by using the spectral properties of the operator  $T$ . Thus the general solution to the transport equation in operator form

$$\Psi(x, \mu) = \exp(-Tx) \Psi(0, \mu) + \int_0^x \exp[-T(x-x')] Q(x', \mu) dx',$$

can be expressed by corresponding functional form for given boundary conditions.

The considered transport process includes an arbitrary scattering anisotropy, while the energy dependence is expressed in multi group approximation with slowing down terms added to the source  $Q$ . The derivation and verification of the proposed analytical expressions are followed by appropriate mathematical methods.

Examples of the computed neutron and photon radiation fields are given at the end.

MONTE CARLO SIMULATION OF THE BACKSCATTERED PEAKS IN  
XRF FOR ANNULAR SOURCE GEOMETRY

I.Bogdanović, I.Orlić and V.Valković  
Ruđer Bošković Institute, Zagreb, Yu

The backscattered peaks of an energy-dispersive x-ray fluorescence spectrum obtained by annular radioisotope excitation are examined. In Monte Carlo simulation each photon is followed from emission to detection in the active layer of the Si(Li) detector. A new technique, developed for Monte Carlo simulation of relative X-ray fluorescence intensities(1), is used. The simulation is done only for pure single-element samples( $Z < 30$ ). All physical parameters for photon scattering process (Compton profiles, form and scattering factors for the cross sections, system and detector efficiency data) are included.

The importance of the backscattered peaks is that they contain information about the unknown sample to be analysed. The low atomic number constituents in the sample may also be qualitatively found by using the incoherent-to-coherent scattered intensity ratios. The results will be used to increase reliability of quantitative analysis in EDXRF spectroscopy.

1. S.M.Tang, P.Kump, C.T.Yap and M.G.Bilal, X-ray Spectrom. 15, 289(1986)

ON THE OPTIMUM HEIGHT OF VOLUMINOUS CYLINDRICAL  
SOURCES IN GAMMA-RAY SPECTROSCOPY

D.Vesić and I.V.Anićin

The Boris Kidrič Institute, Vinča, Belgrade, Yugoslavia

In our previous study of gamma-ray cylindrical sources for the purposes of spectroscopy (ref.1) we have established that the intensity of the given spectral line,  $I$ , saturates as the height  $H$  of the source increases, as

$$I(H) = I_0(1 - \exp(-\mu_{\text{eff}}H))$$

where  $\mu_{\text{eff}}$  is the empirical effective absorption coefficient. The intensity thus reaches p.100% of its saturation value  $I_0$  at the height of the source  $H_p = -(\ln(1-p))/\mu_{\text{eff}}$ . The quantity which is relevant for optimisation purposes is, however, not the intensity itself but rather its relative error  $r = \Delta I / I \approx \sqrt{1 + 2B/I}$ ,  $B$  being the background under the line. In the ideal case with no background one would have

$$r(H) = r_0 / \sqrt{1 - \exp(-\mu_{\text{eff}}H)}$$

with  $r_0 = 1/\sqrt{I_0}$ , leading to  $r(H_p) = r_0/\sqrt{p}$ . Direct consequence of the simple square root dependence is that the relative error will reach given percentage of its saturation value at the smaller height than will the intensity. For instance, the height at which the relative error will reach 90% of  $r_0$  is only 3/4 of the height at which the intensity will reach 90% of  $I_0$ . This already substantially reduces the quantity of the source material needed as compared to that from usual considerations of intensity only.

In realistic cases the background under the line comes mainly from the two types of Compton scattered higher-energy photons; those scattered in the detector which then escape detection and those scattered in the environment, including the source itself, which are then either partially or completely detected. One may expect both of those components to saturate at the rate corresponding to the original higher-energies, generally slower than the energy under consideration, i.e. with smaller  $\mu_{\text{eff}}$ . After the line has been saturated those will continue to contribute to the background eventually increasing the relative error as the height increases over the intensity saturation height. This effect will obviously strongly depend on the actual spectral composition of the radiation and will generally be more pronounced for low-energy gamma-rays when higher energies abound. We present some experimental results which confirm the existence of this effect.

**A Monte Carlo Simulation Study of Electron Loss to the  
Entrance Window in Xenon Filled X-ray Detectors**

E.P.Santos<sup>\*</sup>, T.H.V.T.Dias<sup>\*</sup>, A.D.Stauffer<sup>#</sup>, C.A.N.Conde<sup>\*</sup>

<sup>\*</sup> Departamento de Física, Universidade de Coimbra, 3000 Coimbra,  
PORTUGAL

<sup>#</sup> Physics Department, York University, Toronto, CANADA M3J1P3

**ABSTRACT**

In xenon filled X-ray gaseous detectors such as Proportional Scintillation Counters, for low drifting electric fields a significant distortion of the energy spectra has been experimentally observed when the penetration depth of absorbed soft X-rays happens to be very small.

Using a detailed Monte Carlo simulation of the absorption of low energy X-ray photons in xenon which has previously been developed to study energy resolution and energy linearity intrinsic limitations, we otherwise investigate in this work the effect of tail enhancement on the spectra obtained near the  $M_{45}$  X-ray absorption edge in xenon (683 eV) when a real detector is considered, i.e., when the boundary defined by the entrance window is introduced in the simulation. The above distortion effect is shown to correspond to a loss of electrons to the detector's window, and the correspondent break in energy linearity and energy resolution degradation is analysed and discussed. The influence of the strength of a uniform electric field applied in the detector's X-ray absorption zone is assessed.

POSITION-SENSITIVE PROPORTIONAL COUNTER FOR LOW-ENERGY X-RAY  
SPECTROMETER (100-1000 eV)

R. Katano and Y. Isozumi

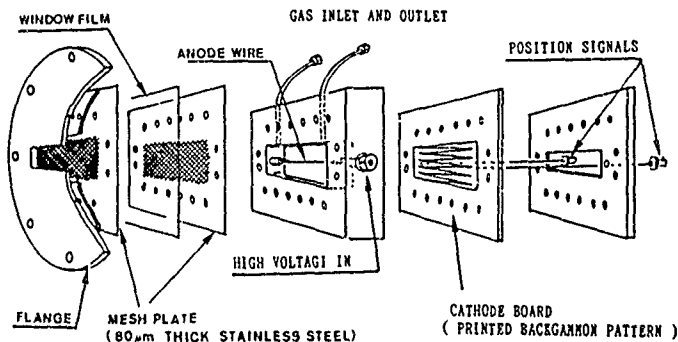
*Institute for Chemical Research, Kyoto University, Uji Kyoto,  
Uji, Kyoto, 611, Japan*

S. Ito

*Radioisotope Research Center, Kyoto University, Kyoto, 606, Japan*

A position-sensitive proportional counter (PSPC) for low-energy X-ray spectroscopy ( $<1$  keV) has been developed. Signals from cathode with the backgammon pattern are used to produce position signals through the charge-division method. The sensitive area of the counter is 7-10 mm (thickness)  $\times$  100 $\times$ 20 mm<sup>2</sup> (window area). The counter gas is methane, ethane, propane or butane with a pressure of 80-450 Torr. The anode is 50-300  $\mu$ m diam gold-coated tungsten wire. The window film is 0.5-5  $\mu$ m thick polypropylene or 2.5  $\mu$ m thick Mylar, which is supported by two stainless steel mesh plates. The gas gain of the counter gases is  $5 \times 10^5$ - $5 \times 10^8$ , depending on X-rays to be detected. The practical position resolution of PSPC coupled with the present electronic system is 250-350  $\mu$ m.

Employing the new PSPC, we are now fabricating a flat-crystal spectrometer to analyze soft X-rays from low-Z elements such as Be(108 eV), B(183 eV), C(277 eV), N(392 eV), O(525 eV) and F(877 eV). The layout of the present PSPC is given below.





P. Marinkovic

Faculty of Electrical Engineering  
University of Belgrade  
Bulevar revolucije 73  
P.O. Box 816

### A B S T R A C T

#### Influence of Neutron Spectra Unfolding Method on Fast Neutron Dose Determination

Accuracy of knowing the fast neutron spectra has great influence on equivalent dose determination. In usual fast neutron spectrum measurements with scintillation detectors based on proton recoil, the main difficulty is confidence of unfolding method. In former ones variance of obtained result is usually great and negative values are possible too, which does mean that we don't now exactly is obtained neutron spectrum real one.

The new unfolding method based on Shannon's information theory, which gives non-negative spectrum and relative low variance, is obtained and appropriate numerical code for application in fast neutron spectrometry based on proton recoil is realized. In this method principle of maximum entropy and maximum likelihood are used together. Unknown group density distribution functions, which are considered as desired normalized mean neutron group flux, are constructed using only constrain of knowing mean value. Obtained distributions are consistent to available information (counts in MCA from proton recoil), while being maximally noncommittal with respect to all other unknown circumstances. For maximum likelihood principle, distribution functions around mean value of counts in the channels of MCA are taken to be Gauss function shape. Optimal non-negative solution is searched by means of Lagrange parameter method. Nonlinear system of equations, is solved using gradient and Newton iterative algorithm. Error covariance matrix is obtained too.

Comperation of equivalent dose measurement by means of fast neutron dose gauge (Nuclear Enterprise NE-1) and calculated dose with measured neutron spectrum of Pu- $\alpha$ -Be neutron source was done too.

## DIGITAL EVALUATION OF ${}^6\text{Li}(n, \alpha)$ REACTION PRODUCT TRACKS IN CR-39 DETECTOR

J. Skvarč, R. Ilić, A. Kodre

"J Stefan" Institute, University of Ljubljana, Jamova 39, 61111 Ljubljana, Yugoslavia

The interpretation of the information recorded by track-etch detectors often depends on subjective criteria due to manual evaluation of the tracks under optical microscope. Distinction between various charged particle tracks and the background is based on size and average greyness of a single track. The increased capabilities of computer technology have opened new possibilities for the development of reliable and relatively cheap systems for the evaluation of digitized images. A microcomputer controlled system was set up at the J. Stefan Institute for the tracks evaluation in solid state nuclear tracks detectors. The digital image processing program which performs several image processing and analyzing operations was developed and applied to the evaluation of  ${}^6\text{Li}(n, \alpha)$  reaction product tracks in the CR-39 detector. By automatic counting, the standard error in  $\alpha$  track density is improved to 15 % from 50 % in manual counting while for triton tracks the error amounts to 15 % in both cases.

## THE ELECTRET IONIZATION CHAMBER AND THE NEUTRON MONITOR

GHILARDI, A.J.P.; PELÁ, C.A.; GHILARDI NETTO, T.; DE PAULA, E.; NAVAS, E. and ZIMMERMAN, R.L. (FÍSICA/CIDRA-DGFM-FFCLRP/University of São Paulo - Ribeirão Preto, São Paulo - Brazil).

We have reported quite recently the use of the electret ionization chamber for gamma, electrons, fast and thermal neutrons. Different parameters have been studied for a better utilization of this chamber. The sensitivity as a function of temperature, mechanical shock, charge stability have been studied in the last years. An electret ionization chamber with boron coated was presented as a new technique for detecting thermal neutrons. Its response to a monoenergetic thermal neutron beam from a critical reactor and to thermal neutron flux in diffusion through a homogeneous moderator medium are determined. The efficiency on electret ionization chambers with different wall materials for the external electrode was inferred from the results. Detection of thermal neutrons with discrimination against the detection of gamma rays and energetic neutrons was shown to depend on the selection of those materials. The charge stability over a long period of time and the charge decay owing to natural radiation were studied. The charge decay owing to humidity was eliminated through a drying chamber constructed and adapted to the detector. Numerical results show that the sensitivity of electret ionization chamber for detection of thermal neutrons could be comparable with that of  $\text{BF}_3$ . A neutron monitor has been constructed by using the electret ionization chamber and cylinders of polyethylene containing in his center a electret chamber. The results from experimental tests have showed that for a optimized thicknesses of polyethylene were found sensitivities of 0.7 nC/mGy approximately.

# TRACK CHARACTERISTICS OF 11.56 MeV/n $^{136}\text{Xe}$ IONS IN MAKROFOL-KG DETECTOR

A. Kumar, P.J. Jojo, A. Rawat and Rajendra Prasad  
Department of Applied Physics, Z.H. College of Engg. and Tech.,  
Aligarh Muslim University, Aligarh, India

Latent damage tracks formed by the energetic  $^{136}\text{Xe}$  ions of 11.56 MeV/n have been recorded in Makrofol-KG plastic track detectors. Stacks of 5 Makrofol-KG detectors were exposed to Xe-ions at GSI Darmstadt, West Germany. The irradiations were made at a dose  $\sim 10^4$  ions/cm<sup>2</sup> at an angle 45° with respect to the detector surface. Etching parameters namely bulk etch rate  $V_B$  and track etch rate  $V_T$  are determined at different etching temperatures - 50, 60, 70 and 80°C - by successive chemical etching. The concentration of the etchant (NaOH) was kept constant at 6.25 N.

The bulk etch rate at different temperatures has been determined using the thickness measurement technique and the track etch rate with track length measurement technique. With the values of  $V_B$  and  $V_T$  obtained at different temperatures the graphs were plotted between  $\log_{10} V_B$  and  $T^{-1}$  and  $\log_{10} V_T$  and  $T^{-1}$ . Using the slopes of the lines the activation energies for track etching  $E_T$  and bulk etching  $E_B$  are determined by an exponential relation  $V_B$  or  $V_T = A e^{-E/KT}$  where A is a constant K, the Boltzmann's constant, T, the etching temperature (°K) and E, the activation energy. Etching efficiency ( $\eta$ ) at various temperatures using  $V_B$  and  $V_T$  are calculated. The threshold value of energy loss rate of Makrofol-KG track detector is also calculated.

# RADIATION DOSIMETERS BUILT WITH PLASTIC SCINTILLATORS.

Raul A. Barrea, Miguel A. Chesta\* and Raul T. Mainardi\*\*.  
Facultad de Matematica, Astronomia y Fisica. Universidad  
Nacional de Cordoba. - Laprida 854 - Cordoba - Argentina.

Gaseous ionization chambers, with air equivalent plastic walls, have been used in x-ray dosimetry systems, since its response permits to measure doses in Roentgens. The commercial availability of a plastic scintillator of air equivalent atomic number have prompted its use in x-ray dosimetry.

We have devised two dosimetric uses of that plastic scintillator. A large volume chamber to make dosimetry of x-ray beams and a small volume cylinder in combination with an optical fiber to allow positioning in phantoms for dosimetry of x-ray fields. Calibration of both systems against existing conventional chambers was carried out for energies between 20 and 180 Kev. They have shown higher efficiency and precision attributable to the large density of the plastic as compared with air. A wide range of applications are presently foreseeable.

\* Under a Fellowship of the Research Council of the Province of Cordoba-Argentina (CONICOR)

\*\* Member of the National Research Council of Argentina (CONICET).

MONTE-CARLO SIMULATION OF ELECTRON AVALANCHES IN  
PROPORTIONAL COUNTERS.

Alfredo L. Falco and Raul T. Mainardi\*.

Facultad de Matematica, Astronomia y Fisica. Universidad  
Nacional de Cordoba. - Laprida 854 - Cordoba - Argentina.

A statistical study of Monte-Carlo simulated avalanches in gases has been performed along the lines set forth by Kundhardt et. al. (Phys. Rev. A34 (1986) 440). We extended this analysis to calculate the second moment of a large number of electron avalanches under different applied electric fields and gas densities.

The results obtained thus far show a qualitative agreement with experimental curves from proportional counters as measured by a large number of workers.

\*\* Member of the National Research Council of Argentina (CONICET).

CALIBRATION OF CELLULOSE NITRATE (R) PLASTIC  
TRACK DETECTOR USING ACCELERATED  $^{16}_8\text{O}$  IONS.

S. M. FARID

Department of Physics, University of Swaziland, Swaziland, Africa.

ABSTRACT

Exposures of Cellulose nitrate ( Russian ) plastic track detector to  $^{16}_8\text{O}$  ions of different energies have been obtained from cyclotron at JINR, Dubna (USSR). The chemical etching is carried out in stirred  $(6.00 \pm .05) \text{N}$  NaOH solution. The bulk etch rate,  $V_b$  and track etch rate,  $V_t$  are measured for different etching temperatures. The dependence of  $V_b$  and  $V_t$  on etching temperature is exponential and can be expressed by Arrhenius correlation. The activation energies for bulk etch rate and track etch rate are determined. The experimental results show that both  $V_t$  and  $V = V_t / V_b$  along the trajectory of the particle depend on etching temperature. The range and the energy-loss,  $dE/dx$  of the ions in the detector material are computed using theoretical equations with the help of computer. The dependence of  $V_t$  and  $V$  on energy-loss,  $dE/dx$  is also presented. The normalized track rate depends on both  $dE/dx$  and etching temperature. The maximum etched track lengths of the ions agree with the theoretical ranges to better than 2%. The experimental results show that the response of this detector can be adjusted by altering the etch bath temperature.

MINIATURISED TISSUE-EQUIVALENT  
DOSE-RATE MONITORS USING  
SYNTHETIC DIAMOND CRYSTALS AS SENSOR ELEMENT

U. KARFUNKEL, M. TAN, T.L. NAM and R.J. EDDY

Schonland Research Centre for Nuclear Sciences

University of the Witwatersrand

Johannesburg, South Africa

and

J.H. GROBBELAAR, R.C. BURNS

De Beers Diamond Research Laboratory

Johannesburg, South Africa

---

Miniaturised tissue-equivalent detectors which can monitor ionizing radiation dose-rates have been constructed with the circuits designed to operate with custom synthesized Type Ib diamond crystals as the sensitive element. Tissue-equivalence is assured because of the use of the diamond sensor and carbon fibre leads attached to the diamond to supply the polarizing voltages.

An important factor which influenced the performance of the devices were found to be the concentrations and types of impurity atoms incorporated into the crystal lattice during synthesis. Also the preparation of the crystal surfaces for forming the electrical contacts and attaching the leads was found to be critical. A technique of ion-implanting opposite, polished surfaces of the diamond crystal was developed which resulted in ohmic contacts and the removal of space charge effects for the low nitrogen concentration specimens. Strict control of the synthesis cycle parameters, including the chemistry, was necessary for the regulation of the impurity atom concentrations. The devices were found to be particularly sensitive to the nitrogen concentrations in the diamond sensors.

With crystals having volumes of  $\sim 10\text{mm}^3$  and containing approximately 60ppm of paramagnetic nitrogen,  $\gamma$ -ray dose-rates down to  $7.5 \mu\text{Gy.h}^{-1}$  could be recorded with linearity of response up to  $1\text{cGy.h}^{-1}$ .

The detectors have been found to respond also to electron and  $\alpha$ -particle beams.



APPLICATION OF VARIOUS GERMANIUM DETECTORS AS ON-LINE  
NEUTRON MONITORS

Chien Chung and Cheng-Jong Lee

Institute of Nuclear Science  
National Tsing Hua University  
Hsinchu 30043, Taiwan R.O.C.

A feasibility study of using germanium detectors as neutron monitors is described. N-type and P-type high purity germanium detectors with various efficiencies are irradiated by neutrons supplied from nuclear reactors and neutron sources. The semiconducting detector emits prompt photopeaks at 596 keV and 691 keV from the  $\text{Ge}(n, \gamma)$  and  $\text{Ge}(n, n' \gamma)$  reactions, respectively. The count rate of these index photopeaks is used to monitor the neutron dose rate equivalent, resulting in a detection range of  $0.08 \mu\text{Sv/h} - 120 \mu\text{Sv/h}$  for thermal and epithermal neutrons and  $0.8 \mu\text{Sv/h} - 75 \mu\text{Sv/h}$  for fast and high energy neutrons. Advantages and disadvantages of using the HPGe detectors as neutron monitors while serving primarily as gamma-ray spectrometers in a mixed neutron/gamma field are discussed.

This work is financially supported by the National Science Council of the Republic of China under contract number NSC 79-0413-E007-14

MEASUREMENT OF  $w$  FOR PROTONS OF 1.3, 1.5 and 2 MeV  
in  $N_2$ ,  $O_2$  and Ar

V. K. Bhargava\* and M. K. Mehta†

\*Division of Radiological Protection, Bhabha Atomic Research Centre  
Bombay 400 085, India

†Vikram A. Sarabhai Community Science Centre, Navrangpura  
Ahmedabad 380 009, India

Neutron Dosimetry with Ionisation Chambers and microdosimetry of protons in general need accurate and simple measurement of the differential value of  $w$  for protons,  $w$  being the average energy required to form one ion pair on partial absorption of energy of protons in measuring gas medium. It is also important to study the variation of this  $w$  value with incident energy. The ' $w$ ' has so far been evaluated for protons above 3 MeV. In the investigation reported here  $w$  measurements have been carried out for protons of energies 1.3, 1.5, and 2 MeV, in Nitrogen, Oxygen and Argon respectively. These gases are the constituents of the detection medium in ion chambers or other types of dosimeters.

The measuring system is a windowless, 40 cm long parallel plate ionisation chamber preceded by a differential pumping system. The beam, after passing through two collimators of 1.61 mm and 1.41 mm diameter respectively, enters the chamber through a 0.47 mm size collimator, and exits to the Faraday cup through a mylar foil of 0.480 mg/cm<sup>2</sup> thickness. A surface barrier detector set up at a fixed forward angle before the Faraday cup is used to determine the spectrum of the protons scattered by the mylar foil. The energy loss of the protons in passing through the gas medium is measured from the shift in the elastic peak of the scattered spectrum with and without the gas in the ionisation chamber. The total ionisation is measured by a charge integrater connected to the collection plates of the ionisation chamber. The charge collected by the Faraday cup yields the number of protons.

The value of  $w$  for 2.0 MeV protons is measure to be 32.7, 30.0, and 25.0 eV for  $N_2$ ,  $O_2$  and Ar respectively while for 1.3 MeV protons it is 36.0, 33.7, 20.2 respectively. These values are different from reported  $W$  (integral measurements) values of 37, 34 and 27 eV respectively for the same gases for a different proton energy, indicating that  $w$  (differential) is energy depednent and is different from  $W$  (integral) values. The paper discusses various aspects of design, measurements and results.

A PIECEWISE LINEAR INTERPOLATION SOLUTION TO  
SPECTROGRAPHIC DIAGNOSIS FOR OPTICALLY-THICK,  
CYLINDRICALLY SYMMETRIC PLASMA

Ding Peizhu,<sup>1</sup> Mu Yingkun<sup>2</sup>,  
and Pan shoufu<sup>1</sup>

1) Jilin University

2) Changchun Finance Manager College

Abstract

A piecewise linear interpolation solution obtaining the radial emission coefficient for optically-thick, cylindrically symmetric plasma is presented. An example is evaluated with the presented interpolation and Young's iteration, it is shown that the present interpolation solution is precise and reliable. By using the present interpolation, the generalized Abel equation is separated to a system of linear algebraic equations and the coefficient matrix of the system is an upper triangular matrix, so the present interpolation solution is very simple to evaluate and easy to master for experimentalists and required computer time is less.

GAMMA-RAY DEPTH DOSE DISTRIBUTION INSIDE

WATER PHANTOM USING LiF-700 THERMOLUMINESCENCE DOSIMETER

M.M. Elissa, M.S. Abdel Wahab<sup>\*</sup>, A.M. Sayed<sup>\*\*\*</sup>, I.M. Arafa

M.A. Fadel and M.A. El-Fiki

National Institute of Standard, Dokki, Cairo, Egypt

\* Phys. Dept., Faculty of Science, Ain Shams University, Cairo, Egypt.

\*\*\* Egyptian Atomic Energy Authority, Rad. Prot. Dep.

Biophysics Dep., Faculty of Science, Cairo Univ., Egypt

ABSTRACT

The distribution of absorbed dose from Cf-252 fission source inside a water phantom using LiF-700 thermoluminescence dosimeter has been performed. The phantom dimensions are 30 x 30 x 30 cm, made from perspex and filled with water. The measurements were carried out at X, Y and Z directions, i.e. (X,Y) at Z = 0 and (X,Z) at Y = 0. Bare and 0.5 mm Cd covered LiF-700 in one side and both sides were used in the study in order to measure the absorbed Gamma dose originated from the Cf-252 source as well as the total Gamma dose covered LiF-700 dosimeter. The high sensitivity small size, stability and reusability of LiF-700 enables accurate measurements at small depths.

PAST, INTERMEDIATE AND THERMAL NEUTRON DOSE EQUIVALENT

M.A. El-Piki, H.M. Eissa, A.M. Sayed<sup>\*\*\*</sup>, E.H. El-Adl,

M.S. Abdel-Wahab<sup>\*\*\*</sup>, I.M. Arafa and M.A. Fadel<sup>\*</sup>

National Institute of Standards, Dokki, Cairo, Egypt

\* Bioph. Dep., Faculty of Science, Cairo Univ., Egypt

\*\*\* Egyptian Atomic Energy Authority, Rad. Prot. Dept.

\*\*\* Phys. Dep., Faculty of Science, Ain Shams Univ., Cairo, Egypt.

Abstract :

Neutron absorbed dose measurements from Cf-252 inside a perspex phantom filled with water has been carried out using LiF-700 and LiF-600. The dosimeters were previously calibrated against Co-60 Gamma radiation. The light output from the dosimeters has been transferred to Gamma dose using the calibration curve of each dosimeter. The phantom dimensions was 30x30x30 cm, and measurements were done in the X, Y and Z directions, i.e. (x,y) at  $z = 0$  and (x,z) at  $y = 0$ . Bare dosimeters as well as 0.5 mm Cd covered in one side and both sides dosimeters were used in the study. The absorbed doses from total thermal neutrons, forward thermal neutrons, and Albedo neutrons were estimated.

THERMOLUMINESCENCE PROPERTIES OF SOME  
EGYPTIAN NATURAL MATERIALS

M.S.ABDEL-WAHAB, H.M.EISSA<sup>1</sup>, M.SHARAF<sup>1</sup>, N.RABIE<sup>1</sup>, M.A.KENAWY<sup>2</sup>,  
and M.A.EL-FIKI

Ain Shams University, Faculty of Science, Physics Department,  
Abassia, Cairo, Egypt

<sup>1</sup> National Institut for Standards, Dokki, Cairo, Egypt

<sup>2</sup> University College for Girls, Ain Shams University, Cairo

ABSTRACT

The thermoluminescence (TL) properties of some natural samples which collected from the Eastern Desert of Egypt have been studied. TL response to gamma rays for the samples under examination show a linear response from 4.5 Gy up to 9 KGy followed by saturation. One of the samples was selected for further TL studies due to its high response for gamma doses and good glow curve shape. The sensitivity of this sample for gamma doses was enhanced by a factor of 85 % using the sensitization method. Fading rate for both material and sensitized sample have been also studied. This results demonstrate the usefulness of the sensitized sample in dosimetry, by storing it at low temperature.

THE FANO FACTOR FOR MIXTURES OF Ar AND H<sub>2</sub>\*

Mineo Kimura, I Krajcar-Brown,<sup>§</sup> Miso Inokui, and M. A. Dillon  
Argonne National Laboratory, Argonne, IL 60439 U.S.A.  
<sup>§</sup>Ruder Bošković Institute, Zagreb, Yugoslavia

This is the first report on the statistical fluctuations of ionization yield, or the Fano factor, for mixtures based on a rigorous treatment of the Spencer-Fano theory.<sup>1</sup> The Fano factor  $F(T)$  is defined as

$$F(T) = \frac{D(T)}{N_i(T)}, \quad (1)$$

where  $D(T)$  and  $N_i(T)$  describe the variance and ionization yield resulting from a single incident electron with initial energy  $T_0$ , respectively. These quantities satisfy equations

$$N_i(T_0) = n \int_1^{T_0} dTy(T_0, T) \sigma_i(T) \quad (2)$$

and

$$D(T) = n \int_1^{T_0} dT' y(T_0, T') p_i(T'), \quad (3)$$

where  $y(T_0, T)$ ,  $\sigma_i(T)$ ,  $p_i(T)$ , and  $n$  represent the electron degradation spectrum, the ionization cross section with threshold  $I$ , a quantity<sup>1</sup> calculable from  $N_i(T)$  and cross sections, and a number density of molecules, respectively.

From Eqs. (2) and (3), the Fano factor  $F(T)$  is readily calculable. The Fano factor for the ionization of the Ar-H<sub>2</sub> mixture is presented in Fig. 1 as a function of composition of Ar at  $T_0 = 1000$  eV. Note that the Fano factors at 0 and 1 of Ar composition correspond to those of pure H<sub>2</sub> and pure Ar, respectively. The Fano factor is a smoothly decreasing function of the composition and shows no sign of structure and anomaly at any certain composition.

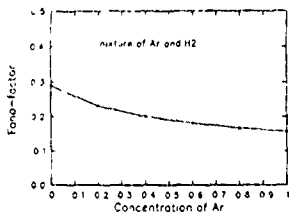


Fig. 1. The Fano factor as a function of the composition of Ar.

## Reference

- 1 M. Inokui, D. A. Douthett, and A. R. P. Rau, Phys. Rev. A 22, 445 (1980)

\*Work supported in part by the U.S. Department of Energy, Assistant Secretary for Energy Research, Office of Health and Environmental Research, under Contract W-31-109-Eng 38, and by the U.S./Yugoslavia Cooperative Research Program of the National Science Foundation

The submitted manuscript has been authored by a contractor of the U.S. Government under contract No. W-31-109-ENG-38. Accordingly, the U.S. Government retains a nonexclusive, royalty-free license to publish or reproduce the published form of this contribution, or allow others to do so, for U.S. Government purposes.

ENERGY DISPERSIVE X-RAY FLUORESCENCE SPECTROMETER  
USING RADIOISOTOPE SOURCE FOR EXCITATION

M.ENNAHI, M.FADEL, M.ABDULAZIZ, M.GADDARI  
and G.I.SAVELYEV

RADIOCHEMISTRY DEPARTMENT  
TAJOURA NUCLEAR RESEARCH CENTRE  
P.O.BOX 30878  
TRIPOLI LIBYA

The design of energy dispersive X-ray fluorescence spectrometer using annular radioactive sources F-55, Cd-109 and Am-241 for excitation and HPGe detector are described.

The aim of this work is to improve the sensitivity in trace element analysis by the optimization of the physical parameters of radioisotope source-specimen-detector system, the detector unit construction, the incident scattered radiation flow on the detector and the sample preparation techniques for analysis.

A calculation of the geometrical efficiency for analysis of the source-specimen-detector system is carried out. The obtained results for the system with different distances between its elements and the diameter of the specimen are presented.

The influence of the different surface regions of the specimen on the incident scattered radiation flow are investigated in detail. This work and the related data can be applied to create similar high efficiency spectrometer. Optimum conditions where annular source Cd-109 specimen distance is 7mm, pellet specimen diameter is 13mm, its weight is 0.15g and source activity is 320MBq then a detection limit below  $10^{-5}$  g for uranium is achieved.



PORTABLE GENERATOR OF NEUTRONS  
TYPE GN-01

Gulko V. M., Kolomietz N. F., Kuchnagra A. A., Mikhailenko B. V.,  
Yakovlev K. I.

Nuclear Research Institute of Ukrainian Academy of Sciences  
(252028, Kiev, USSR)

This work presents the results of the effort aimed at the development of a miniature neutron generator of 14 MeV for the radiation-aided explorations at laboratories and in the field.

The generator is capable of producing a flux of the D-T neutrons ranging from  $10^7$  to  $10^8$  s<sup>-1</sup> in a pulsed mode with a pulse repetition frequency of the 7 kHz and duty factor 2. Constructionally, the generator is an assembly of two units: the emitting unit and control unit interconnected by a cable about 10 m long. The emitting unit comprises the sealed accelerating neutron tube, type NTG-3, and high-voltage source of Cockcroft-Walton type. The neutron tube makes it possible to produce a neutron flux within the above-specified range as supplied from a cylindrical target 30 mm long with a diameter of 60 mm. The target, which is at a 'ground' potential, is surrounded by no hydrogen-containing materials and, therefore, the specimens to be irradiated can be arranged directly on its surface. The high-voltage source supplies an accelerating voltage of up to 110 kV and the pulsed voltage for the neutron tube ion source which is energized with high voltage. The emitting unit has been constructed as an airtight device 300 mm high with a diameter of 250 mm filled with liquid dielectric (transformer oil). The function of the control unit is to supply the power and control voltages to the emitting unit and to stabilize the neutron flux at a desired level with a precision of 10 per cent by controlling the parameters of the neutron tube. Provisions have also been made for suppressing the electronic component of the accelerating tube current.

# EFFECTIVE $\text{Bi}_4\text{Ge}_3\text{O}_{12}$ -CRISTALL $\gamma$ -SPECTROMETER IN EXPERIMENTS USING 14 MeV NEUTRONS

N.A. Belyusenko (The Krzhizhanovsky Power  
Institute, Moscow, 117927, USSR )  
N.F. Kolomiets (Institute of Nuclear  
Research of UAS, Kiev, 252028, USSR)  
V.K. Maidanyuk, V.M. Neplyuev, G.I. Primenko,  
Yu.A. Sedov, V.K. Tarakanov (Kiev State  
University, Kiev, 252017, USSR)

The nuclear physical micro- and macro experiments are carried out to confirm a working capacity of received data-programm complexes for research a propagation of ionizing radiation in matter [1-4]. In particular the application of  $\text{Bi}_4\text{Ge}_3\text{O}_{12}$ -cristall  $\gamma$ -spectrometer is very effective to improve the nuclear constant sistem for second foton angle distributions arising after neutron irradiation on micro-pieces of material.

We have determined the absolute effectivity of such spectrometer with 50 x 50 mm cristall taking into account of simultaneous  $\alpha$ -particle radiation from  $^{11}\text{B}(p,\alpha)^8\text{Be}$  reaction. The energetic calibration of the detector is carried out in the range up to 2 MeV using radioisotope sources in the range above 2 MeV using  $\gamma$ -radiation ( $E_\gamma = 4.44, 11.67, 16.11$  MeV) from resonance  $^{11}\text{B}(p,\gamma)^{12}\text{C}$  reaction with 163 keV proton beam.

The created spectrometer is used in exeperiments on irradiation  $^{27}\text{Al}$  samples with 14 MeV neutron source ( $\Phi_n = 5 \cdot 10^{11}$  n/s). The results on using this spectrometer for angle dependence investigation of second foton cross sections are reported.

## References:

1. Proc. of the 7th Inter. Conf. on Radiation Shielding. -V.1-3, Bournemouth- England:1988. -1195 pp.
2. Properties of Neutron Sources. IAEA-TECDOK 410. -Vienna: 1987. -430 pp.
3. Proc. of the 1 Inter. Symp. on Fusion Nuclear Technology. Parts A,B,C. -Amsterdam: Elsevier Science Publ. B.V. 1989.
4. Proc. of the 4th Inter. Symp. on Radiation Physics. - Sao Paulo, Brazil, 1988.

METAL-AND-TRITIUM (DEUTERIUM) TARGET  
FOR PRODUCING THERMONUCLEAR NEUTRONS

Golubev V. S., Kolomoietz N. F.  
Nuclear Research Institute of Ukrainian  
Academy of Sciences. (252028, Kiev, USSR)

Extensive use is now made of non-isotope sources of neutrons, the latter being generated as a result of these nuclear reactions:  $T(d,n)^4\text{He}$ ,  $D(d,n)^3\text{He}$ .

In this case the tritium (deuterium) is contained in the target bombarded by an accelerated neutron beam.

Employed most frequently are the solid-body targets which are made of metal hydrides applied to a metal base. The metals functioning as the base are copper, molybdenum and stainless steel. The tritium (deuterium) sorbents are titanium, zirconium, scandium. The Nuclear Research Institute has developed and is manufacturing the tritium and deuterium-containing targets capable of producing neutron fluxes in a range of up to  $10^{13}$  n/s.

Such targets of a standard series are manufactured with the sorbent mass density ranging from 0,5 mg/cm<sup>2</sup> to 3 mg/cm<sup>2</sup>. Whenever requested by customer the sorbent coats may be made extra thin (50 mg/cm<sup>2</sup>) and thick (up to 100 mg/cm<sup>2</sup>). This being the case, the minimum ratio of the quantity of the tritium (deuterium) atoms to one atom of the sorbent is 1,5. The sorbent coat thickness nonuniformity over the target surface is within 10 per cent, the tritium (deuterium) distribution irregularity does not exceed 15 per cent. The guaranteed storage term of the targets before the beginning of their operation is 18 months in the case of the titanium sorbent and 12 months - in the case of the zirconium or scandium sorbent. The target service life is dependent on numerous factors such as the deuteron beam ion composition, beam scanning over the target surface, target cooling method, contamination of the target surface by volatile hydrocarbons from the evacuation compounds.

EMPLOYMENT OF MINIATURE CONTROLLABLE NEUTRON SOURCES OF NEW  
GENERATION IN GEOPHYSICAL PROSPECTING FOR PETROLEUM AND GAS

Bespalov D.F., Martyanov I.A., Shikanov A.E.  
(Ramenskoe Branch of VNIIGeoInformsystem,  
Ramenskoe, Moscow Region, USSR)

In today's nucleonics-aided geophysical prospecting for petroleum and gas an extensive use is made of the pulsed neutron logging (PNL) methods based on the employment of the accelerative tubes (AT) to provide the information about the oil pool thermal-velocity neutron density decrement which is indicative of its petroleum content, transmissibility, position of the water-and-petroleum interface, etc. The utmost utilization of the PNL equipment capabilities requires better stability, greater neutron flux and longer life of the accelerating tube, efficient detector record, minimized resolution time of the analyzed signal processing system combined with the optimum time structure of the neutron field. With this purpose in view RB VNIIGeoInformsystem the designers of the NRI of the UAS have developed neutron sources based on the gas-filled AT capable of generating a high-stability flux of  $10^8$  n/s in pulsed periodic duty with a frequency of 0.1 to 1.0 KHz and of maintaining such mode of operation during 200 hours. These parameters provide for the realization of modern technologies based on the pulsed neutron-neutron and neutron-gamma logging as well as on their combinations employing the injection of a liquid labelled by a component with a high section of capturing the thermal-velocity neutrons. Besides, the development of the sources with a flux of  $10^9$  to  $10^{10}$  n/s utilizing the vacuum AT is now in progress for oxygen logging, direct finding of carbon, activation analysis and preparation of short-lived radionuclides for radioactive tracer techniques.

The results of the equipment tests are now analyzed while the geophysical data will be interpreted by modern computer-aided facilities specially developed for the particular purpose.

# MINIATURE NEUTRON TUBES FOR RADIATION-AIDED AND GEOPHYSICAL EXPLORATION

Gulko V.M., Kolomietz N.F., Mikhailenko B.V.,  
Tzibin A.S., Shikanov A.E., Yakovlev K.I.

Nuclear Research Institute of Ukrainian Academy of Sciences  
(252028 Kiev, USSR), Ramenskoe Branch of VNIIGeoinformsystem  
(Moscow Region, 140100, USSR)

Extensive application of the neutron radiation to the radiation-aided and geophysical explorations requires the development of more efficient controllable small-size neutron sources with accelerative tubes (AT) convenient in use.

The particular work is dealing with the theoretical investigation of the processes that occur in the sealed neutron tube while discussing the problems of obtaining, shaping and accelerating the ions and offering the analyses of the target thermodynamic characteristics.

The work also presents the results of the research effort aimed at the development of the vacuum neutron tubes with the laser-type ion source (LNT-2M), those with the vacuum-arc source (DIN-1), as well as of the gas-filled neutron tubes with the penning source (NTG-2) and with the orbitron source (NTG-3).

The main physicotekhnical characteristics of the above-mentioned neutron tubes are tabulated below.

Parameter	Neutron tube type designation			
	LNT-2M	DIN-1	NTG-2	NTG-3
Neutron Flux, n/s	$4 \cdot 10^9$	$1 \cdot 10^9$	$3 \cdot 10^8$	$2 \cdot 10^8$
Voltage, kV	150	130	100	100
Frequency, Hz	50	20	$(10 \cdot 10^4)$	$(10 \cdot 10^4)$

# MODELING OF $\alpha$ -, $\beta$ -, $\gamma$ - AND NEUTRON SOURCES USED FOR RADIATION PROCESSING OF SEMICONDUCTIV ELEMENTS

A.S. Tsybin (Moscow Engineering Physics  
Institute, Moscow, 115409, USSR)  
N.A. Belyusenko (The Krzhizhanovsky Power  
Institute, Moscow, 117927, USSR)  
N.F. Kolomiets (Institute for Nuclear Research of  
Ukrainian Academy of Sciences, Kiev, 252028, USSR)  
G.I. Primenko (Kiev State University, Kiev,  
252017, USSR)

The projecting, setting and using sources of  $\alpha$ -,  $\beta$ -,  $\gamma$ - and neutron radiation for processing of semiconductiv elements need mostly express consideration of optimal characteristics of dose radiation fields in objects and in protecting compositions [1,2].

The new issues of the analitical and physical modelling of these fields are reported. In particular this modelling gives a visual numeral (graphic or tabulated) interpretation of the radiative-physical characteristics formation. The results presented are concerned with:

- fast neutron ( $E_n=14$  MeV,  $\Phi_n=5 \cdot 10^{11}$  n/sec) irradiation for disk plate semiconductiv elements with taking into account of anisotropy and inuniformity of the radiation field;
- $\alpha$ -particle irradiation using  $^{238}\text{Pu}$ -source (square up to  $2400 \text{ cm}^2$ ) with taking into account of an accompanying  $\gamma$ -radiation from  $^{236}\text{Pu}$ -impurity and ( $\alpha$ ,  $n\gamma$ ) reactions in protecting screens including polymethylmethacrylate, Al, Fe, Pb;
- $\beta$ -particle and  $\gamma$ -ray irradiation using plate sources.

The modelling of penetrating  $\gamma$ - and n-radiation in multilayer protecting compositions (Fe + polyethylene, concrete, Pb, Li, U) is conducted by using one- and many dimensional computer programmes of multigroups calculation and on base of different nuclear constant systems.

## References:

1. V.I. Strizhak, G.I. Primenko e.a. - Proc. of the First Inter. Conf. on Neutron Physics. - V.4. - Moscow, TSNIATOMINFORM. 1988. - P.136.
2. N.A. Belyusenko, N.F. Kolomiets e.a. - Proc. of the XIX Inter. Symp. on Nuclear Physics. - Gaussig- DDR: Dresden, TUD, 1989.

# NEW SOURCES OF 14 MEV NEUTRONS FOR RADIATION PHYSICS AND THERMONUCLEAR RESEARCHES

A.S.Tsybin (Moscow Engineering Physics  
Institute, Moscow, 115409, USSR)  
N.A.Belyusenko (The Krzhizhanovsky Power  
Institute, Moscow, 117927, USSR)  
N.F.Kolomiets (Institute for Nuclear Research of  
Ukrainian Academy of Sciences, Kiev, 252028, USSR)  
G.I.Primenko (Kiev State University, Kiev,  
252017, USSR)

In the course of numerous radiative-physical and thermonuclear researches sufficiently intensive and relatively safety in maintenance the sources of 14 MeV neutrons with flux  $10^{10}$ - $10^{12}$  n/sec performed on the basis of low-voltage ion accelerators [1,2] were widely spread.

Modernized generator development of NG-200 type (accelerating voltage 200 kV) with flux  $2 \cdot 10^{10}$  n/sec and NG-300 (up to 300 kV) with flux to  $5 \cdot 10^{11}$  n/sec (Kiev State University) is reported. These sources were subjected to the necessary metrological certification in the automated complex of nuclear-physical and radiotechnical equipment. On the NG-300 generator basis the radiative-physical NOP-10 setting with flux up to  $10^{12}$  n/sec for neutron processing of semiconductiv elements has been developed.

Power sources increase of the considered thermonuclear neutrons type in the pulse mode is achieved by the neutron generator with laser-plasma ion source developed in Moscow Engineering Physics Institute. In frequency mode, at pulse duration  $\sim 10^{-6}$  sec neutron yield is about  $10^9$  imp $^{-1}$  and flux is  $\approx 10^{11}$  n/sec. On the collective ion acceleration basis at the initial accelerating voltage of 200 kV, the deuterons acceleration up to 1,2 MeV energy has been realized. At pulse duration  $\sim 10^{-8}$  sec the neutron yield achieves  $5 \cdot 10^7$  imp $^{-1}$ .

## References:

1. M.I.Dekhtyar, V.E.Maydanyuk e. a. - IAEA Advisory Group Meeting on "Properties of Neutron Sources". - Vienna, 1987, pp.365-367.
2. Yu.A.Bykovsky, A.S.Tsybin. - 4th Inter. Symp. on Radiation Physics. - Sao Paulo, Brazil, 1988, PD-2.

## INTENSE PULSE NEUTRON SOURCE BY LASER USED

A.S. Tsybin, K.I. Kozlovsky  
(Moscow Engineering Physics Institute,  
Moscow, 115409, USSR)

The creation of the intensive neutron sources (up to  $10^{12}$  n/sec) in conjunction with their small-size, comparative radiation safety, control advantage still remains to be the actual scientific technology task. One of the directions of its decision is connected with the realization of the more effective deuterium ion acceleration in the neutron generator with the double- and three-electrode accelerating system in a small-size accelerator tube.

Complex of researches directed to the pulse neutron generator creation with the laser-plasma ion source and the enhanced current value accelerating up to 200-300 keV ions is reported in the present work. The ion current increase is achieved by the effective magnetic isolation of the electron current component in a accelerating gap. The detailed physical researches of laser plasma produced by the radiation of the moderate intensity ( $10^9$ - $10^{11}$  W/cm<sup>2</sup>) on deuterium-rich targets, its behavior in magnetic fields up to 10 kGs allowed to realized a number of devices with the density of the emitted ion current more 10 A/cm<sup>2</sup>, pulse duration of 0,5-1,5 msec and stable functioning with 100 Hz frequency. The unique technical decisions of magnetic insulating system realization give a possibility to obtain the acceleration efficiency on the ion current of 75-80% [1]. All these results allowed to produce the source of neutrons (reactions D+D and D+T) with the yield up to  $10^9$  n/imp and and flux up to  $10^{11}$  n/sec at sufficiently low energy consumption. the energetic neutron price is less  $10^{-7}$  joule to one neutron.

The operation laser neutron generator project on the basis of the high current diode with magnetic isolation allowed to accelerate deuterons up to 1,0-1,2 MeV is presented.

## References:

- 1 V.M. Gulko, K.I. Kozlovsky et al. - Sov. News of Universities. Radiophysics. - 1990, V.33, N 8, pp.965-970.



## ESTIMATION OF COLLECTIVE DOSE DUE TO COSMIC RAYS IN EGYPT

M.A. Gomaa, A.A. Tawfik and H. Abu-Zaid\*

Radiation Protection Department, Atomic Energy Authority,  
Cairo, Egypt

As a part of the national plan for estimation of the ionizing radiation exposure of the population of the Arab Republic of Egypt, the collective dose equivalent due to Cosmic Rays is estimated.

In general, the calculated value indicated that the average annual effective dose equivalent due to the neutron and the ionizing components are found to be around 20 and 240  $\mu\text{Sv}\cdot\text{a}^{-1}$  respectively.

The estimated collective dose equivalent for Egypt is found to be around 12600 man-Sv, hence, the number of fatal cases due to cosmic rays in Egypt is 126 cases yearly.

---

\*Phys. Dept., College of Girls, Ain Shams University, Cairo, Egypt

X-RAY DETECTION CHARACTERISTICS OF GOLD PHOTOCATHODES  
AND MICROCHANNEL PLATES USING SYNCHROTRON RADIATION  
(10 eV - 82.5 keV)

M. Hirata, T. Cho, E. Takahashi, N. Yamaguchi,  
T. Kondoh<sup>1)</sup>, S. Aoki, H. Maezawa<sup>2)</sup> and S. Miyoshi  
Plasma Research Centre, University of Tsukuba,  
Tsukuba, Ibaraki 305, Japan

Recently synchrotron radiation from a storage ring has been utilized for calibration studies of various X-ray detectors. For incident X-ray beam monitors, gold photocathodes<sup>1</sup> are widely used. However, basic data on the photoelectric yield of Au are not available even at this time; in particular, for low energy photons from a few tens of eV to a few keV, only a limited amount of references is available. This energy range is important for the observation of radiation energy losses from fusion oriented plasmas.<sup>2,3</sup> According to this requirement, our investigations are motivated as a fundamental research to prepare the database for X-ray detector calibration (for microchannel plates (MCP)<sup>4</sup> and silicon surface barrier detectors<sup>5</sup>). The quantum efficiency of gold<sup>1</sup> is compared with the published data at some discrete energies, and we add several new data points in the 12-39.5 eV and the 2-8 keV.

From precise calibration of the incident X-ray monitoring system, the detection response of MCP<sup>4</sup> has been represented for X-rays from 10 eV to 82.5 keV along with its incident angle dependence. The MCP response shows jumps and humps at the edge energies of C, O, Si, Ba and Pb, and remains within about one order of magnitude for this wide energy range

\* Permanent address: <sup>1)</sup>JAERI, <sup>2)</sup>KEK

<sup>1)</sup>T. Cho et al., Rev. Sci. Instrum. **59** (1988) 2453

<sup>2)</sup>T. Cho et al., Phys. Rev. Lett. **64** (1990) 1373.

<sup>3)</sup>M. Hirata et al., Nucl. Fusion (to be published)

<sup>4)</sup>M. Hirata et al., Rev. Sci. Instrum. **61** (1990) 2566,  
N. Yamaguchi et al., *ibid.* **60** (1989) 368 and 2307.

<sup>5)</sup>T. Kondoh et al., *ibid.* **59** (1988) 2452

<sup>6)</sup>T. Cho et al., Nucl. Instrum. Methods **A289** (1990) 317

X-RAY DETECTOR CHARACTERIZATION AND APPLICATION TO  
PLASMA RESEARCHES

T. CHO, M. HIRATA, E. TAKAHASHI, N. YAMAGUCHI, T. KONDOH<sup>1</sup>,  
K. OGURA<sup>2</sup>, S. AOKI, H. MAEZAWA<sup>3</sup>, K. YATSU, AND S. MIYOSHI  
*Plasma Research Centre, University of Tsukuba,  
Tsukuba, Ibaraki 305, Japan*

Recent developments in controlled thermonuclear fusion experiments require new developments in wide energy range X-ray detectors (for example, microchannel plates (MCP)). For precise analyses of plasma electron behaviours, it is important to characterize these newly developed detectors as well as conventional type detectors (for example, silicon surface barrier (SSB) detectors), since even for these conventional detectors their X-ray responses were not reported experimentally except only in a few papers (1).

This paper reports the X-ray energy response of SSB detectors as well as their application to the observation of keV range electron component in the central-cell region of a plasma fusion oriented device of the GAMMA 10 tandem mirror (2). These data are essential to study the electron confinement property due to thermal barriers.

X-ray tomographic reconstruction technique is employed for the investigation of the 60 keV electrons in the thermal-barrier region (3) of GAMMA 10. Here, the first application of two sets of 50-channel MCP to plasma X-ray tomography has been carried out. This application of the MCP detectors has clarified the two dimensional structure of thermal barriers. The effect of the thermal-barrier potentials on the confinement of the central-cell electrons will also be presented for the first time at this symposium.

(1) T. Cho *et al.*, Nucl. Instrum. Methods A289 (1990) 317.

(2) T. Cho *et al.*, Phys. Rev. Lett. 64 (1990) 1373.

(3) T. Cho *et al.*, Nucl. Fusion 27 (1987) 1421

<sup>1</sup> Japan Atomic Energy Research Institute, Japan.

<sup>2</sup> Niigata University, Niigata, Japan.

<sup>3</sup> National Laboratory for High Energy Physics, Japan.

Session III

RADIATION IN FUNDAMENTAL RESEARCH

## SEARCH FOR RARE DECAYS USING LOW-LEVEL GAMMA-RAY SPECTROMETRY

I. Sykora, J. Staníček, M. Durčík, P. Povínek  
Comenius University, Department of Nuclear Physics,  
842 15 Bratislava, Czechoslovakia

In the low-level gamma-ray spectrometry the crucial problem is the level of background, because the probabilities of investigated rare processes are very low (usually below  $10^{-3}$ ). Therefore, these investigations require a very good passive shield, accommodating single or coincidence/anticoincidence spectrometers.

In this work we tested a special low background HPGe detector (70% relative efficiency, 2.12 keV energy resolution for 1.33 MeV, low background Cu cryostat) in a large shield - (the inner dimensions of 0.8 m x 0.9 m x 1.7 m) designed for low-level gamma-ray spectrometry. The shield was made of lead, iron, copper and polyethylene. The background reduction of 60-250 times has been obtained in the energy interval 0.1-3 MeV (e.g. 330 times for the  $^{40}\text{K}$  peak).

The background levels in the shield may be considerably influenced by high radon concentrations in the air. The long term measurements have shown 11 times increase of the intensity of 609 keV peak if the shield was not properly ventilated.

A typical higher-order process, the internal bremsstrahlung, has been measured for  $^{32}\text{P}$ ,  $^{54}\text{Mn}$  and  $^{204}\text{Tl}$ . The internal bremsstrahlung spectra of  $^{55}\text{Fe}$  have been looked for from the point of view of a search for a heavy 17 keV neutrino.

Effects of Irradiation by High Energy Particles  
on Oxygen Precipitation in Cz Silicon.

A. A. Groza, V. I. Varnina, L. G. Nikolaeva, M. I. Starchik,  
G. G. Shmatko, K. M. Shevtsov.

Institute for Nuclear Research, Ukrainian Academy of Science,  
Kiev, USSR

The oxygen precipitation kinetics in Cz-silicon was investigated in dependence of irradiation conditions (neutrons, protons,  $\gamma$ -rays, flux variation) and subsequent heat treatment.

It is known that oxygen precipitate growth is controlled not only by diffusion flows of impurity but point defects (interstitials, vacancies) also. That's why the point defects supersaturation can lead to the increase (decrease) of critical radius of precipitate nuclei. It is possible to create the conditions for the supersaturation of both types of point defects by high energy particles irradiation and to affect the oxygen precipitation in silicon. It was received the acceleration of oxygen precipitation in irradiated crystals. The increase of nuclei concentration and the change of precipitation kinetics were observed. The effect of the type and the value of irradiation fluence on the structure of oxygen precipitates was shown. It was stated that point defects concentration was the main factor affecting the precipitate structure. The accumulation kinetics for some types of defects with the increasing of irradiation flux and annealing time was studied. It was shown the prevail over formation of stacking faults in high irradiated crystals after heat treatment take place. The useful factors of radiation at using of gettering action of oxygen precipitates are noted.

## METASTABLE CENTERS FORMATION IN IRRADIATED SILICON.

R. I. Guchetl, P. M. Gringhtein  
State Institute for Rear Metals "Giredmet", Moscow, USSR

Initial FZ-Silicon, n-type conductivity, resistivity 500 Ohm cm was irradiated by high-energy (20-30 MeV) gamma-quantums in order to introduce  $10^{14}$  cm<sup>-3</sup> atoms of Al in the result of nuclear reactions ( $\gamma, n$ ) and ( $\gamma, p$ ).

After irradiation the sample was annealed in the gradient of temperatures in the range 300-800°C for different times with different rates of cooling. After each cycle of annealing the resistivity was measured along the sample with the help of 2-probe technic and also type of conductivity by thermal probe method. The following main features of annealing were discovered:

- in the range 300-550°C the defects of acceptor type are forming similar to the case of neutron irradiation;
- in the range of 550-650°C these defects anneal with the forming of centers (concentration  $\sim 10^{13}$  cm<sup>-3</sup>) that anneal at temperatures greater than 200°C (metastable centers). These centers may be frozen when cooling the sample with the speed 20 °C/sec to room temperature. The stage of formation of metastable centers can be well seen on resistivity-temperature dependence measured after fast cooling of the sample. In this case the dependence has a maximum of resistivity in the range 550-650°C. This maximum disappears after annealing at temperatures higher 200°C or after full annealing of radiation acceptors. This stage of annealing of radiation acceptors followed by metastable centers formation has never been observed earlier;
- while the temperature becomes greater than 650°C the resistivity goes to the value depends on the concentration of Al.

In the whole range of temperatures of annealing p-type conductivity was observed.

Similar stages of annealing were observed in silicon irradiated by high-energy protons with consequent nuclear formation of Al, and in p-type silicon (boron doped) irradiated by reactor neutrons. We suppose that the stage of metastable centers formation is connected with reaction between the products of radiation acceptors annealing (vacancies or self-interstitials) and atoms of acceptor impurities.

# FREE-CARRIER SCATTERING IN ELECTRON-IRRADIATED III-V SEMICONDUCTORS

E.Yu. Brailovsky, N.E. Grigoryan, Z.A. Demidenko and I.G. Megela

Institute of Nuclear Research, Academy of Sciences of the  
Ukrainian SSR, Kiev, Ukraine

The free-carrier scattering mechanism peculiarities in irradiated GaP and InAs crystals have been studied by optical IR absorption and electrical measurements. Irradiation was made with 7.5 to 50 MeV electrons (total flux up to  $1.5 \cdot 10^{16} \text{ e cm}^{-2}$  at room temperature). Optical transmission measurements were done at 300 and 80 K in the wavelength region from 2 to 15  $\mu\text{m}$ . In this study the single crystal samples n- and p-type GaP doped with Te and Zn and n-type InAs undoped and doped with Sn (carrier concentration  $n = 2 \cdot 10^{18}$  to  $2 \cdot 10^{19} \text{ cm}^{-3}$ ) were used.

Free-carrier absorption (FCA) coefficient for all non-irradiated samples have the frequency dependence  $\alpha \sim \omega^{-r}$ , the value of  $r$  is determined by the scattering mechanism and is equal to 1.7, 2.15 and 2.9 for n- and p-type GaP and n- InAs respectively.

We observed the monotonously decrease in  $n$  value in the n- and p-type GaP crystals as a result of irradiation. On the contrary, in the n- InAs crystals the  $n$  value increase with irradiation dose as  $\phi_0^{0.5}$ . Hall mobility decrease for all cases but its change cannot be explained by the additional ionized centre scattering.

From the general consideration it follows that the value of  $r$  must increase with introduction of the charged radiation defects (RD). However from absorption measurements we found the value of  $r$  decrease with irradiation dose in all cases up to 1.1, 1.5 and 1.6 for n- and p-type GaP and n-InAs crystals respectively. Simultaneously with  $r$  decrease we observed the growth of FCA cross section ( $\alpha/n$ ) at fixed wavelength. The chemical doping do not results in similar of changes  $r$  and  $\alpha/n$  values. These facts show the appearance of the additional scattering mechanism caused by the RD introduction.

It is known that RD in the III-V compounds is characterized by great specific deformations.

So we have considered within the framework of the theory of deformation potential a mechanism of the scattering by the static deformation fields which appear in the vicinity of RD. The absorption coefficient was calculated in the second order of perturbation theory. It is obtained that the scattering intensity for this mechanism  $A^*(\omega) \sim \omega^{-r}$ , and therefore the total coefficient of FCA can be described approximately by the dependence  $\alpha \sim \omega^{-r}$ , where  $1/2 \leq r \leq 7/2$ . With increasing the concentration of RD the contribution of this mechanism into FCA grows. Thus, the suggested mechanism allows one to explain the  $r$  decrease in the frequency of local deformation fields in the vicinity of the point RD.



# Electronic Structure and Spectra of Irradiative Impurity Crystals

N.Kulagin

Physics-Technology Institute, 244030 Sumy, USSR

The letter is devoted to consideration of new approach in the investigation of the radiation colour centers - RCC in impurity wide-zone solid states. Experimental technoks for study before and after  $\gamma^-$ ,  $e^-$  irradiation are: optical absorption and luminescence (140-100 000 nm), ESR 5X-band) and original valence shift method of X-ray lines[1]. The theoretical foundation is self-consistent field theory for clusters [2]; The method of valence shift of X-ray lines allow to determine of ion's valency and constructe to the model of RCC.

It was founded for oxide single crystals with garnet, perovskite and simple oxide structure and others doped by ions of iron and lanthan group elements the types and concentration of RCC are connected with structure defects and impurities. After irradiation in that crystals we have several main RCC: impurity clusters with change of ions valency, F-like and  $V_K$ -centers with local or nonlocal charge's compensation. Mechanizms of charge compensation was investigated by ESR-method and thermoluminezcence technik. We have the best correspondity of the theoretical calculations of electronic structure of RCC and data of optical and ESR experimants in most cases. And in that cases our identification of RCC is true and we have real picture if radiation stimulation processes in doped wide zone crystals[3].

1. N.Kulagin, D.Sviridov. Methods of Electronic Structure Calculations for Free and Impurity Ions. M. 1986.
2. N.Kulagin. J.Mol.Struct. 19 (1990) 16
3. N.Kulagin, D.Sviridov. Introduction to Doped Crystals Physics. Kharkov. 1990.

MOSSBAUER EFFECT OF  $^{57}\text{Fe}$  IN BARIUM FERRITE

Li Xiang-dong and Zeng Ling-zhi \*

Polymer Research Institute, Chengdu University of Science and  
Technology, Sichuan 610065, P.R. China

\* The 44th Electronics Research Institute, P.O.Box 1102 Yongchuan,  
Sichuan 632163, P.R. China

Mossbauer spectra were taken of barium ferrite at temperatures ranging from 15K to 733K. The hyperfine field  $H$ , centre shift  $\delta$ , and recoilless fraction  $f$  for ferric ions as function of temperature at different lattice sites were determined. Above 300K, the effective vibrating mass of the Mossbauer atom at the Fe(2) site  $m_{\text{eff}}=65\pm5$  (in U) is larger than those at other sites, indicating a stronger covalent bonding with the neighbour oxygen atoms. We also discuss the temperature dependence of the unusually large quadrupole splitting due to ferric iron in the bipyramidal position, with a very small Mossbauer lattice temperature  $\theta=233\pm15\text{K}$ .

# THE REFLECTION OF FAST ELECTRONS FROM A SURFACE OF SOLIDS

Luo Zhengming and Cheng Bo

Center for Radiation Physics,  
Institute of Nuclear Science and Technology,  
Sichuan University, P.R.China

Using the bipartition model of electron transport, this paper puts forward an effective method to calculate reflection of fast electrons from a surface of solids. The method can not only calculate the total reflection coefficients with high precision, but also give precise angular distribution, energy spectra and the angular correlations of energy spectra of reflected electrons. This paper will systematically give out the reflection data for electrons with various energies normally incident into C, Al, Cu, Sn and Pb by using the bipartition model of electron transport.

EXCITATION FUNCTIONS FOR ALPHA INDUCED  
REACTIONS AND PRE-EQUILIBRIUM EFFECT

B. P. Singh and R. Prasad

Department of Physics, A. M. U. Aligarh (India)

In  $\alpha$ -induced reactions initiated by few tens of MeV particles, the reaction mechanism is considered to proceed through equilibrium as well as pre-equilibrium (PE) emissions of particles. The relative contribution of these processes is still not well known. Pre-equilibrium emissions are characterised by slowly descending tails of the excitation functions, forward peaked angular distribution of particles and stretched particle distribution in the angular momentum space. The study of excitation functions (particularly the high energy tail portion) may give useful information about pre-equilibrium emission. With a view of studying pre-equilibrium emission, a programme of precise measurement of excitation functions for  $\alpha$ -induced reactions in light medium and heavy nuclei at moderate excitation energies has been undertaken. The analysis of the excitation functions has been done using Hauser-Feshbach model for the compound nucleus component and exciton model is used for simulating pre-equilibrium component. From the analysis of the data, interesting trends in the pre-equilibrium fraction (FR), which is the measure of relative strength of PE-component, with energy and mass number have been observed.

## SUM PEAK METHOD FOR K-CAPTURE PROBABILITY STUDIES

Kulwant Singh and K.S. DhillonDepartment of Physics, Guru Nanak Dev University,  
Amritsar-143005, India

Sum peak method is based on the summing of cascade gamma ray photons of two different energies which fall within the resolving time of the detector. In addition to singles, X-ray and gamma-ray peaks, sum peaks of energies equal to the sum of the energies of the individual cascading photons also appear. This method is used to determine relative K-capture probabilities to the 1085, 1233, 1529 and 1649 Kev excited states of Sm-152. The radioactive isotope Eu-152 in the form of EuCl in HCl solution was obtained from NBS, Washington, USA. For intensity measurements a weak point source was prepared by drying solution in a cavity drilled on a piece of perspex sheet under an infra red lamp. Similarly a very weak point source was prepared for taking sum spectra in the close geometry set up. Since the accuracy of the relative K-capture probability is sensitive to the correctness of the sum peak area, clean and well resolved sum peaks were used. The count rate was adjusted to be of the order of 1000 counts per second to avoid accidental coincidences. To measure gamma ray intensities the areas under the various peaks were corrected for summing loss or gain due to cascading gamma rays by a computer programme KORSUM.EXE, developed by Debertain and Schotzig.  $1086 + K_{\alpha}$ ,  $1112 + K_{\alpha}$ ,  $1408 + K_{\alpha}$  and  $1529 + K_{\alpha}$  Kev sum peaks were analyzed and K-capture probabilities were found to be 0.853(79), 0.848(79), 0.830(70) and 0.805(81) to the 1085, 1233, 1529 and 1649 Kev levels respectively.

## Change of Ion's Valency in Solid States in External Fields

N.Kulagin

Physics-Technology Institute, 244030 Sumy, USSR

One of the main problem of radiation solid state physic is stability of the electronic state of ions. Change of ion's valency under irradiation lead to change of electronic structure, conductivity, optical properties and others. For ions with unoccupied d- or f-shell (iron, lanthan etc. group elements) in different crystals that problem solved by method of valence shift of X-ray lines[1]. The experimental procedure of this method was realized with help of microanalyser (Cameca or Jeol). We determined ion's valency and its change under  $\gamma$ -,  $e^-$ - and  $n$ - $\beta$ - irradiation and thermal treatment for different ions in oxide wide zone crystals such as: simple oxide, perovskite structure and complex garnets, halogen crystals and phosphat ceramics.

The ion's valency stability of ions in their compounds have been defined for different amount of radiation. Kinetic and mechanisms of decay of radiation centers was study in detail in our approach of impurity clusters [2];

1. N.Kulagin, D.Sviridov. Methods of Electronic Structure Calculation for Free and Impurity Ions. M. 1986.
2. N.Kulagin, D.Sviridov. Introduction to Doped Crystals Physics. Kharkov. 1990.

ON THE DEPOPULATION OF THE 6 h ISOMERIC STATE OF Tc-99  
BY PHOTON IRRADIATION

M. Krmar, I. Bikit, J. Slivka, M. Vesković, Lj. Čonkić, Z. Kuzmanović\*

Institute of Physics, Faculty of Science,  
\*Institute of Oncology, Faculty of Medical Science,  
University of Novi Sad, Yugoslavia

The ( $\gamma, \gamma'$ ) reactions on isomeric states can excite levels, which in subsequent decay cascade skip the isomeric level. Such depopulation of the isomeric states is easily measured in rare cases where the isomer decays much slower than the ground state. Recent results<sup>1</sup> on the depopulation of Ta-180m exhibit a cross section two orders of magnitude higher than that for isomer production. In the most common cases where a short lived isomer decays to a stable ground state the observation of the depopulation is much more difficult because a small change in the activity of the isomeric state due to photon irradiation must be detected. The results of such measurements at high count rates are strongly influenced by systematic errors. In order to explore the limitations of this type of measurements we investigated the depopulation of Tc-99m by irradiation with the bremsstrahlung of the 15 MeV linac. The decay of the 40 mCi activity source was followed before and after the 2 h irradiation. In the first runs an unexpectedly high activity change of 0.2% was registered. The possible explanations of this result in terms of systematic error analysis and open reaction channels will be given in detail.

1) C. Collins, C. Eberhard, J. Glesener and J. Anderson, Phys. Rev. C37 (1988) 2267

SLOWING-DOWN OF POLARIZED MUONS ( $\mu^-$ ) IN A AL-C-AG TARGET

ANA PROYKOVA

UNIVERSITY OF SOFIA, FACULTY OF PHYSICS, ATOMIC PHYSICS  
DEPARTMENT, SOFIA-1126, 5 A.IVANOV BLV., BULGARIA

The present study is a part of vast investigation of the muonic neutrino helicity in the reaction  $^{12}\text{C}(\mu^-, \nu)^{12}\text{B}$  (ground state) from a simultaneous measurement, [1], of the average polarization ( $P_{av}$ ) of the recoil ( $^{12}\text{B}$ ) along the muon polarization ( $P_\mu$ ) at capture and the polarization ( $P_L$ ) of the recoil along its velocity  $\vec{v}$  (opposite to the direction of the emitted neutrino).  $P_{av} = \langle \vec{J} \cdot \vec{v} \rangle / J$  is a mirror invariant and  $P_L = \langle \vec{J} \cdot \vec{P}_\mu \rangle / J$  is a parity violating quantity;  $\vec{J}$  is the nuclear spin of B. The alignment of the recoil nucleus with respect to  $\vec{v}$  is, unless parity is conserved, not an independent observable. The ratio  $P_{av}/P_L$  depends stronger on the dynamics of all the processes involved than either, and is a function of  $P_\mu$ .

To obtain  $P_\mu$  for an initially polarized muon beam  $P_\mu^0=1$ , the scattering processes depending on the particles polarization are studied when a negative muon slows down in a Al-C-Ag target consisting of 1000 sandwiches of a very thin carbon foil (so as the recoil nucleus  $^{12}\text{B}$  to be able to escape from the foil) between layers of Al and Ag, [1]. The kinetic energy of the muons captured in  $^{12}\text{C}$  is considered to be less than 100 eV. The kinematics of the muon slowing down is similar to that in [2], but with the scattering cross sections which are polarization dependent.

The angular distributions of muons having a kinetic energy in the intervals (10-50) eV, (50-80) eV, and (80-100) eV are presented. The fractions of muons retained their initial  $P_\mu^0$  polarization are calculated. The number of muons captured by C atoms is determined under the assumption that a muonic atom can be created in all the cases of the muon energy given above.

1. L. Ph. Roesch, V. L. Telegdi, P. Truttmann, A. Zehnder, L. Grenacs and L. Palfy, Phys. Rev. v. 46(1981)No. 23, p. 1507.
2. A. Proykova, J. Phys. D, v. 12(1979)p. 87.



# COMBINATION OF DIRECT X-RAY METHODS IN ATOMIC STRUCTURE STUDIES OF DISORDERED ALLOYS

N.V.Ershov. Institute of Metal Physics, Ural Branch of the  
USSR Academy of Sciences, 620219 Sverdlovsk GSP-170

Review of the atomic structure investigations of disordered alloys by such direct methods as X-ray diffraction and X-ray absorption spectroscopy, using synchrotron radiation, is presented. Analysis of the results shows that the short-range order in solid solutions, local structure of quasicrystal phases, metal glasses etc. are among the most intricate subjects. In such studies an approach, when the same samples are investigated by different methods and all gained information is used for the analysis of the results, becomes almost traditional.

Another approach utilizes the regular methods of the solution of the inverse problems /1/. The data of several experiments may be processed in the frameworks of the single mathematical algorithm /2/ and/or applied as an a priori information, that permits to restrict the multitude of the obtained solutions. This ensures more reliable structural parameters and reduces the errors of their determination.

New approaches allowed us to obtain unique physical results. So, our study of the short-range order structure of amorphous Fe-B alloys by EXAFS and X-ray diffraction has confirmed that the relaxed random closed packing model is suitable for description of their atomic structure /3/. For the first time we have obtained the local distribution of nitrogen atoms around copper atom in the Cu-aluminum complexes /4/. The study of local ordering in iron-nickel Invar alloys has shown that in initial quenched state there is a short-range decomposition.

## REFERENCES

- /1/ A N Tikhonov, V Ya Arsenin Methods of Solving Ill-Posed Problems, Izd Nauka Moskva 1979, 285 p
- /2/ Yu A Babanov et al. Phys stat.sol (b),105,747(1981)
- /3/ Yu A Babanov et al J.Non-Cryst.Solids,79,1(1986)
- /4/ K A Asaturian et al NIM,A261,187,1987)

INVESTIGATION ON THE EFFECT OF SOLVENTS ON THE DIFFUSION  
OF IONS BY RADIOACTIVE TRACER METHOD

A. Das and S.N. Changdar

Physics Laboratories, Bose Institute, 93/1, A.P.C.Road,  
Calcutta-9, INDIA

In recent years there have been spectacular developments in the study of diffusion phenomena in liquids. Computer simulation techniques have added a new dimension in this field and there has been some new additions in the radioactive tracer technique <sup>1</sup>. But most of the Inelastic neutron scattering, pulse NMR and optical measurements in electrolyte solutions centered around ion-ion interaction with no emphasis on ion-solvent interaction. By using the sliding cell method developed in our laboratory <sup>2</sup> and using both  $H_2O$  and  $D_2O$  as solvent we are trying to see both ion-ion and ion-solvent effects.

Instead of the conventional method of measuring diffusion coefficient by noting the change in radioactivity at a fixed plane in a liquid as a function of time, our technique measures the time dependence of what is effectively an weighted spatial average of radioactivity. This not only allowed a simplification of experimental arrangement but also pushed down the uncertainties associated with experimental diffusion coefficients by almost an order of magnitude. The technique is based on sliding cell mechanism and the experimental geometry consists of radioactive and non-radioactive columns of equal lengths with the radiation detector placed vertically over the diffusion column.

The experiments clearly show a decrease in diffusion coefficient with increasing concentration in both  $D_2O$  and  $H_2O$  systems. The diffusion coefficients at lower concentrations obey Nernst's law but at higher concentrations they can be explained by Onsager's phenomenological theory. The difference of diffusion coefficients in  $D_2O$  and  $H_2O$  systems of  $^{204}Tl$  ion showed indications of fundamental changes in the structure of solvent upon dissolution of a salt. We are carrying out experiments with other radioactive isotopes also.

<sup>1</sup> P.Passiniemi - J.Soln.Chem. 12, 801 (1983)

<sup>2</sup> S.N.Changdar - J.Pure and Appl. Phys. 11, 811 (1973)

<sup>3</sup> D.E. Woessner et al - J.Chem. Phys. 49, 371 (1968)

PION-INDUCED FISSION OF  $^{209}\text{Bi}$ , R.J.Peterson (University of Colorado, USA); S. de Barros, I.O. de Souza, M.B.Gaspar, H.Schechter and R.Donangelo( Universidade Federal do Rio de Janeiro, Brasil)

For fission in  $^{209}\text{Bi}$  we have collected an extensive body of data over a wide range of beam energies. These data in several parasitic setups are illustrated in Fig. 1. We note the data show a sharp drop in the fission cross section when compared to the calculated reaction cross section at approximately 200 MeV. We suggest that this drop could be due to some fast mechanism that de-excites the  $^{209}\text{Po}$  system into a daughter of much lower fission probability. The sharpness of the drop suggest a phase change.

We have used the multifragmentation code of Bondorf et al.<sup>1)</sup> to compute the probability of fragments (Z,A) being produced for a range of excitation in  $^{209}\text{Po}$ . We use earlier<sup>2)</sup> computed fission probabilities (for Bi itset) to estimate the yield of fissioning final nuclei. Residual nuclei with A above 200 were included. These probabilities are shown in Fig. 2, demonstrating a strong maximum at  $E^*/A$  near 1.4. This value is close the nuclear excitation obtained through complete absorption of a 132 MeV pion. The similarity in shapes measured and computed is suggestive that enough nucleons are removed through this mechanism so as to diminish the fission yields.

More runs are planned to verify the data, and a more precise weighting of the computed fission probabilities is being carried out. If our approach is correct, the observed drop in fission cross sections should not be observed for very heavy targets, since removal of a handful of nucleons still leaves a highly fissionable system. It is also important to remark that a detailed study of track lengths for spontaneous fission and pion-induced fission of U and of Bi show differences that may also be indicative of some process other than simple fission.

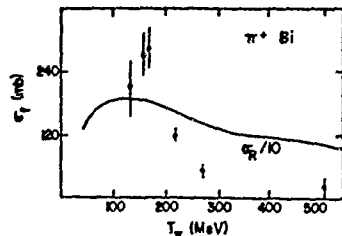


Fig. 1 Preliminary measured cross sections for fission of  $^{209}\text{Bi}$  induced by  $\pi^+$ . The curve shows the reaction cross section computed by a first order optical potential.

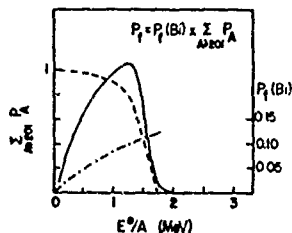


Fig. 2 Probabilities to form nuclei with mass number above 200 calculated with the multifragmentation model of ref. 1 (dashed curve). The solid curve shows the fission probabilities after multifragmentation, assuming the residual nuclei fission with the same energy dependence as Bi. The dot-dashed curve shows the fission probabilities calculated for Bi using a standard code<sup>3)</sup>.

#### References:

- 1) J.P.Bondorf et al., Nucl. Phys. A443, 231 (1985);  
ibid, A444, (1985) 460.
- 2) K.H.Hicks, Ph.D. Thesis, University of Colorado (1984).
- 3) M.Blann (ALICE) Report Rochester.

## Fundamental Parameters Determination Using the Tilt of the Propagation Plane

Héctor Jorge Sánchez \* and Marcelo Rubio <sup>†</sup>

Facultad de Matemática, Astronomía y Física,  
Universidad Nacional de Córdoba,  
Laprida 854 CP 5000 Córdoba  
ARGENTINA

### Abstract

A method to obtain fundamental parameters, as fluorescence yields ( $\omega$ ) and emission probabilities ( $\Gamma$ ), based on the propagation plane inclination is presented. Measurements on binary samples were carried out to determine the product  $\omega\Gamma$ , for  $k_{\alpha}$  lines in elements such as Cr, Fe and Ni.

The results shown in this work are confronted with the ones reported in well known compilations of other authors.

Our procedure can be considered a new alternative to increase the available set of methods to fundamental parameters measuring.

---

\*Fellowship of CONICOR, Córdoba ARGENTINA

<sup>†</sup>Member of CONICET, ARGENTINA

Session IV

RADIATION IN MEDICAL, ENVIRONMENTAL AND EARTH SCIENCES

MONTE CARLO CALCULATIONS OF ELECTRON  
ENERGY LOSS SPECTRA IN WATER\*

C. J. Tung and T. J. Chen  
Institute of Nuclear Science  
National Tsing Hua University  
Hsinchu, Taiwan, R. O. C.

## ABSTRACT

Energy loss spectra of monoenergetic electrons and beta particles in water have been calculated using the Monte Carlo technique. Differential inverse mean free paths of electrons for inelastic interactions with the valence band of water were estimated using the Born-Bethe formula together with the Moller exchange effect terms. Differential cross sections of electrons for ionizations of inner shells were evaluated using the quantum mechanical hydrogenic model. Computed results on transmitted energy loss spectra, slowing down spectra and pathlength distributions of electrons in water were compared with those calculated using the Landau theory and the convolution method. These results have direct applications in radiation dosimetry, microdosimetry and quantitative surface analysis.

---

\*This research was supported by the National Science Council of the Republic of China.

# EFFECT OF AIR BENT DUCT ON THE DISTRIBUTION OF GAMMA DEPTH DOSES IN CONCRETE SHIELD

S.A.BENAYAD , T.S.AKKI, F.A.EL-BARKOUSH and R.M.MEGAHID

Radiation Shielding and Neutron Physics Division,  
Department of Physics and Material Science,  
Tajura Nuclear Research Center,Tripoli ,Libya

## ABSTRACT

This work is concerned with the study of the effect of air bent duct pierced in ordinary concrete shield on the distribution of total gamma-rays depth dose when collimated beam of reactor radiation is passing through the duct. The concrete medium under investigation is made from limestone ,sand and portland cement and has a density of  $2.3 \text{ ton.m}^{-3}$ . The air bent duct was made from polyethylene with diameter of 10 cm and has two right angle bents. The gamma dose was measured by thermoluminescence dosimeter discs of  $^7\text{LiF}$  embedded in teflon matrix . The depth doses were measured at different locations in planes normal to the beam entrance and located at different concrete thicknesses. Measurements were initially performed in solid concrete shield then repeated in concrete shield pierced with duct.

The measured responses of the detector were reduced to absolute values of gamma doses using the calibration and normalization coefficients.The obtained results are presented in the form of attenuation curves in planes normal and parallel to the beam axis for solid and ducted concrete media .In addition,the duct effect,i.e. the ratio between the dose value measured at any location in presence of duct and that measured in solid concrete was derived and plotted versus concrete thickness for planes normal and parallel to the beam axis.



## TRANSMISSION MEASUREMENTS OF 0.77 MeV ELECTRONS THROUGH LIQUIDS

R.K. BATRA

PHYSICS DEPARTMENT, PUNJAB AGRICULTURAL UNIVERSITY, LUDHIANA

- 141004 (INDIA)

Measurements of the mass attenuation coefficient  $\mu$  and the range  $R$  of 0.77 MeV electrons from  $Tl^{204}$  in Aluminium as a standard absorber and the liquids such as Methanol, Benzene, Toluene, Water, Heavy Water and Glycerine whose densities vary from 0.79 to 1.26 g/c.c., are reported using a thin window Proportional Counter. The electron transmission in all the liquids is found to follow the exponential behaviour down to 4 o/o. The measured  $\mu$  values in liquids except Glycerine are larger by a factor of 1.7 to 2.3 relative to Aluminium. However, the experimental and the predicted values of the penetration constant ( $\mu \times R$ ) are in excellent agreement. Further, the measured difference of 13% in mass attenuation coefficients in Benzene and Toluene (equal density liquids) is, perhaps, due to the difference in their structures or compositions.

## SHIELDING STUDY FOR THE 8 GEV SYNCHROTRON RADIATION FACILITY IN JAPAN

N.Sasamoto, N.Kurosaka and Y.Harada  
Japan Atomic Energy Research Institute

In Japan a project is in progress to construct the 8 GeV class Synchrotron Radiation Facility (SPring-8) aiming to promote the most advanced research in a wide range of scientific and technological fields. Its construction started in FY1990 and is scheduled to be completed in FY1997, starting services in FY1998. SPring-8 is an electron(positron) accelerator complex consisting of a 1 GeV linear accelerator and an 8 GeV synchrotron as injectors, and a full energy storage ring, circumference of which is 1436 m, with the maximum stored beam of 100 mA.

Based on ALARA principle, dose limit for the bulk shield design to the controlled area is set to be  $2\mu\text{Sv/h}$  and to members of general public at the nearest access is  $50\mu\text{Sv/y}$ .

For shielding calculations in the forward direction to the electron beam ( $\theta = 0^\circ$ ), Swanson's formula including inverse square law was used for the photons(bremsstrahlung). Muons were also necessary to be taken into account in the forward calculations. On the other hand, for lateral calculations ( $\theta = 90^\circ$ ), Jenkins' formulas were employed for neutrons and photons, separately.

Beam loss assumption is one of the most important but actually indefinite parameter for estimating radiation sources. In the linear accelerator, beam loss is generally considered to be very small for regions but for 7 slit parts. In the synchrotron and storage ring, however, large beam loss is assumed at their injection regions and the rest parts of beam loss are assumed to be equally divided into 34 and 52 points where  $\beta$  function takes its maximum, in the synchrotron and storage ring, respectively. In addition to the above steady state beam loss, accidental beam loss scenario was also considered.

For a distance of about 100 m to the site boundary, the annual skyshine dose was estimated to be  $15.5\mu\text{Sv}$ , based on Stevenson-Thomas' formula. Here, we assumed maximum annual operation time as 5,500 hours. Further, in order to fit to Stevenson-Thomas' formula which requires neutron intensity as radiation source data, total dose at the shield surface is assumed to be due to neutrons only, i.e. photon dose there is equivalent to neutron one. Besides, 1/E energy spectrum is conservatively assumed for the leakage neutrons from the shield wall.

## RADIOLOGICAL IMPACT OF POWER PLANTS DURING CONVECTIVE STORM

Boško Telenta<sup>1</sup>, Dragoljub Antić<sup>2</sup><sup>1</sup>Federal Hydrometeorological Institute, Belgrade<sup>2</sup>The Boris Kidrič Institute of Nuclear Sciences, Vinča,  
POB 522, 11001 Belgrade

The transport of radionuclides from the power plants ( nuclear or fossil fuel plants ) can be simulated using various numerical simulations. A two-dimensional version of the cloud model has been adapted and used to simulate transport of radionuclides emitted from the power plant to the atmospheric environment.

A convective storm has been analysed. A set of realistic meteorological conditions ( radiosonde sounding temperature, humidity and pressure data ) has been used. A low-level temperature perturbation is inserted 6 km from the center of the domain to initiate the convection. The cloud and pollutants progression in the near-surface layer ( planetary boundary layer ) has been demonstrated by a numerical simulation approach. The current model has been tested by comparative numerical experiments with convective storm and without convective storm. Various horizontal and vertical grid spacings are also analysed.

A set of calculated data for release rates of radionuclides from a lignite fired power plant is used for this study. The model can be used also for the analysis of the nuclear power plants and for the comparative studies.

The specific activity of the radionuclides in air downwind on the ground has been calculated. The dose rates from inhalation for stochastic effects for an adult has been assessed using the conversion factors for inhalation. The assessed dose rates are compared with the results from literature for similar calculations.

These numerical investigations have shown that the cloud model gives an encouraging degree of realism. It can be used for simulation transport of radionuclides and radiological impact assessment.

## PENETRATION OF 20 TO 35 MEV NEUTRONS THROUGH IRON AND CONCRETE

Ishikawa Toshio and Nakamura Takashi

## Abstract

The attenuation factors of direct neutrons and the neutron spectra penetrated through iron and concrete have been measured, using the quasi-monoenergetic source neutrons produced by  $\text{Li}(p,n)\text{Be}$  reaction.

The experiments were made at Cyclotron and Radioisotope Center of Tohoku University, Japan. The  $100 \text{ mg/cm}^2$  thick  $\text{Li}$  target was bombarded by 35 and 25 MeV protons accelerated by the AVF cyclotron. The produced quasi-monoenergetic neutrons were confirmed to have the 32.6 and 21.8 MeV average energies and the 1.4 and 1.6 MeV FWHMs, respectively by the TOF measurement.

These source neutrons were injected into iron with 10, 20, 30, and 40 cm thicknesses and concrete with 25, 50, 75, and 100 cm thicknesses. The neutrons penetrated through them were measured by the NE213, the hydrogen proportional counter, and the multi-sphere moderated  $^3\text{He}$  proportional counter and unfolded to the neutron energy spectra. The number of neutrons produced from the  $\text{Li}$  target was monitored during experiment with another NE213 placed in front of the material. The attenuation factors of direct neutrons were obtained by integrating the neutrons in the peak energy region at every thickness and normalizing them to one at the 0 cm thickness.

The neutron spectra penetrated through iron have a broad peak around 200 keV to 2 MeV and those through concrete have  $1/E$  slowing-down spectra below 1 MeV. The attenuation factors of direct neutrons for iron and concrete were pretty different from the macroscopic total cross section of the DLC-87 cross section library.

## TRANSMITTED PHOTON SPECTRA OF GAMMA RAYS THROUGH WATER PHANTOM

A. S. Mollah

Institute of Nuclear Science and Technology,  
Atomic Energy Research Establishment,  
Ganakbari, Savar, GPO Box 3787,  
Dhaka-1000, Bangladesh.

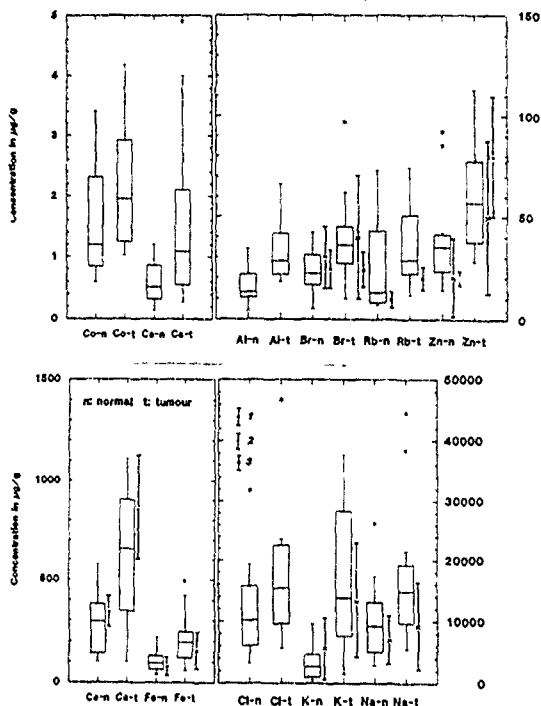
## Abstract

A knowledge of the spectrum of gamma rays through a human body is useful for better estimation of health hazards due to transmitted radiation. Measurement of the transmitted spectra available in the literature have perhaps been carried out from the view point of shielding the radiations. A study has been undertaken to determine the transmitted spectra of gamma rays through a human body. In this study, a tissue equivalent water phantom has been used to characterize the shape of the transmitted gamma ray spectra through the medium. The transmitted spectra of gamma-rays from  $^{60}\text{Co}$  and  $^{137}\text{Cs}$  through different depths of water phantom have been measured using a collimated 7.5 cm  $\times$  7.5 cm NaI(Tl) detector. The output pulses of the detector were recorded using a 4096 channel analyzer. In the degradation process of gamma ray photon energy in the water phantom, a multiple-scatter peak is observed in the analyzer at an energy below 100 keV. The multiple-scatter co-efficients of gamma-rays in water phantom medium and the exposure buildup factors under conditions of measurements have been determined. From this study, it is found that the contributions from multiple scatter photons to total transmitted exposure dose increasing the thickness of the medium and can not be ignored while assessing the health implications. As the transmitted spectrum is continuous from primary energy downwards, these transmitted spectra can be used for calibrating radiation monitors, dosimeters, etc. with continuous radiation - a practice now being carried out with discrete energy sources for use in continuous gamma radiation fields.

## ELEMENTAL COMPOSITION OF BREAST TISSUE BY INSTRUMENTAL NEUTRON ACTIVATION ANALYSIS

K H Ho<sup>1</sup>, D A Bradley<sup>2</sup>, L M Looi<sup>3</sup>, C Seman Mahmood<sup>4</sup>, A Khalik Wood<sup>4</sup><sup>1</sup>Department of Radiology & <sup>2</sup>Pathology, University of Malaya, Kuala Lumpur<sup>2</sup>Department of Radiology, National University of Malaysia, Kuala Lumpur<sup>4</sup>Nuclear Energy Unit, PUSPATI Complex, Bangi, Selangor, Malaysia

We report multi-elemental analysis of 15 paired samples of normal and tumour human breast tissue by instrumental neutron activation analysis. Fresh biopsy tissue were freeze-dried, and irradiated together with a standard (NBS bovine liver) in a TRIGA MK II reactor providing a thermal flux of  $10^{12}$   $\text{n cm}^{-2} \text{s}^{-1}$ . The elements, Al, Br, Ca, Cl, Co, Cs, Fe, K, Na, Rb, Zn were detected. This data represents the result of an on-going attempt to obtain a profile for the elemental composition of normal and abnormal states of breast tissue.



1. Spyron WM. Proc of the First Inter Conf on Elements in Health and Disease 1983; 225-234.

2. Mangel PC, Kumar S. Indian J Phys 1984; 58A:355-360.

3. Risk SL, Sky-peck EH. Cancer Res 1984; 44:5390-5394.

A NEW METHOD FOR CONTINUOUS MEASUREMENT OF  
RADON IN GROUND WATER

R.C.Ramola\*, M.Singh, S.Singh & H.S.Virk  
Department of Physics  
Guru Nanak Dev University  
Amritsar-143005, India

ABSTRACT

Radon is being monitored extensively all over the world in air, soil and water for uranium exploration, earthquake prediction and environmental pollution. For earthquake prediction continuous and long term measurements of radon both in soil and groundwater are necessary in order to get the signal in time. A new method for the continuous measurement of radon in groundwater is suggested and discussed in this paper. This is a simple, easily designed method and have used successfully in the field. Some of the field data with this method are also reported in this paper. This method will be very useful for radon measurement and earthquake prediction studies in near future.

\*Present address: Division of Biophysics, University of Salzburg  
Hellbrunner Strasse 34, A-5020 SALZBURG; AUSTRIA

## ENVIRONMENTAL IMPACT OF COAL BURNING POWER STATIONS

E. Cereda

C.I.S.E., SpA, Segrate (Milano), Italy

V. Valković\*

Ruđer Bošković Institute, POB 1016, 41001 Zagreb, Croatia, Yugoslavia

When considering environmental impact of coal burning power plants three main components should be included:

- gases produced during combustion process;
- particulates emitted and trace elements carried by them;
- radioactivity.

The problem associated with  $\text{SO}_2$  and  $\text{NO}_x$  emission have been treated in many details. Environmental impact of coal burning power plant due to particulate emission has been studied to a lesser degree.

Radionuclides including isotopes of uranium, thorium, and their series members - and large number of other toxic elements are released into the atmosphere as a result of coal burning plant operations. The quantity released depends on the particulate control system, furnace design, mineral content of the coal and existing emission control standards.

The source term for evaluating environmental impact of coal burning power stations is characterized by following parameters:

- mass of particulate matter escaping through electrostatic filters;
- radionuclide and elemental composition, total mass of individual elements and radioisotopes,
- size distribution of escaping particles and fraction of elements and radioisotopes carried by them;
- radial distribution of elements and radioisotopes within single particles,
- biological effectiveness of different fly ash fractions.

In this report we discuss the potential of the nuclear analytical techniques for the determination of source term parameters. Examples of some types of coals being used in conjunction with specific emission control equipment are presented.

---

\*Present address:  
IAEA, Agency's Laboratories, Seibersdorf, Austria



## TRITIUM IN THE ATMOSPHERIC AIR

G. Uchvářin, K. Kozák, E. Csaba

Institute of Isotopes of the Hungarian Academy of Sciences,  
Budapest, P.O.Box 77. H-1525 Hungary

Tritium originating from natural and man-made sources is present in the atmosphere mainly in the form of tritiated water vapour (HTO), tritiated hydrogen gas (HT) and as hydrocarbons. The present background levels may be significantly altered on regional and on global scale as tritium is being to be used as fuel in fusion reactors.

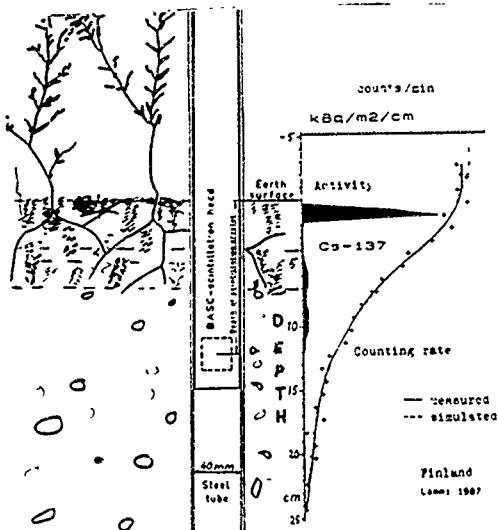
A differential HT/HTO sampler, based on molecular sieve, has been developed and tested. Water vapour is collected in 4A molecular sieve while HT is converted and adsorbed on a Pd coated molecular sieve. Using  $H_2$  carrier gas at a concentration of 2000 ppm allows complete conversion of HT at room temperature. Regular sampling of the atmospheric HT and HTO has been started three years ago at a "clean" and at a locally contaminated site in Budapest. Atmospheric HTO and HT concentrations varied between 0.06-0.6  $Bq.m^{-3}$  and 0.02-2  $Bq.m^{-3}$ , respectively.

Atmospheric tritium data are evaluated together with results of analysis of precipitation from the same sampling site and with tritium discharge data affecting the concentration determined. A project aimed at the investigation of environmental atmospheric tritium on a regional scale has been started three years ago involving six institutions from different countries at the present. The structure of this project and preliminary achievements are presented and the future radiological significance of atmospheric tritium is assessed.

# CESIUM-GAMMA MEASUREMENTS

Servo Kasi  
Helsinki University of Technology  
Otakaari 1  
SF-02150 Espoo  
Finland

1. Inversion determination of vertical radiocesium profiles /1,2/. The activity distribution  $q(z)$ , assuming the density  $\rho(z)$  is also stratified, is calculated from the measured counting rates at different depths  $z$ . The purpose is to follow the cesium distributions at different soils.



2. Snow cover mass /3/ and surface soil moisture determination by cesium-137 and potassium-40 radiation.

Cesium-137 is close by the soil surface, but potassium is distributed in all soils and rocks.

3. Erosion and suspension examinations.

We must hurry-up for taking advantages of cesium-134 (2.062 a). It still helps to separate the old cesium-137 from the 1986 one.

- /1/ Kogan, R.M., I. M. Nazarov and S. D. Fridman: "Gamma spectrometry of natural environments and formations", Israel program for scientific translations, Jerusalem 1971  
Original in Russian, Moscow 1969
- /2/ Kasi, S. S. H., First radiocesium profile and snow cover measurements, The publications of the Academy of Finland 5/1988, 101
- /3/ - , Cesium-137 for snow cover water equivalent measurement, IRPS-News 2(2), 3-7, and 2(3), 24

## AN R-FUNCTION METHOD FOR RADIATION TRANSPORT CALCULATIONS IN COMPLEX GEOMETRY

D.V. Altiparmakov and N. Dašić

The Boris Kidrič Institute of Nuclear Sciences  
P.O.Box 522, 11001 Belgrade, Yugoslavia

### ABSTRACT

This paper presents a new computational method for neutral particles transport through media of complex geometric shape. Two main features on which the method relies are (a) R-function solid modeling and (b) iterative solution of integral transport equation by multiple collisions. Similarly to combinatorial geometry based Monte Carlo codes, the R-function solid modeling makes this method able to cope with arbitrary three-dimensional models. On the other hand, like the direct methods, computations result in particle flux distribution rather than an estimate of some region integrated quantity (detector response) as it is usually the case with Monte Carlo methods. Pointwise flux calculation is carried out by linear interpolation and point kernel integration. The angular integral is replaced by a cubature formula reducing the problem to radial integration along a number of rays. To determine ray/solid intersections the RFG (R-Function Geometry) technique is applied which has been already proven to be faster than the geometric module of the worldwide used Monte Carlo code MCNP.

The presented approach combines both the advantageous and disadvantageous features of Monte Carlo and direct methods. Most of the disadvantages, for instance, large CPU time consumption or high memory request, are computer related. Taking into account the advances in computer technology they become less important making the method convenient for a wide range radiation transport problems.

ENVIRONMENTAL NEUTRONS AS SEEN BY A GERMANIUM GAMMA-RAY  
SPECTROMETER

G.Škoro, I.V.Aničkin, A.H.Kukoč, Dj.Krmpotić, P.Adžić  
R.Vukanović and M.Župančić

The Boris Kidrič Institute, Vinča, Belgrade, Yugoslavia

The 693 keV spectral structure is the prominent feature in the background spectra of heavily shielded low-background germanium spectrometers which are ground based. It is formed by the inelastic neutron scattering on  $^{72}\text{Ge}$  followed by the emission of EO radiation for which the detection efficiency is the convenient 100%. To determine the total detection efficiency for the fast background neutrons we used the very thin and point-like  $^{252}\text{Cf}$  source sandwiched between a surface barrier Si and the germanium detector. The germanium spectrum was gated by the fission fragments detected in Si, the alphas being discriminated and the prompt gammas in Ge being partly suppressed by the intervening 2 cm of lead. The recoil tail of the 693 keV distribution, assuming the flat energy dependence of the inelastic cross-section, speaks about the difference between the background and fission neutron spectrum. From those data alone, we have thus been able to deduce the flux of the fast background neutrons and to get an impression of their spectral distribution.

From the lines at 140 keV, 198 keV and 596 keV we have also estimated the background thermal neutron flux (ref.1). According to our results the sensitivity of germanium detectors to neutrons may be as high as  $1 \text{ n/m}^2\text{s}$ .

- 
1. A.Kukoč, I.Aničkin, P.Adžić, R.Vukanović, M.Župančić:  
14-th Europhys.Conf.Nucl.Phys., Bratislava 1990,p.55

## THE FIRST ATOMIC BOMB - 45 YEARS LATER

I.V. Aničin, A.H. Kukoč and Dj.M. Krmpotić

The Boris Kidrič Institute, Vinča, Belgrade, Yugoslavia

The first atomic bomb exploded on July 16, 1945 on the test site in New Mexico with code name Trinity. The desert soil, mostly sand, which was fused into the glass-like solid by the blast was later named "trinitite" (ref.1). The 2g piece of trinitite which we obtained thanks to the kindness of Prof. C.S. Wu we analysed by the X and gamma-ray spectroscopy. On a Si(Li) detector we could identify the spontaneously emitted  $X_L$  rays of uranium and the  $X_K$  rays of Cs, Ba, La, Ce and Sm. The X-ray spectra excited by the 241-Am radiation revealed the presence of Fe, Rb, Sr, Y, Zr, Nb, Ag, Ba, La, Ce. The spontaneously emitted gamma-rays as seen by the low-background germanium spectrometer were due to 133-Ba, 137-Cs, 152-Eu, 154-Eu and 155-Eu. We also did the neutron activation in the flux of  $10^{13}$  n/cm<sup>2</sup>s for 30 minutes. The gamma-ray spectra taken after 5 hours at the earliest and at many later intervals showed the presence of some 50 isotopes common in similar analyses of geochemical samples. However, the presence of both the 141-Ce and 143-Ce offered the opportunity to test the abundance ratio of the typical fission product from the peak of the yield curve. The 140-Ce/142-Ce ratio in trinitite turned out to be  $4.3 \pm 1.0$ . The natural abundance ratio is 7.345 while from the fission yields it is estimated to be close to one. It follows that about half of the stable cerium in the sample is of the fission origin! To conclude, we may say that the traces of explosion did not only survive for 45 years but that it also left identifiable permanent marks on the soil infinitely.

A FORMULA FOR TRANSMISSION OF NUCLEAR RADIATION  
DOSE EQUIVALENT IN ORDINARY CONCRETE

V. Stanić, R. Simović, N. Marinković  
Nuclear Engineering Laboratory  
Boris Kidrič Institute of Nuclear Sciences-Vinča

For the need of radiation shield design a simple exponential two parametric formula was proposed for computing transmission of nuclear radiation dose rate equivalent through ordinary, rather thick concrete slab:

$$I(x) = e^{-(A\rho_c + B\rho_v)x},$$

where parameters  $\rho_c$  and  $\rho_v$  represent concrete density and density of chemically bound water in the concrete, A and B are coefficients describing the nature of nuclear radiation computed by sensitivity analysis methods and x is the concrete slab thickness.

Transmission of neutron and gamma doses were computed by ANISN and SABIIE-3 codes for a typical ordinary concrete composition. Based on these results and sensitivity analysis theory the coefficients A and B were defined by least square method for neutron, primary and secondary gamma radiation according to the following formulae:

$$A = -\frac{1}{x} \frac{\partial \ln I}{\partial \rho_c},$$

$$B = -\frac{1}{x} \frac{\partial \ln I}{\partial \rho_v}.$$

The procedure was applied to compute transmission of neutron and gamma radiation as well as coupled neutron-gamma radiation from fission, fast and thermal neutron sources as well as 14 MeV neutron source. In this way a practical tool was obtained for determining the transmission of coupled neutron-gamma radiation which is tiresome to achieve by applying existing engineering tables in modern handbooks.

Feasibility of tissue characterization by Compton scattering profile measurements.

A TARTARI, E CASNATI, J FELSTEINER\* AND C BARALDI

Dipartimento di Fisica Università, I-44100 Ferrara, Italy  
\*Technion, Israel Institute of Technology, 32000 Haifa,  
Israel

The R/C ratio of photons coherently scattered due to Rayleigh effect (R) and those incoherently scattered due to Compton effect (C) has proved useful for bone tissue characterisation in term of mineral contents. However, the range of application of this techniques is limited by the fact that the coherent scattering is a very weak process, with low atomic numbers. MacKenzie<sup>1)</sup> recently suggested that the Compton scattering profile - which reflects the momentum distribution of the target electrons - can also be used in assessing the bone mineral content.

In this paper, we examine the possibility of extending the Compton scattering profile evaluation technique to the soft tissues. The single and multiple Compton scattering profiles are generated, starting from the individual electron Compton profiles of the atoms composing the tissue, by means of analytical and Monte Carlo methods<sup>2)</sup>. Accurate experimental testing on animal tissues and tissue-like materials - performed using Am-241 sources and backscattering geometry - has (in principle) demonstrated the feasibility of utilizing this techniques to characterize a biological tissue in terms of soft tissue, fat and bone mineral contents.

REFERENCES

1. IK MacKenzie. Nucl Instrum Meth A299, 377 (1990);
2. A Tartari et al. Phys Med Biol 36, (1991).

Evaluation of shielding for ALPI Heavy Ion Accelerator

S. Fazinic, Rudjer Boskovic Institute, Zagreb, Yu

An existing Tandem accelerator at the Istituto Nazionale di Fisica Nucleare, Laboratori Nazionali di Legnaro (INFN-LNL), Italy, will be upgraded and extended with a superconducting linac booster (ALPI) to provide heavy ions (from Oxygen to Uranium) with energies ranging from 6 up to 20 MeV/nucleon. X-rays, Gamma and neutron fields are expected to be potential radiation hazard, with neutrons as the dominant one.

The shielding calculation was done using Thomas, Stevenson and Tesch approach, and following NCRP Rep. No 51 guide-lines[1]. The source term was estimated using Clapier parametrisation[2] based on experimental data about neutron production in heavy ion reactions. The Tesch empirical equations[3] for one, two, and three legged labyrinth were used for the attenuation of the neutron dose equivalent in alabyrinths. The empirical expressions proposed by Ladu and Thomas[1,4] were used to estimate "skyshine" contribution to dose equivalent in the neighbourhood of the accelerator.

- [1] R.H.Thomas, G.R.Stevenson, Technical Report Series No.283, IAEA, Wiena, 1988; A.Tesch, Radiat. Prot. Dosim. 11 3(1985)165; Radiation Protection Design Guidelines for 0.1 - 100 MeV Particle accelerator Facilities, NCRP Report No. 51, 1977
- [2] F.Clapier, C.S.Zaidinis, Nucl.Instr.Meth.217(1983) 489
- [3] K.Tesch, Part. Accel. 12(1982)169
- [4] M.Ladu, M.Pelliccioni, P.Picchi, G.Verri, Nucl. Instr. Meth. 62 (1968) 51



Radon Studies for Earthquake Prediction

H.S. VIRK & BALJINDER SINGH  
Physics Department  
Guru Nanak Dev University  
Amritsar-143005

Abstract

Radon monitoring for earthquake prediction is part of an integral approach since the discovery of coherent and time anomalous radon concentration prior to, during and after the 1966 Tashkent earthquake. Earthquake forecasting has not achieved the same degree of success and confidence level as in case of weather forecasting. It is encouraging to note that during the last two decades, more than a dozen earthquake precursors which hold out considerable promise, have been identified.

Our own programme is based on using radon as a precursor. Radon concentration is being monitored daily in soil gas and groundwater since 1984 at the University Campus and in Kangra valley, Himachal Pradesh (India) since 1989, identified as a highly seismic zone in the Himalayan belt. Laboratory experiments and the development of soil gas and groundwater radon monitoring systems are described. The effect of meteorological variations on radon emanation rate is studied. It is observed that radon anomalies are correlated to some of the earthquakes which occurred in the region and appear to be caused by strain changes which incidently precede the earthquakes.

## TRACE URANIUM IN WATER SAMPLES

P.J. Jojô , A. Rawat and Rajendra Prasad  
Department of Applied Physics, Z.H. College of Engg.  
and Tech., Aligarh Muslim University, Aligarh, INDIA.

Determination of uranium concentration in water samples is quite significant from the point of view of radiation hygien and environmental control. Uranium is transferred to water through leaching action when it passes through soil and rocks etc. In the present investigation, trace analyses of Uranium in water collected from different sources (tap, Hand pump, tube well etc.) from different places of India have been done using fission track registration technique.

A known volume (0.06 ml) of water is placed on clean circular disc (dia 1.3 cm) of Makrofol KG track detector and is allowed to evaporate inside an oven leaving behind a thin film of non volatile constituents including uranium. Dried droplet on the detector was covered with another similar circular disc of the detector. Several such pairs (pellets) of different water samples alongwith a blank pallet and standard glass of known uranium concentration were irradiated with thermal neutrons at APSARA reactor at Bhabha Atomic Research Centre, Trombay India.

After irradiation, the detectors were separated, washed and etched in 6.25 KOH solution at 80°C for 20 min. and the resulting fission tracks were counted using binocular research microscope having magnification 400 X. For finding the thermal neutron dose, the irradiated glass was etched in 48% HF at 23°C for 5 sec. and scanned for track density. The uranium concentration is found to vary from 1.84 µg/l to 13.75 µg/l and depends on the source and place of the water collected.

# AUTOMATIC MONITOR OF RADON-222 DAUGHTER ELEMENTS CONCENTRATION IN AIR.

Edgardo V. Bonzi and Raul T. Mainardi\*.

Facultad de Matematica, Astronomia y Fisica. Universidad  
Nacional de Cordoba. - Laprida 854 - Cordoba - Argentina.

A new procedure to find the concentration of Radon-222 daughter elements in air has been developed. The alpha emissions of atmospheric aerosols are measured simultaneously discriminated in two energy intervals, one for Po-218 and the other for Po-214. The counting times have been optimized by a variational method. Emissions from Po-214 are counted in a period of 16 minutes after the accumulation time, while for Po-218 it is done simultaneously in two equal consecutive periods of time.

In order to implement this procedure in practice, a non continuous monitor was built to measure the concentration of those elements in air.

The fundamentals of the analytical method and construction details of the monitor are presented.

\* Member of the National Research Council of Argentina (CONICET).

X-RAY SPECTRA DETERMINATION, INCLUDING CHARACTERISTIC  
LINES, BY INDIRECT METHODS.

Raúl T. Mainardi\*, Miguel A. Chesta\*\*, Facultad de  
Matemática, Astronomía y Física, Universidad Nacional de  
Córdoba. 5000 Córdoba, Argentina and Donald L. Smith.  
Engineering Physics Division. Argonne National Laboratory  
- Argonne, Ill. 60439-USA.

The method of x-ray spectra determination by  
successive attenuation of the beam (R.T. Mainardi and R.A.  
Barrea NIM A280 (1989) 387 ) has been extended to include  
characteristic lines. The emission from a tube is assumed  
to be composed by a continuum due to bremsstrahlung and  
characteristic lines of known energies as well as relative  
intensities. To the three parameters already needed for the  
Kramers type continuum model, one additional adjustable  
parameter is added per each series of lines to set its  
intensity in relation to the continuum.

Computer codes have been written to calculate  
the model parameters from the measured attenuation data and  
with a linear least square procedure propagate errors from  
the measured points to the model parameters and provide the  
error correlation matrix. A considerable reduction of the  
experimental errors was achieved by using high purity  
aluminum filters and a specially designed dose monitor  
using a plastic scintillator that provides a higher  
detection efficiency and better homogeneity throughout the  
volume.

\* Member of the National Research Council of Argentina  
(CONICET)

\*\* Under a Fellowship of the Research Council of the  
Province of Córdoba-Argentina (CONICOR)

Proposed for presentation in general topics section # 4

SSNTD METHOD FOR THE MEASUREMENT OF WORKING LEVELS OF  
INDOOR RADON AND THORON

M.C. Subba Ramu, T.S. Muraleedharan, T.V. Ramachandran  
and K.S.V. Nambi

Environmental Assessment Division,  
Bhabha Atomic Research Centre, Bombay - 400 085, India.

It is necessary to measure radon and thoron daughters in WL unit to obtain the effective dose equivalents and assess the inhalation hazard. Solid State Nuclear Track Detectors (SSNTD) can be used by exposing them in the bare mode for obtaining the sum of radon and thoron daughter concentration in WL units and in cups with appropriate membrane and filter for getting radon and thoron concentrations in  $\text{Bq m}^{-3}$ . A calibration procedure has been devised to obtain a correlation between the ratio of radon to thoron concentration and the ratio of radon to thoron daughter WLs, with the help of which the individual radon and thoron daughter WLs can be obtained.

The paper describes the calibration procedure followed by using a system consisting of an exposure chamber, an aerosol generator and radon and thoron sources. LR-115 detector was used in different exposure modes to different concentrations of radon and thoron. Track density obtained in the bare mode exposure was correlated with the sum of the WLs of radon and thoron daughters. Exposures in cups with membrane and filter enabled to obtain radon and thoron concentrations. A correlation has been obtained between the radon to thoron WL ratio and the radon to thoron concentration ratio. It has been seen that these ratios are not dependent on the ventilation and plate-out rates. It is thus possible to estimate the individual WL.

The calibration using radon and thoron daughters of AMAD  $0.2 \mu\text{m}$  dia have given a sensitivity of  $0.32 \text{ tracks cm}^{-2} \text{ day}^{-1}$  per unit total mWL and 4.6 as the ratio of the tracks due to radon and thoron concentrations per unit ratio of the WLs of radon to that of thoron daughters, the measured range of the ratio being 1.2 to 6.5.

## THE RADIATION SAFETY DESIGN OF THE JAPANESE HADRON PROJECT

Yoshitomo Uwamino and Tokushi Shibata

*Institute for Nuclear Study, the University of Tokyo*

*3-2-1, Midori-cho, Tanashi, Tokyo 188 Japan*

### ABSTRACT

The Japanese Hadron Project (JHP) is proposed by Institute for Nuclear Study, the University of Tokyo. A 1-GeV 400- $\mu$ A proton beam will be accelerated by a linac, and reformed its time structure by a compressor/stretcher ring, and distributed into 3 experimental arenas of neutron, meson and exotic nuclei for the secondary particle production.

Because of its big beam power, many problems related to radiation hazards must be solved, that is, deep penetration, skyshine, and streaming of high energy neutrons, and activation of machine components, structures, air, cooling water, soil, and under ground water.

These problems were evaluated by simple analytical formulae, such as the Moyer model, and also the scaling method at first. The present design is as the following. The beam line passes 14 m below the surface, and the tunnel is made by 1.5-m-thick concrete. Before releasing the activated air from the ring and the experimental rooms, short lived activities is reduced in reservoir tanks.

The production and the deep penetration of high energy neutrons were evaluated by the HETC-KFA-2 Monte Carlo code and the ANISN code. The neutron production was calculated by the HETC code, and compared with the experimental data of Clerjacks and Raupp. The calculated angular distribution has stronger forwardness than the measurement. The deep penetration in iron and concrete slabs was calculated by the HETC and ANISN codes, and compared with other calculations and experiments. Our calculations of the two codes agreed well each other, and showed larger dose rates than the evaluation by the Moyer model. The value of the shielding lengths of our calculations is surrounded among the other estimations which have various values.

RADIOACTIVE NUCLIDES IN GLOBAL STUDIES OF  
RECENT ENVIRONMENTAL CHANGES.

P. El-Daoushy \*

Department of Physics

Box: 530

S-751 21 Uppsala

Sweden

Global studies of recent environmental changes require the construction of reliable chronological records for various depository systems around the world. However, the different inputs of radioactive nuclides (used in dating recent deposits such as Pb-210, Cs-137 and others) to global depository systems and the complexity of the processes involved in such systems require good controls of essential factors/parameters influencing the reliability and quality of dates obtained. A summary on different requirements for radioactive dating of recent deposits will be reviewed.

---

\* Present address: Department of Physics, P.O.Box: 17551,  
U.A.E. University, Al-Ain, United Arab Emirates.

NEW PATCHES OF MONAZITE AND DISTRIBUTION OF RADIONUCLIDES IN THE  
ENVIRONMENT OF MANGALORE - SOUTH INDIA

K Siddappa, A P Radhakrishna, H M Somashekarappa, Y Narayana  
and N Lingappa  
Department of Physics, Mangalore University  
Mangalagangothri-574 199, India

ABSTRACT

Mangalore is an important city situated amidst the beautiful natural environment of Coastal Karnataka, in the west coast of South India. The city and surrounding region is now on the threshold of major industrial activities with proposed nuclear power plant, super thermal power station, an oil refinery in addition to the already existing fertilizer factory and other industries. We have undertaken a systematic study on the background radiation level and the distribution of natural and artificial radionuclides in the environment of this region for future impact assessment of industrial endeavours. A systematic ambient gamma radiation level survey conducted using a 2" x 2" NaI(Tl) scintillometer showed some conspicuously high levels at certain locations of Mangalore beach. Soil and sand samples from such high activity locations were analysed employing a high resolution HPGe detector and the results clearly indicate the presence of patches of monazite activity in Mangalore beach. External exposure rates were also measured using thermoluminescent dosimeters. Natural samples of soil, sand, vegetation, vegetables, and marine samples of the region were investigated for gross alpha, gross beta and individual radionuclide activities employing well established nuclear techniques and radiochemical methods. The concentrations of important radionuclides were determined in vegetarian and non-vegetarian composite meal samples and the daily intake of these radionuclides by the population of the region was estimated. The results of these investigations are presented and are compared with the literature values reported for the environs of other parts of India and other countries.



A SEMI-ANALYTICAL, MODIFIED PRE-DOSE  
EQUATION: EXPERIMENTAL VERIFICATION  
AND APPLICATION OF THE EQUATION

L. S. CHUANG, Department of Applied Science, City Polytechnic of Hong Kong, Kowloon, Hong Kong.

Y. K. NGAR, Department of Physics, The Chinese University of Hong Kong, Hong Kong.

ABSTRACT

In thermoluminescence (TL) dating using the pre-dose techniques, the assumption made for the empirical pre-dose equation adapted for use in determining the archaeological pre-dose of a sample cannot always be justified. In coping with the situations a modified pre-dose equation has been semi-analytically formed. In this paper, a brief introduction of the modified pre-dose equation with an experimental verification is presented. An application of the modified equation in actual dating of ancient pottery sherds, which require different magnitudes of the test-dose for a legible  $110^{\circ}\text{C}$  glow peak in quartz is also illustrated. Detailed procedures for convenient use of the modified pre-dose equation in the dating is introduced.

**Attenuation coefficients of different soils  
in the energy range 10-300 keV**

Roberto Cesareo<sup>1)</sup>, Joaquim Teixeira de Assis<sup>1,2)</sup>

1. Centro per l'Ingegneria Biomedica, Università di Roma "La Sapienza"  
Rome, Italy.

2. COPPE/UFRJ - C.P. 68501 Rio de Janeiro, Brazil/CNPQ

Soil samples have a chemical composition characterized by the presence of  $\text{SiO}_2$ ,  $\text{Al}_2\text{O}_3$ ,  $\text{Fe}_2\text{O}_3$ ,  $\text{CaO}$  and  $\text{MgO}$  in variable concentration, and of other optional oxides like  $\text{TiO}_2$ ,  $\text{MnO}$ ,  $\text{K}_2\text{O}$  and others<sup>1)</sup>.

Using the literature concentration data, and the Berger-Hubbell program for the calculation of mass attenuation coefficient of a mixture according to the weighted average formula<sup>2)</sup>, the theoretical values of mass attenuation coefficients of these soils in the energy interval 10-300 keV have been obtained. Further, measurements have been carried out on some selected soil and sand samples, at energy values between 10 and 120 keV. Monoenergetic radiation was obtained both using a X-ray tube with external changeable targets and collimating the output radiation at about  $90^\circ$  respect to the incident beam<sup>3)</sup>, or employing a 200 mCi  $\text{Am}^{241}$  source or a 1 mCi  $\text{Co}^{57}$  source.

Experimental and theoretical attenuation coefficient values are compared, and some considerations are made, concerning the effective atomic number of soils, and the relationship between soil physical parameters and tomographic images.

1. G.S. Mudahar and H.S. Sahota; Appl. Radiat. Isotopes 39 (1988) 1251.
2. M.J. Berger and J.H. Hubbell; U.S. Dept. of Commerce, Nat. Bureau of Standards NBSIR 87-3597.
3. R. Cesareo, G. Viezzoli; Phys. Med. Biol. 28 (1983) 1209.

## Microtomography in soil physics

Roberto Cesareo<sup>1</sup>, Joaquim Teixeira de Assis<sup>1,2</sup>,  
 Silvio Crestana<sup>3</sup>, Giovanni E. Gigante<sup>1</sup>.

1. Centro per l'Ingegneria Biomedica, Università di Roma "La Sapienza",  
 Rome, Italy
2. COPPE/UFRJ - C.P. 68501 - Rio de Janeiro, Brazil/CNPQ
3. Embrapa, NPDI, Rua XV de Novembro, Sao Carlos, S.P., Brazil

In the last few years, with the advent of new methodologies originating from different disciplines, some experimental techniques have been proposed or applied for the first time in the domain of soil and related research. Among them, neutron radiography, ultrasound, dielectric conductivity and laser can be cited.

Particularly, the X and gamma-ray computerized tomography (CT) have been successfully used for imaging soil samples<sup>1)</sup>, and in the last year also X-ray computerized microtomography<sup>2)</sup>. Microtomography is a technique for obtaining the distribution of X-ray attenuation coefficients within small objects, with a geometrical resolution (of the order of tenths of microns or less). A very strong monoenergetic source having a beam size of tenths of microns is therefore required.

In this work a X-ray tube was employed with external absorbers, carefully studied in order to obtain a quasihomogeneous intense beam of variable energy and high intensity.

Several soil samples have been scanned, for determining the characteristics of the microtomography respect to geometrical and contrast resolution versus beam size and energy.

1. S. Crestana, R. Cesareo, S. Mascarenhas; Soil Sci. 142 (1986) 56.
2. S. Crestana, H.E. Martz, D.R. Nielsen, A. Orhun and J. Biggar; EOS Trans. Am. Geophys. Union 70 (1989) 337.

# VERY LOW ENERGY $\beta$ MEASUREMENTS IN TRITIUM CONTAMINATED PARTS

S. K. ARBI, B. M. BAHAL, U. M. EL-GHAWI,

A. A. GULAK and H. H. ENBIA

*Tajura Nuclear Research Centre,*

*P. O. Box 30878, Tripoli, Libya*

Neutron Generator laboratories producing neutrons from D-T reaction use high activity tritium targets either as solids in a solid material matrix or as gas targets. Inevitably the accelerator parts are contaminated due to it and eventually, inspite of usual precautions, tritium leakage finds its way to unexpected areas, causing a possible health hazard if internally taken. Tritium being a very low energy  $\beta$  emitter is difficult to detect by conventional radiation detectors. Therefore a  $4\pi$  gas proportional counter sensitivities has been enhanced with suitable modifications to detect tritium beta particles. With this setup  $\beta$  spectrum is recorded for different sources such as  $H^3$ ,  $C^{12}$ ,  $Y^{90}$  and  $Bi^{207}$ . The linearity of energy is established for different high voltage conditions. Swap samples from all over the Neutron Generator and Accelerator laboratory & our research centre are collected over a large period of time. Sampling is done on a routine basis and contaminated part is rechecked after cleaning. The results of these measurements are presented. On the basis of our experience, recommended tritium safe handling is also made.

POSSIBILITY OF USING LOW ENERGY PROTON BEAM  
FOR PIXE MICROANALYSIS

U. M. EL-GHAWI, B. M. BAHAL and S. K. ARBI

*Tajura Nuclear Research Centre  
P.O. Box 30878, Tripoli , LIBYA*

The utilization of low energy PIXE has been explored for the analysis of biological materials, metal and alloy samples, soil samples and silicon wafers. Impurities of a thick carbon light matrix and elemental analysis of stainless steel havey matrix have been made using low and conventional proton energies, and the sensitivities compared in the present work. ECPSSR theory has been used to calculate ionization cross-section and  $K_{\alpha}$  X-ray production cross-section of these elements was calculated for carbon and stainless steel matrices. Elements below zinc were detected in low and high range of concentrations. At 2.0 MeV proton energy, a large background due to the Bremstrahlung secondary electrons was seen in the X-ray energy region below 6.0 and 8.0 keV for the carbon and stainless steel matrices respectively. This is considerably reduced at 0.25 MeV proton energy. sensitivity limit of low Z elements in heavy matrix was better than light matrix for low bombarding energy. The sensitivity limit of elements below calcium for heavy matrix at low energy is comparable to that of conventional PIXE. The ability of 0.25 MeV proton beam to reach these elements is in the micron range which is much less than that of 2.0 MeV, making it more suitable for surface analysis.

THE STUDY OF SERUM TRACE ELEMENTS  
IN MALNOURISHED CHILDREN IN TANZANIA  
BY USING X-RAY FLUORESCENCE SPECTROSCOPY

G.M. Mwiruki, M.G. Bilal, L.M. Chuwa\* and J.W.A. Kondoro  
Department of Physics, University of Dar es Salaam,  
P.O. Box 35063, Dar es Salaam, TANZANIA.

ABSTRACT

The blood serum of children of age up to 7 years has been studied by X-Ray Fluorescence (XRF) analysis. The serum trace elements content of malnourished children has been compared with those of healthy ones. Malnutrition is characterized by chronic diarrhea, bleached hair, underweight, and preterm birth in some cases. Serum has mainly iron, copper, zinc and bromine as trace elements. The malnourished children have been found to have significantly lower mean values of serum copper than their healthy counterparts.

\* Department of Clinical Chemistry,  
Muhimbili Medical Centre,  
P.O. Box 65002, Dar es Salaam.

5<sup>th</sup> International Symposium on Radiation Physics, Dubrovnik, Yugoslavia,  
June 10-14, 1991

---

THE AIR KERMA-RATE CONSTANT OF  $^{192}\text{Ir}$

M.M.NINKOVIĆ, J.J.RAIČEVIĆ

Boris Kidrič Institute of Nuclear Sciences, Vinča, Belgrade, Yugoslavia

Abstract: The air kerma-rate constant  $\Gamma_0$  and its precursors, as one of the basic radiation characteristic of  $^{192}\text{Ir}$ , was determined by many authors. Analysis of accessible data on this quantity led us to the conclusion that calculated data are rather inaccurate. That is the reason we calculated this quantity on the base of our and many other authors gamma-ray spectrum data and latest data for mass-energy-transfer coefficients for the air. In this way it was obtained for  $\Gamma_0$  value of  $(30,0 \pm 0,9) \text{ aGym}^2\text{s}^{-1}\text{Bq}^{-1}$  for unshielded  $^{192}\text{Ir}$  source and  $(27,8 \pm 0,9) \text{ aGym}^2\text{s}^{-1}\text{Bq}^{-1}$  for standard packaged radioactive source taking into account self-absorption and attenuation of gamma-rays in the platinum source wall and in the air.

PHOTOTRANSFER-THERMOLUMINESCENCE OF HIGH TEMPERATURE  
TL PEAKS IN ZIRCON

Y.M. Amin, M. Fathony and S.A. Durrani  
School of Physics and Space Science  
University of Birmingham  
Birmingham B15 2TT  
United Kingdom.

**Abstract**

Phototransfer-thermoluminescence(PTTL) of high temperature ( $>500^{\circ}\text{C}$ ) natural and gamma induced thermoluminescence(TL) was studied in zircon using UV light Source. It was found that the PTTL intensity increases with illumination time. The amount of PTTL was also found to be proportional to the initial gamma dose given to the sample. Fading study of the high temperature peak was also determined. For the duration of ~6 weeks it was found that ~10% of the artificially induced TL faded while the natural TL showed no fading. The location of the high temperature peak was determined using a step heating followed by PTTL measurements. The position of this peak was found to be at temperature of  $620-720^{\circ}\text{C}$ .



# GAMMA-RAY TRANSMISSION STUDIES OF SOIL INTERFACE TRANSITION DURING WATER INFILTRATION AND REDISTRIBUTION

Carlos Roberto Appoloni; Hélio Saito and Aírton Algozini Junior  
Universidade Estadual de Londrina  
Departamento de Física - Caixa Postal 6001  
86051 - Londrina - PR - Brasil

The horizontal erosion process in the inner layers of the soil, where there is the interface of different horizons or a compactation zone, can be put in evidence through changes in the conductivity and diffusivity functions.

With this aim we have measured the vertical infiltration and redistribution of water in the following compound soil samples: L.E.a. (dark red latosol) with A and B horizons; L.E.a. - sand fase and L.E.a. - clay fase; L.R.d. (dusky-purple latosol) with an inner compactation layer.

The spacial and temporal moisture profiles  $\theta(z,t)$  were obtained using gamma ray attenuation method with a  $^{241}\text{Am}$  source, standart spectrometry eletronic and scintillation detector NaI (Tl). In this experimental arrangement the soil column moves vertically through the fixed source, collimators and detector. The acrylic 5,33cm inner diameter and 92,0cm long soil column was attached to a pressure controlled wetting system through a perforated acrylic plate and filter papers. The vertical flow was made in the same direction of the gravitational field.

The  $\theta(z,t)$  data were collected during a 4 hours infiltration process and in redistribution at 0.25, 0.50, 0.75, 1.0, 2.0, 3.0, 6.0, 10.0, 15.0, 20.0 and 24.0 days after infiltration. The moisture temporal evolution was determined along 20 different places inside the column. Moisture was measured within a 3-5% precision, computing statistical and other source of errors.

The hidraulic diffusivity  $[D(\theta)]$  and conductivity  $[K(\theta)]$  functions of the soil samples were determined using diffusion mathematical models and the  $\theta(z,t)$  data, and were obtained at various places inside the soil samples, away, near and at each interface. For the L.E.a. soil the results were: at the A horizon region,  $K(\theta) = 16,3 \text{ EXP } [44,4 (\theta - 0,5)]$ ; at the interface between A and B horizons,  $K(\theta) = 3,6 \text{ EXP } [21,9 (\theta - 0,5)]$  and at the B horizon region,  $K(\theta) = 17,8 \text{ EXP } [38,3 (\theta - 0,5)]$ . Results clearly show the abrupt hidraulic conductivity change at the AB interface. Similar results were obtained for the other samples.

PARALLEL MONITORING METHOD: DETERMINATION OF THE MASS  
ATTENUATION COEFFICIENT OF CORTICAL BONE FOR POLIENER-  
GETIC X-RAY BEAMS.

Carlos Oyarzún Cortés (\*) Luis Flores Viza (\*\*).

(\*) Chilean Nuclear Energy Commission, Ionizing Radia-  
tion Metrology Laboratory.

(\*\*) Clinical Hospital Catholic University, Radiology  
Service.

Using the method "Monitoring in Parallel", based on  
NaI(Tl) crystal scintillation detectors, the Mass Atte-  
nuation Coefficient of cortical bone for Polienergetic  
X-ray beams was determined.

The simultaneous use of the NaI(Tl) use of the NaI  
(Tl) Monitor and main Detector intercepting the collima-  
ted X-ray beams, permits the control of the fluctuations  
in Intensity and Energy of the incident and emergent  
beams from the thickness of bone.

The Mass Attenuation Coefficients obtained for corti-  
cal bone, whose average macroscopic density is 1.84  
gr/cm<sup>3</sup>  $\pm$  3%, were 0.44667 g<sup>-1</sup>/cm<sup>2</sup> and 0.2216 gr/cm<sup>2</sup> for  
beams of 48  $\pm$  27% (FWHM) KeV and 83  $\pm$  33% (FWHM) KeV of  
energy.

EFFECT OF HIGH Z FRONT LAYER  
ON SATURATION THICKNESS FOR  
RADIATION SHIELDING MATERIALS

A.K. Sinha, A. Bhattacharjee and B. Purakayastha  
Department of Physics  
Regional Engineering College  
Silchar-788 010, Assam (INDIA)

Measurements of energy albedo for backscattered gamma rays from binary combination of shielding materials are important in designing gamma ray shields which are useful in nuclear installations. In these applications the characteristic parameter which gives an integral measure of gamma ray scattering is the albedo of the materials involved. It has been observed that a layer of high Z material when placed before a radiation shield improves the shielding property and considerably decreases the saturation thickness. The atomic number and the varying thickness of the front layer play significant role in the determination of optimum saturation thickness of a radiation shield and in reducing its cost involved.

Most of the authors made albedo measurements for backscattered photons with scintillation counter coupled with multichannel analyser. The modified spectrum of gamma ray was corrected by inverse matrix method. The indigenously designed Proportional Response Photon Counter whose efficiency is proportional to the energy of the incident photon has been used in the proposed measurement which has the advantage that its sensitivity is independent of the mixed energy of the backscattered gamma rays.

In the present investigation energy albedo as well as saturation thickness measurements for 1250 keV energy have been reported using lead, tin and iron as front layer material and aluminium, concrete, and iron as shielding materials.

**MODEL TO EVALUATE IRRADIATION FIELD  
DISTORTIONS CAUSED BY MISALIGNED FLATTENING  
FILTER OF A MEDICAL ELECTRON ACCELERATOR**

**G. GESKE, UNIVERSITY OF JENA/ GERMANY**

Field flatness and symmetry besides other beam parameters are necessary for a successful radiation therapy with the photon beam of electron accelerators. Field distortions by a misaligned flattening filter may be analyzed by a model which depends on a semiempirical formula for the measured dose distributions in water. The method and an example are presented.

AIR-COLLISION-KERMA TO DOSE-EQUIVALENT CONVERSION  
COEFFICIENTS FOR THE CALIBRATION OF INDIVIDUAL DOSEMETERS  
IN X-RAY FIELDS

B. Grosswendt

Physikalisch-Technische Bundesanstalt,  
W-3300 Braunschweig, Federal Republic of Germany

Individual dosimeters provided to be worn on the trunk and to indicate dose equivalent quantities defined at depths  $d$  of the human body must be calibrated in a suitable way. The calibration is commonly performed in such a way that the dosimeters are fixed at the surface of a phantom and irradiated by a well-known x-ray field. The dosimeter reading is converted to individual dose equivalent afterwards by means of a conversion coefficient which relates the air kerma in free air and the dose equivalent at depth  $d$ . Therefore these conversion coefficients must be known for the x-ray quality and the phantom used in the calibration procedure. To determine these conversion coefficients the ratio of the collision kerma for ICRU tissue-equivalent material and the receptor-free air collision kerma was calculated for a variety of cube and slab phantoms when irradiated with broad parallel x-ray beams of different directions of incidence with respect to the phantom's front face. The procedure used was the Monte-Carlo method in the kerma approximation taking the photoelectric effect, Rayleigh scattering and Compton scattering into account. The influence of electron binding on both scattering effects was included in the calculation. The results of the conversion coefficients for perpendicular x-ray beam incidence and of the angular-dependence factor for various depths  $d$  are given in tabular form.

TRANSFORMATION OF ACONITIC ACID ADSORBED  
ON A CLAY-MINERAL BY  
GAMMA IRRADIATION.

S. RAMOS-BERNAL<sup>2</sup>, A. NEGRON-MENDOZA<sup>2</sup> AND G. ALBARRAN<sup>1</sup>.

<sup>1</sup>Instituto de Ciencias Nucleares, UNAM.  
Circuito Exterior, C.U. A. Postal 70-543 México  
<sup>2</sup>Departamento de Física, Facultad de Ciencias, UNAM.  
Circuito Exterior, C.U. México, D.F. México.

The mechanism of radiation-catalytic activity from clay-minerals is of particular importance due to the fact that these solids are important constituents of the earth crust and act as catalysts for natural processes. In the present work we investigate the irradiation of aconitic acid adsorbed on a clay-mineral (Na-montmorillonite) and to compare with the irradiation of the acid without the solid. To get an insight into the mechanisms leading to the transformation of this acid adsorbed in the clay a systematic study was carried out. The results were interpreted in terms of two possible mechanism that are driving the system. The first one involves changes in the valence state of the transition metals at the surface and edges of the solid. The second one comes via the energy transfer processes from the excited solid to the adsorbed molecules through an interaction of non-equilibrium charges carriers with these adsorbed molecules. Both of them lead to an enhancement of the effect of decarboxylation of the aconitic acid in comparison with the irradiation of this acid without the presence of the solid.

## AN IMPROVED MULTIPLE SCATTERING MODEL FOR CHARGED PARTICLE TRANSPORT

A. FERRARI\*, P.SALA\*\*, R.GUARALDI\*\*\*, F.PADOANI\*\*\*

- \* Istituto Nazionale di Fisica Nucleare INFN, Sez.di Milano, Lab. LASA,  
Via F.lli Cervi 201, 20090 Segrate (MI)
- \*\* Istituto Nazionale di Fisica Nucleare INFN, Sez.di Milano,  
Via Celoria 16, 20133 Milano
- \*\*\* Comitato Nazionale per la Ricerca e Sviluppo dell'Energia Nucleare e delle Energie  
Alternative ENEA, Dipartimento Reattori Innovativi,  
Via Martiri di Monte Sole 4, 40129 Bologna

### ABSTRACT

An extended model for charged particle transport through the multiple scattering formalism based on the Molière Theory has been developed. Using as starting point the electron transport algorithm used in EGS4, the new model has been implemented independently through two different algorithms in the Monte Carlo codes FLUKA and MCNPE.

FLUKA treats hadrons and leptons with energies up to 10-20TeV. The electromagnetic part of the code has been further improved to meet the high energies foreseen for the LHC collider.

MCNPE, based on the coupled neutron photon code MCNP3a with the addition of an electron transport capability, was written to provide a user-friendly and robust code for radiation protection and dosimetry applications.

Major features of the extended model are:

- the inclusion of lateral displacements as well as angular deflections;
- a new path length correction (PLC);
- correlation of both path length correction and lateral displacement with the final scattering angle;
- the introduction of first order corrections to the spin relativistic effect (FLUKA);
- the inclusion of nuclear form factors in high energy scatterings (FLUKA).

The codes are currently being benchmarked on a variety of reference problems in their respective fields of application.

Determination of Arsenic Content in the Waste Sludge from a  
fertilizer factory of Bangladesh using XRF and NAA Techniques.\*

N.N.Mondal, T.Debnath, T.K.Roy, K.D.Saha, B.Alam & M.Sarkar  
Department of Physics  
University of Dhaka  
Dhaka- 1000  
Bangladesh

&  
F. Henrich and M. Mommsen  
ISKP, Nussallee 14 - 16  
5300 Bonn 1, Germany

Few pieces of the waste sludge from a fertilizer factory of Bangladesh have been analysed both by the X-ray fluorescence technique (XRF) and Neutron Activation Analysis (NAA). For the XRF, a  $^{109}\text{Cd}$  radioactive source, a proportional/Si(Li) detector, and a multichannel analyser (both conventional and computer based) were used. For the NAA, a  $^{252}\text{Cf}$  spontaneous fission neutron source, a NaI(Tl) ( 7.6 cm X 7.6 cm ) detector along with the necessary electronics were employed. The amount of arsenic detected in the sludge was found to  $\sim 50$  in wt% . indicating that the waste sludge is highly poisonous. The arsenic content was also cross checked with the finding of the chemical analysis and another set of XRF result obtained from the University of Bonn, Germany. The industry has taken adequate measure in disposing the waste sludge to save the environment from pollution.

\* Supported by the University Grants Commission, Bangladesh.



Session V  
RADIATION IN TECHNOLOGY

## STUDY OF RADIATION BY SOLID-STATE LASERS

Burhan Davarcioglu  
Gazi University, Institute of Science and Technology,  
Ankara, Turkey

Solid-state lasers structures is related with different types of solid-state laser materials. At this study, crystalline host materials are described, pointing out their characteristics pertinent for laser systems. Rare-earth and transition metal impurities used as laser materials are tabulated and the role of sensitization in increasing the overall efficiency of laser systems is described.

COMPTON PROFILES OF Co-Ni- AND Fe-Ni-BASED  
AMORPHOUS ALLOYS

A. Andrejczuk\*, L. Dobrzyński\*, E. Zukowski\*, M. J. Cooper\*,  
S. Hamouda\*, J. Latuszkiewicz&

\* - Faculty of Physics Warsaw University Branch,  
Lipowa Str. 41, 05-474 Białystok, Poland

# - Department of Physics University of Warwick,  
Coventry CV4 7AL, UK

& - Borsucza Str. 74, 05-807 Podkowa Leśna, Poland

The Compton profiles in  $\text{Fe}_{82-x}\text{Ni}_x\text{B}_{18}$  amorphous alloys for  $x=12$  and 70 have been measured using 412 keV (Białystok) and 60 keV (Warwick)  $\gamma$ -radiation. In addition the sample with  $x=41$  has been measured at Warwick. The interpretation of Compton difference profile, based on charge transfer from 4s to the 3d band, supports our earlier results from Co-Ni amorphous alloys [1]. Experimental data for both alloy families were analysed identically, taking into account the difference of the free atom Compton profiles (Biggs data) for Fe, Co, Ni and B compounds. The 4s-3d charge transfer in Ni-Fe alloys is 0.07(2) at the total change of the number of electrons of 1.16 per formula unit. The re-analysis of the Co-Ni data [1] shows the transfer of 0.08(2) 4s-electrons at the total change of 0.55 electrons. It suggests that 3d band in nickel is filled more effectively in Co-Ni than in Fe-Ni alloys. This can explain the disappearance of nickel magnetic moment in former and its conservation in the later when Co and Fe are substituted by nickel atoms.

- [1] E. Zukowski, L. Dobrzyński, M. J. Cooper, D. N. Timms,  
R. S. Holt and J. Latuszkiewicz, J. Phys.: Condens. Matter,  
2 (1990) 6315-6321

## RADIATION EFFECTS ON HYDROGEN RELATED POINT DEFECTS IN QUARTZ CRYSTALS

HARISH BAHADUR  
National Physical Laboratory,  
Hillside Road, New Delhi-110012  
INDIA

A study of irradiation and electrodiffusion (sweeping) has been carried out on good quality optically clear natural quartz crystals. The crystals were of Arkansas and Brazilian origin which are generally used as starting material in hydrothermal synthesis of high purity cultured quartz. In particular, various OH<sup>-</sup> related defects have been monitored using infrared absorption measurements in the 3100-3700 cm<sup>-1</sup> range. Essentially, crystals of both origins have same spectral features except that the bands are much more intense in the Brazilian quartz than the Arkansas quartz used in the present investigation. Some of the low strength bands in the Brazilian crystal are not observable in the Arkansas sample. Our estimates show that the two crystals have almost the same aluminum ratio but the hydrogen ratio in the Brazilian sample is as high as more than three times in of that in the Arkansas stone. Therefore, we have labeled the Brazilian quartz as high-H sample and the Arkansas quartz as low-H sample. The Li ratio is also higher in the high-H sample. This leads to an H-limited Li-H defect concentration in the low-H sample. With this H-limitation, only the most preferred defects sites are occupied. In a previous study [1], it has been shown that all natural quartz in its unswept condition has a set of major bands at 3476 cm<sup>-1</sup> associated with the presence of a Li ion<sub>i</sub> (designated as N<sub>i</sub>-Li<sup>+</sup> band) and the Al-OH<sup>-</sup> bands at 3367 and 3306 cm<sup>-1</sup> designated respectively as e<sub>1</sub> and e<sub>2</sub> bands. Other band in natural quartz may or may not be present in conjunction with these bands. Electrodiffusion (sweeping) of natural quartz with Na and H results in major bands appearance at 3451 and 3468 wavenumbers respectively.

We present here the results of our investigation on radiation-induced ion movements in natural quartz samples of matching thickness as a function of H-concentration (high and low) and the irradiation temperature; 77K, room temperature and the final irradiation at 77K. The study included major bands designated as N<sub>i</sub>-H<sup>+</sup>, where H<sup>+</sup> is either Li<sup>+</sup> or Na<sup>+</sup> and e<sub>1</sub> and e<sub>2</sub> bands. Measurements show that for the same radiation dose (2 Mrad used at every stage) the N<sub>i</sub>-H<sup>+</sup> centers exhibit a relatively fast decay at room temperature irradiation than at 77K. On the other hand, the N<sub>i</sub>-H<sup>+</sup> centers do not show any depletion at 300K irradiation while at 77K irradiation their strength is significantly reduced to about 10% of their original value. Both Al-OH<sup>-</sup> bands in natural quartz show their irradiation characteristics that are identical to those of high purity cultured quartz. For both samples, the N<sub>i</sub>-Na<sup>+</sup> centers show a faster depletion to the similar extent than the N<sub>i</sub>-Li<sup>+</sup> centers at 300K irradiation. Occasionally, after irradiation there appear some low strength OH<sup>-</sup> infrared bands in all versions of swept and unswept natural quartz. This occurs at the expense of already existing OH<sup>-</sup> defect centers.

This work was conducted at the Oklahoma State University and was supported by Sandia National Laboratories and the Rome Air Development Command, Hanscom, MA.

GENERATION AND ANNEALING POINT DEFECTS DURING PULSED  
RADIATION OF SILICON

D.A.Sechenov, A.M.Svetlichny, S.I.Solovev

Department of Microelectronics, Kalmykov Institute,  
Taganrog, USSR

The pulsed radiation is already used in VLSI technology sufficiently widely for activation ion implanted dopants, recrystallization amorphous and polycrystalline silicon films, oxidation and so on. Highly intensive electron and photon flows not only considerably reduce a duration of thermal treatment due to a pulsed influence but they can considerably modify properties of radiated structures. Since the heat process proceeds very rapidly, the equilibrium state of a defect system is violated. Therefore additional hole and electron trapping centers can be formed. At present the model describing this effect adequately is absent. In this work a behaviour of point defects during pulsed radiation was investigated by numerical modelling in silicon substrate doped phosphorus and radiated by photon incoherent light.

The model is based on a system of partial differential equations describing reactions of interaction between point defects and ionized doped atoms. Moreover, continuity equation for electron is included in the model in order to account a change of charge during radiation. The surface is assumed as an ideal source (sink) in the boundary conditions for defect equation, and it is assumed by an ideal barrier in the boundary conditions for dopant equations.

Theoretical concentration profiles for point defects differ from their equilibrium values in consequence of a quench effect which takes place while a fast cooling. It is shown that under certain conditions radiation (substrate temperature, radiation duration) considerably modification of a substrate specific resistance occurs affecting on the parameters of semiconductor devices and VLSI.

ELECTRON INELASTIC MEAN FREE PATH VERSUS  
ATTENUATION LENGTH IN SOLIDS\*

C. M. Kwei and Y. F. Chen  
Department of Electronics Engineering  
National Chiao Tung University  
Hsinchu, Taiwan, R. O. C.

ABSTRACT

The electron inelastic mean free path is a quantity of basic importance in many applications in radiation physics and surface physics. This quantity represents the average pathlength traveled by an electron between two neighboring inelastic interactions. It can be calculated using the dielectric function for the valence band and atomic generalized oscillator strengths for inner shells of a solid. Although the experimentally measured attenuation length is conceptually distinct from the mean free path, they are frequently used interchangeably in a loosely defined manner. For electrons of energy in the keV region, elastic interactions play an important role in relating these quantities. This work used elastic cross sections derived from the phase shift method to evaluate an increase of the pathlength over the penetration depth for an electron transmitted through a solid film. Monte Carlo technique as well as analytical multiple scattering formulations have been employed in the investigation.

---

\*This research was supported by the National Science Council of the Republic of China.

INVESTIGATIONS ON THE CHANGE OF VISCOSITIES OF POLYMERS AND  
APPLICATION OF RANDOM RESISTANCE NETWORK MODEL

L. Santra, B. K. Chatterjee, D. Bhaumik\* and S. C. Roy  
Dept. of Physics, Bose Institute, Calcutta - 700 009, INDIA  
\*Saha Institute of Nuclear Physics, Calcutta- 700 064, INDIA

In this paper we present the experimental observations of damage produced in polymeric silicone fluids of six different grades by gamma irradiation by measuring the change of their dynamic viscosities. We also present a theoretical approach (model) to explain our observations on the basis of the random resistor network (RRN) model.

Silicone fluids of initial kinematic viscosities 50, 200, 500, 1000, 2000 and 3000 centistokes were irradiated by a  $^{60}\text{Co}$  source at the dose rate of 2 Gy/s. The change in viscosities due to irradiation were measured using a sensitive differential viscometer developed in this laboratory<sup>1</sup>. It has been observed that the viscosity increases smoothly with the dosage of  $\gamma$  irradiation and diverges at some asymptotic value of the dosage. The samples with smaller viscosity (average initial molecular weight) diverge at a much higher dosage compared to the ones with larger viscosities. We demonstrate that the observed behaviour can be interpreted in terms of RRN model. To do this, the correspondence between viscosity and resistivity was worked out in detail, comparing the Navier-Stokes equation of liquid flow with that of the current flow. The equivalence of dose with the production of recombined polymers was established from a simple picture of rate kinetics. The recombined polymers, in turn play the role of blocking the fluid flow pathways similar to random blocking of the current flow in RRN model. The results obtained using the model agree well with the experimental observations.

---

1. L. Santra, D. Bhaumik and S. C. Roy. J. Phys. E21 (1988) 896

RADIATION DAMAGE IN THE SURFACE OF MATERIALS  
CREATED BY HYDROGEN, DEUTERIUM IONS

Luo Zhengming and Zhu Qi

Center for Radiation Physics,  
Institute of Nuclear Science and Technology,  
Sichuan University, Chengdu, P.R.China

ABSTRACT

By applying PANDA-CSDA program based on the improved bipartition model of ion transport, the calculation has been made for the radiation damage in materials bombarded with hydrogen and deuterium ions of different incident angles and energy. These data may be of use to fusion research. The results obtained possess high reliability and precision mainly because of the inclusion of surface effects and the use of a new, better elastic scattering cross section and electronic stopping power. This program has demonstrated much higher calculation efficiency than other codes based on Monte Carlo simulation and could be extended to be applied to multi-elemental and multi-layer materials.



INVESTIGATION OF DISTRIBUTION OF CALCIUM, POTASSIUM AND  
CHLORINE IN DIFFERENT PARTS OF SPINACH PLANT  
USING XRF TECHNIQUES

Raj Mittal, Anita, N. Singh and B.S. Sood  
Department of Physics, Punjabi University, Patiala-147002, India

The distribution of trace elements Ca, K and Cl has been investigated in soil, roots, stems, leaves and seeds of spinach plant using XRF technique. A low background triaxial double reflection geometrical setup [1] fabricated from a single block of iron is used to selectively ionise the K-shell electrons of Ca, K and Cl in the samples respectively, by suitable choice of secondary target elements, whose external conversion K X-rays are used for the K-shell electron ionisation in the elements of the sample. The concentration of the desired elements in the samples of various parts of the plant is made with the help of linear calibrations of the set up obtained by using two standard targets [2]. Theoretical corrections for absorption and enhancement effects are not required in the present method. Enhancement effects are avoided using selective excitation and absorption is estimated in terms of intensities of the measured X-rays. The details of the experimental set up, methods of sample preparation and the results of analysis will be presented.

References

- 1 K.L. Allawadhi, Raj Mittal and B.S. Sood, J. Instrum. Soc. India 15 (1985) 191.
- 2 Raj Mittal, K.L. Allawadhi and B.S. Sood, X-Ray Spectrom. 16 (1987) 1

Study of the Effect of Reactor Neutron Irradiation and High-Temperature Annealing on the Electrophysical and Optical Properties of High- $T_c$  Materials.

R.F.Konopleva, V.A.Evseev, B.A.Borisov, V.Yu.Davydov\*,

I.V.Nazarkin, and V.A.Chekanov.

Leningrad Nuclear Physics Institute, Academy of Sciences of the USSR; \* Ioffe Physical-Technical Institute, Academy of Sciences of the USSR.

An analysis of the temperature dependence of conductivity in original and neutron - irradiated samples of the  $\text{YBaCuO}$  ceramic in the normal and superconducting (SC) phases has been carried out to reveal the mechanism of carrier transport. The carrier transport over the Cu-O planes was shown to be two-dimensional. The analysis in the normal phase of the temperature behaviour of conductivity of the  $\text{YBaCuO}$  ceramic near the transition to the SC state for  $T > T_c$  was based on percolation theory. For all investigated samples, both original and neutron - irradiated ( $\Phi \sim 10^{17} - 10^{18} \text{ cm}^{-2}$ ), the critical index of conductivity was found to be  $t = 0.85 - 1.19$ , which corresponds to two-dimensional carrier transport in the vicinity of the transition temperature,  $T > T_c$ .

Studies of the IR reflectance and Raman scattering of  $\text{YBaCuO}$  films on  $\text{SrTiO}_3$  and  $\text{MgO}$  substrates, as well as of the  $\text{YBaCuO}$  samples irradiated by neutrons and subjected to thermal annealing revealed considerable changes in the phonon spectra associated with oxygen deficiency during the annealing and with the irradiation-formation of oxygen vacancies.

The effect of high temperature annealing ( $100^\circ\text{C} - 950^\circ\text{C}$ ) in nitrogen, argon and air environment on the electrical parameters of the original and neutron-irradiated  $\text{YBaCuO}$  ceramic has been investigated. The SC properties have been formed to recover at  $T_{\text{ann.}} \sim 700^\circ\text{C}$  after the loss of SC state at  $T_{\text{ann.}} \sim 600^\circ\text{C}$  in nitrogen atmosphere at a temperature variation rate of  $5^\circ\text{C}/\text{min.}$  with the oxygen concentration decreasing monotonically from  $X = 6.94(100^\circ\text{C})$  down to  $X = 6.68(950^\circ\text{C})$ .

Gravimetric and EPR studies of the  $\text{YBaCuO}$  ceramic have shown the effect of recovery of the SC properties to be due to both to a disordering in the oxygen subsystem and to a change in the oxygen stoichiometry.

STRUCTURAL STUDIES OF SOME HIGH  $T_c$  OXIDE SUPERCONDUCTORS  
THROUGH XANES AND XPS TECHNIQUES

S.G.Saxena, Rekha Govil and K.B.Garg\*, Department of Physics,  
University of Banasthali Vidyapith(Raj.) 304022, INDIA.

\* Department of Physics, University of Rajasthan, Jaipur  
302004, INDIA.

ABSTRACT

The superconducting behaviour at high temperatures of the defect perovskite layered oxidic compounds, with vacant oxygen positions in the lattice, has been the key issue for structural investigations through many a technique such as XANES, EXAFS, XRD, XPS etc. in recent years /1,2,3,4/. Some structural investigations have been carried out in case of  $YBa_2Cu_3O_{7-x}$  and  $Bi_{1.2}Ca_{2.1}Sr_{0.7}Cu_2O_y$  using XANES as a probe and  $Cu_2O$  and  $CuO$  as reference compounds. While such studies have been performed in terms of the pre-edge structure, principal absorption maximum and shoulder structure beyond the principal absorption maximum, complementary information obtained from 2p core-level XPS of Cu has been used to ascertain charge transfer from oxygen 2p states to vacant 3d states of Cu.

Plausible arguments in favour of the shoulder structure, beyond the principal absorption maximum, being a 5s resonance peak rather than due to 3+ state of Cu have been extended /3,5/. A comparison of the XPS spectra of these superconductors with those of  $Cu_2O$  and  $CuO$  also suggests that Cu in these compounds is in 2+ state. It is, however, not possible to label Cu with the normal 2+ state as it is in dynamic mode in these superconductors /4/. The results are in agreement with those of Bianconi et al who have logically established the absence of  $Cu^{3+}$  in such compounds and pointed to the probability of ground state being a mixture of  $3d^9$ ,  $3d^9L$  and  $3d^{10}L$  states /5/.

**References:**

- /1/. Bednorz J.G. and Muller K.A., Z.Phys. B64, 189 (1986).
- /2/. Padalia B.D., Menta P.K. and O.Prakash, Int. Symp. on High Temperature Superconductivity, Department of Physics, University of Rajasthan, Jaipur 302004, India, July 6-8, 1988.
- /3/. Saxena S.G., Rekha Govil and Garg K.B., Conf.Proc. 2nd European Conf. on Progress in X-ray Synchrotron Radiation Research, Rome, Italy, Oct.2-6, 1989.
- /4/. Lottici P.P., Antonioli G., and Licci F. Conf.Proc. 2nd European Conf. on Progress in X-ray Synchrotron Radiation Research, Rome, Italy, Oct. 4-6, 1989.
- /5/. A.Bianconi et al, Proc. of the Adriatico Research Conf. on High Temp. Superconductivity, Trieste, Italy, July 6-8, 1987.

USING OF SOL-GEL PROCESS FOR PREPARATION OF  
HIGH-DENSITY  $\text{UO}_2$  MICROSPHERES FROM THE U(IV) SOLS.

SHABAN I.S., MOHAMED F.O. AND NIKITENKO S.I.

RADIOCHEMISTRY DEPARTMENT  
TAJOURA NUCLEAR RESEARCH CENTRE  
P.O.BOX 30878  
TRIPOLI LIBYA

Solutions of 1 mol/l U(IV) were prepared by the hydrazine reduction of U(VI) in nitric acid solutions in the presence of Pt on silica-gel as a catalyst. It was shown that U(IV) in highly concentrated solutions in the presence of nitric acid is stable when the concentration of hydrazine is more than 2 mol/l.

The U(IV) sols were prepared by de-nitration of concentrated U(IV) solutions, containing urea, with the hexamethylene tetramine (HMTA). It was shown that after neutralization of "free" nitric acid the U(IV) sols are stable for few hours when the ratio U/urea and U/HMTA are 1/(3.0-3.5) and 1/(1.5-2.0) accordingly.

The microspheres were formed by dropping the conditioned sols into perfluorodecaline heated to about 80°C, which serves as an innert heat transfer medium. The process of washing, drying and burning of obtained microspheres were described. The major advantage of the presented method is the absence of necessity of U(VI) reduction by  $\text{H}_2$  gas.

STRUCTURE CONTROL OF FILLED POLYOLEFINS EXPOSED  
TO IONIZING RADIATION AND PREDICTION OF THEIR  
PROPERTIES

V.Yu.Barinov, V.P.Gordiyenko

Physico-Mechanical Institute of the Ukrainian SSR  
Academy of Sciences, Mauchnaya, 5, Lvov, 290047, USSR.

The addition of fillers to polymers is a promising method of producing new composite materials. Irradiation of many a filled highly molecular compound opens up new possibilities for their modification.

In polyolefins exposed to radiation effects, the additives will fulfil a dual function. First, depending on their nature and concentration, they can promote changes in the structure of polymers prior to irradiation by controlling the power and directivity of the radiation effect on the composite. Second, the additives will directly participate in radiational modification of polymers.

On the basis of the structure and property analysis of irradiated filled polyolefins, some concentration regions have been identified where the action of dispersant additives is of varying nature. On irradiation with exposure doses ranging from 0.05 to 0.5 MGy, optimization of polyolefins is most effectively attained when the filler content is either to 1-3% or from 5-10 to 20-30%.

The introduced fillers will also be responsible for the distribution of absorbed energy via secondary electrons. So, a polymer with the electron density smaller than that of a filler will receive more energy, particularly in boundary layers.

Thus, the fillers exert a profound influence on every stage of processes occurring in polyolefins under irradiation. Hence, the information about the transformation pattern in filled polymers will be most helpful to control modification of composites and predict their properties.

A COMPARISON OF PIXE AND ENERGY DISPERSIVE XRF FOR THE ANALYSIS OF MOCVD GROWN EPITAXIAL LAYERS OF  $\text{Hg}_{1-x}\text{Cd}_x\text{Te}$  AND  $\text{CdTe}$  WITH INGROWN DOPANTS

Peter N. Johnston, Salvy P. Russo, Robert C. Short

Department of Applied Physics, RMIT,  
GPO Box 2476V, Melbourne 3001, Australia

and G.N. Pain

Telecom Australia Research Laboratories,  
770 Blackburn Road, Clayton 3168, Australia

ABSTRACT

Epitaxial layers of  $\text{Hg}_{1-x}\text{Cd}_x\text{Te}$  grown by MOCVD are being developed for infra-red optoelectronic devices. These layers can be very non-uniform in stoichiometry particularly in the direction of gas flow. PIXE analysis has been successfully applied to the elemental analysis of these materials for determination of stoichiometry over a wafer<sup>1,2</sup>.

Due to strong X-ray attenuation, Hg M, Cd L and Te L X-rays are not used in these analyses. Rather Hg L, Cd K and Te K X-rays are used. These atomic shells have proton and alpha-particle ionisation cross-sections that are smaller than those normally associated with PIXE analysis. However, for these high-Z elements photon ionisation cross-sections are large. This makes energy dispersive XRF an attractive alternative to PIXE.

An energy dispersive XRF system using  $^{241}\text{Am}$  as an excitation source has been developed. It has been used to measure x for  $\text{Hg}_{1-x}\text{Cd}_x\text{Te}$ . The results obtained from XRF are not distinguishable from those from PIXE after correction for secondary fluorescence. This form of XRF analysis is simpler, quicker, causes little damage and is much less expensive than PIXE. This has great attractions for production testing on commercially manufactured wafers.

Initial results indicate that this method has a greater sensitivity for ingrown dopants of In and Sb in  $\text{CdTe}$  than PIXE analysis.

References

1. 'RBS and PIXE analysis of  $\text{Hg}_{1-x}\text{Cd}_x\text{Te}$  and related structures grown by MOCVD', S.P. Russo, P.N. Johnston, R.G. Elliman and G.N. Pain, Proc. Mat. Res. Symp., November 1990 (To be published).
2. 'RBS and PIXE analysis of  $\text{Hg}_{1-x}\text{Cd}_x\text{Te}$  Epitaxial layers on GaAs grown by MOCVD', S.P. Russo, P.N. Johnston, R.G. Elliman and G.N. Pain presented to the Fourth Australian Conference on II-VI semi-conductor compounds, Warburton, April 1990.

**RADIATION EFFECTS IN OPTOELECTRONIC DEVICES AND DOSIMETRY**

Ladislav Musilek, Anita Daříčková, Jan Schmidt, Josef Gerndt: Czech Technical University in Prague, Faculty of Nuclear Sciences and Physical Engineering, Břehová 7, 115 19 Praha 1, Czechoslovakia

A considerable amount of work has been done on the study of radiation effects in semiconductors in the last three decades. Now, as optoelectronic devices propagate more and more, the effort turns also to them.

The paper deals with the results of an investigation of radiation induced changes of parameters of some active and passive elements of optoelectronic systems. Light emitting diodes (LED), phototransistors and photo-couplers consisting of these parts were studied in the field of gamma radiation and fast neutrons. Relatively high sensitivity to fast neutron doses was found, doses of the order of Gy causing very remarkable degradation of parameters. Sensitivity to gamma radiation is more than two orders lower.

Various light guides, made mostly of glasses were also studied and a remarkable decrease of optical transparency was observed even in gamma-ray fields with partial recovery depending on the type of glass.

These radiation effects may be useful for dosimetric purposes. Degradation of LED has good prospects for neutron dosimetry in accidental range of doses and gamma dosimetry of high doses, especially in combination with phototransistors in photo-couplers. Glass light guides give good possibilities for gamma dosimetry, the sensitivity being variable in wide limits by the change of length of the light guide. These devices are simple and compact and may represent a new alternative of dosimetric equipment especially in the nuclear industry, radiation technologies and similar branches, where higher radiation doses appear.



## RADIATION IN TECHNOLOGY OF THE VLSI FABRICATION

Alexander Y. Usenko

NPO Rotor, Cherkasy, P.O. Box 257036, Ukraine, USSR

Physical fundamentals of 'radiplanar' integrated circuits technology early proposed by author<sup>1</sup> are described. Advantages and shortcomings of this novel technology and radiplanar devices are discussed. It is concluded that the new approach shows promise as a technology for low temperature operating VHSIC, latch-free CMOS IC and Si MESFETs.

The processing sequence for radiplanar (briefly):

- i formation of transistors in Si wafer by standard methods as oxidation, mask patterning and impurity doping
- ii high dose irradiation of whole wafer with hi-energy electrons (MeV range)
- iii local pulse annealing of the surface by laser
- iiii metal contacts and interconnections fabrication.

High dose high energy electron irradiation leads to the point radiation defect accumulation up to they saturated values in whole bulk of the Si including the transistor's active regions and substrate. It causes the Si conductivity decreasing to the value as it has the completely compensated Si and the transistor structures become inoperable. Under the pulse annealing the point radiation defects are annealed in the transistor active regions only and the high substrate resistivity is kept. The annealing locality on depth is designed by the choice of the laser wavelength and the annealing locality on plane is designed by annealing through the mask. After such a treatment the inoperable irradiated transistors become operable inversely. This is a key step of the novel approach.

Resulting transistors have a drastically decreased parasitic capacitances on substrate and thus the highly increased switching speed. Also, these transistors are isolated by compensated Si.

## References

- 1. A. Usenko. "Si modification by beam treatments to form the ICs", *Elektronnaya tekhnika, seriya 3*, 1989, N°5, p.74 (in Russian)

# KINETICS OF IRRADIATION INDUCED RECOIL MIGRATION IN SOLIDS

Yu.F. Blinov, P.V. Serba (V.D. Kalmykov Radiotechnical  
Institute, Chekhov str. 22, Taganrog, SU347915, USSR)

Irradiation induced recoil migration is caused by an elastic collision of recoil atoms with projectile particles. Both primary flux of irradiating particles and secondary flux of lattice atoms, appeared due to cascade processes, influence on stimulation of recoil migration. This process may be describe using the diffusion theory [1]. The depth distribution of recoil atoms is reached solving Fokker-Planck equation. Kinetics of migration is defined by the diffusion coefficient tensor, which is given by

$$D = \begin{vmatrix} D_x & 0 & 0 \\ 0 & D_y & 0 \\ 0 & 0 & D_z \end{vmatrix}$$

where

$$D_x = \int_E \{ [\bar{\Sigma}_0' + \frac{1}{2} \bar{\Sigma}_0] \varphi_0(x, E) + [\bar{\Sigma}_0 - \frac{1}{2} \bar{\Sigma}_0] \varphi_1(x, E) \} dE$$

the diffusion coefficient component in the direction of irradiation beam

$$D_y = \int_E \{ [\bar{\Sigma}_0' + \frac{1}{2} \bar{\Sigma}_0] \varphi_0(x, E) + [\frac{1}{6} \bar{\Sigma}_0 - \frac{1}{2} \bar{\Sigma}_1] \varphi_1(x, E) \} dE$$

the diffusion coefficient component in the lateral direction (y or z)

$$\bar{\Sigma}_0' = \frac{1}{2} N \sigma_{TF}^2 \int_0^{\bar{t}} \overline{R_L^2(t)} f(t^{1/2}) t^{-3/2} dt,$$

$$\bar{\Sigma}_0 = \frac{1}{2} N \sigma_{TF}^2 \int_0^{\bar{t}} [\overline{R_L^2(t)} - \overline{R_L^2(t)}] f(t^{1/2}) t^{-3/2} dt,$$

$$\bar{\Sigma}_1 = \frac{1}{2} N \sigma_{TF}^2 \bar{E} \int_0^{\bar{t}} [\overline{R_L^2(t)} - \overline{R_L^2(t)}] f(t^{1/2}) t^{-1/2} dt$$

$\sigma_{TF}$  - Thomas-Fermi radius,  $f(t^{1/2})$  - Thomas-Fermi function, defined by projectile with recoil interaction potential,  $\bar{E}$  - dimensionless energy,  $\overline{R_L^2}$  and  $\overline{R_L^2}$  - mean square longitudinal and lateral ranges of recoil,  $\bar{t}$  - recoil energy,  $\varphi_n(x, E)$  - resolution coefficients of the projectile flux on Legendre polynomials, which may be obtained solving transport equation.

The diffusion coefficient is increased with increasing of projectile atomic number and energy and decreasing of recoil atomic number. Recoil migration is caused by cascade processes in a case of light projectile. Role of cascade process is decreased with increasing projectile mass. However, recoil migration is caused by cascade processes on the large depth. When light recoil migration takes place process of migration is isotropical.

## USE OF RADIATION TECHNOLOGY FOR SCREENING SEMICONDUCTOR DEVICES AND ICs

E.A. Ladygin, N.N. Gorjunov, A.P. Galeev, A.V. Panichckin, A.M. Musalitin  
Moscow Institute Steel and Alloys, Crimea Wall-Street, House 3, room 500,  
Moscow, USSR

Unlike long time high-temperature reverse bias tests, generally carried out for evaluating the stability of the semiconductor devices parameters, a new radiation screening method suggests a short time effect of electron or gamma irradiation. Tests are carried out in accordance with the scheme irradiation-anneal. The electron irradiation dose is usually limited to 10-10 rad, and the subsequent anneal is done at the temperatures of 398-523 K during 1-100 hours. During irradiation the semiconductor devices are under electrical bias. Radiation screening can be used both for wafers and for encapsulated devices. By analysing the behaviour of semiconductor devices parameters and using the mathematical apparatus of statistical treatment of measurement results it is possible to establish criteria for selection of devices with minimum sensitivity to ionizing radiation. The use of ionizing radiation reduces semiconductor device test period due to acceleration of the generation process of charges in all the regions of structure and their moving in the electrical field of junctions.

The radiation screening permits to select from the semiconductor devices or the microcircuits lot, manufactured by planar-epitaxy bipolar and MOS technology, samples with parameters stable for a long time within a wide temperature range different applications.

## RADIATION TECHNOLOGICAL PROCESSES IN PRODUCTION LSI CMOS IC

E.A. Ladygin, A.V. Panichkin, N.N. Gorjunov, D.G. Krylow  
Moscow Institute Steel and Alloys, Crimea Wall-Street, House 3, room 500,  
Moscow, USSR

Radiation technological process (RTP) widely used by manufacturing of bipolar IC different types on purpose to operate by parameter, improvement of the electrophysical and exploitation characteristics, decrease their radiation response.

At the same time application RTP for the class CMOS LSI have a number of specific particulars, connected with strong influence surface radiation effects, conditioned technology creation metal-isolator-semiconductor system.

In our works received results, present in practical possibility application operation high-energy electrons (6 MeV) and the next temperature anneal for operate the value threshold voltage n- and p-channel transistors, manufacturing for different technology, controlling change a complex state and dynamic parameters CMOS IC, different degree integration, overwhelm parasitic effect "latch-up", carry out radiation screening structure with secret defects, decrease the total radiation response for the impulse and the permanent ionizing radiation.

On base carried out investigation worked the practice recommendation by using RTP in manufacturing CMOS LSI IC, and also develop model performances about kinetics radiation processes into passive regions transistor MOS structure on stages irradiation and anneal.

## RADIATION TECHNOLOGICAL PROCESSES IN PRODUCTION BYPOLAR MICROCIRCUITS

E.A. Ladygin, A.C. Gaev, N.N. Goryunov, A.P. Galeev  
Moscow Institute Steel and Alloys, Crimea Wall-Street, House 3, room 500,  
Moscow, USSR

Radiation technological processes (RTP) received wide spreading in technology as discrete semiconductor devices, so and integrate circuits (IC). However, for some types IC, in particular for the fast IC series TTLS (transistor-transistor logic), possibilities use RTP practically had not been studied.

In this work we have carried out the research of the elimination parametric and functional spoilage possibility in the TTLS IC of the epitaxial-planar and the isoplanar technology by use the RTP. Experimentally, it is shown that the application radiation technologies allow effectively eliminate spoilage by the dynamical parameters (basically by account of decrease relaxation time of majority charge carriers, so and for account of improvement of the parameters integrate diodes shottky).

The fulfillment researches show, that the use of the RTP allow also to decrease deviate element parameters of IC on a crystal. That give a possibility to liquidate, in some cases, the spoilage by the IC function, that open new possibilities by the use radiation technologies.

It is expect, that the more effective application of the RTP for elimination the functional spoilage, will be reached in LSI and VLSI IC. In this direction it is necessary further investigations.

# RADIATION EFFECTS ON LASER CRYSTALS FOR SPACE APPLICATIONS

F. Brioschi<sup>1</sup>, A. Caridi<sup>1</sup>, E. Cereda<sup>1</sup>, G.M. Braga Marcazzan<sup>2</sup>  
and E. Zanzottera<sup>1</sup>

1 CISE SpA, P.O. Box 12081, 20134 Milan, Italy

2 Istituto Fisica Generale Applicata, University of  
Milan, Italy

In the frame of a research program supported by ESA (European Space Agency) a solid state laser for space based Lidar (Light detection and ranging) application has been designed and is now being completed. This device will operate for three years on the ESA polar platform scheduled to be launched into a polar orbit (800 Km) in 1997.

In the space environment the laser optical components will be exposed to a radiation field whose effects on the optical properties and laser performance should be estimated.

In this work the radiation environment was simulated by using a proton beam provided by a 3.5 MV tandem VdG accelerator in order to study the radiation effects on the optical transmission coefficients of four different laser crystals: Nd:YAG (laser active medium), BBO, KD\*P and Lithium Niobate (for Q-switch and harmonic generation).

In the present paper the experimental set up for crystal irradiations is described and results about radiation effects are presented and discussed.

## **CORRECTIONS FOR VOLUMIC HYDROGEN CONTENT IN COAL ANALYSIS BY PROMPT GAMMA NEUTRON ACTIVATION ANALYSIS**

J. Salgado and C. Oliveira

Dep. Física - Laboratório Nacional de Engenharia e Tecnologia Industrial  
Estrada Nacional 10, 2685 Sacavém - Portugal

The prompt gamma neutron activation analysis, PGNA, is a useful technique to determine the elemental composition of bulk samples in on-line measurements.

Monte Carlo simulation studies performed in bulk coals of different compositions for given sample size and geometry have shown that both the gamma count rate for hydrogen and the gamma count rate per percent by weight for an arbitrary element due to  $(n, \gamma)$  reactions depend on the volumic hydrogen content, being independent of coal composition [1, 2].

Experimental results using a  $^{252}\text{Cf}$  neutron source surrounded by a lead cylinder were obtained for nine different coal types. These show that the  $\gamma$ -peak originated by  $(n, n' \gamma)$  reactions in the lead shield depends on the sample density. Assuming that the source intensity is constant, this result enables the measurement of the coal bulk density.

Taking into account the results just described, the present paper shows how the  $\gamma$ -peak intensities can be corrected for volumic hydrogen content in order to obtain the percent by weight contents of the coal. The density is necessary to convert the volumic hydrogen in percent by weight content and to calculate the bulk sample weight.

### **References**

- [1] Oliveira, C. and Salgado, J. Analysis of fast neutron flux distributions in bulk coal by Monte Carlo simulation studies, Nuclear Geophysics, 5, 2 (1991) (in press).
- [2] Oliveira, C. and Salgado, J. Analysis of thermal neutron flux distributions in bulk coal by Monte Carlo simulation studies, Nuclear Geophysics, (1991) (in press).

## A COMPARATIVE DAMAGE IN TRANSISTORS FROM 14 MeV NEUTRONS AND $\gamma$ IRRADIATIONS

K. K. EL-DUBALI, B. M. BAHAL, A. A. MOHABIS,  
B. W. MAHDAWI AND A. A. GULAK

*Tajura Nuclear Research Centre,  
P.O.Box 30878 , Tripoli, LIBYA*

Importance of 14 MeV neutron induced damages in electronic components are mainly due to their use in the environment of a future TOKAMAK reactor where D-T fuel may be used. The fluence to produce surface effects in materials is more than  $10^{17}$  n/cm<sup>2</sup> and bulk effects in materials is at more than  $10^{20}$  n/cm<sup>2</sup>, however, the radiation induced damage effects in electronic components are observable at a much lower fluence of  $10^{11}$  n/cm<sup>2</sup>. Therefore such a study can be carried out by conventional neutron generators. In our laboratory at Tajura Nuclear Research Centre fast neutron damage in semiconductor transistor is investigated while it is actually working in the radiation medium ( on line ). The room temperature recovery is very small ( < 5 % ) over a period of one year. The recovery is enhanced ( 15 to 30 % ) by elevating the temperature of the components upto 250 °C for 24 hours. The damage of components from Co<sup>60</sup>  $\gamma$  cell, and its subsequent recovery is also measured . The damage mechanism of gamma is different from that of fast neutrons. The results are compared and the differences in the produced effects are discussed.



STUDIES ON CERTAIN WOOD-PLASTIC-COMPOSITES PREPARED BY  
GAMMA IRRADIATION

P.T.Thomas,  
Government Arts and Science College, Calicut, India.  
B.R.S. Babu and K. Neelakandan,  
Department of Physics, University of Calicut, Calicut, India.

Abstract

The timber resources of the forests in India are fast getting depleted due to indiscriminate cutting of trees. The growing demand for high quality timber can be met only by utilising the weaker varieties of wood known as soft wood more effectively. Considerable work has been done on the so-called Wood-Plastic-Composites (WPC) formed by the irradiation method.

In the present investigation, WPC have been formed using two species of soft wood, viz. Erthryna Stricta Roxb (Local name: Murukku) and Hevea brasiliensis (H.B.K) Muell. Arg. (Rubber) in conjunction with the monomers styrene, methylmethacrylate, acrylonitrile and vinyl acetate. The method used to form the WPC is vacuum impregnation of monomer in wood and subsequent polymerization of the monomer by gamma irradiation. Wood samples impregnated with monomers have been irradiated by means of a  $^{60}\text{Co}$  source of strength 50,000Ci at a rate of 0.2Mrad/Hr.

Measurements of radiation dose required for maximum conversion of monomer into polymer yielded the result that in all cases except styrene the total dose required was less than 2Mrad. Styrene requires much larger dose of about 10Mrad. It was found that the impregnation efficiency is more in Murukku than in Rubber, the former having more pore volume. The impregnation efficiency also depends on the ambient pressure; the more the vacuum, the more is the impregnation efficiency.

Mechanical strength of the WPC was measured. The largest enhancement of the tensile strength was 185% in the case of the composite acrylonitrile-MMA-murukku and the lowest was 74% in the case of acrylonitrile-vinylacetate-murukku.

WPC subjected to prolonged exposure to water showed very little water absorption of about 6 to 14% in the case of Murukku based composites and about 4 to 10% in the case of rubber based composites whereas control samples of these wood showed 300% and 80% water absorption, respectively.

X-ray diffraction studies appear to suggest that the crystallinity of the cellulose does not get affected by the radiation polymerization.

**References:**

1. "Impregnated Fibrous Materials", IAEA, Vienna (1968).

**SMALL-ANGLE NEUTRON SCATTERING STUDY OF MICROSTRUCTURAL  
INHOMOGENEITIES IN A STEEL FOR FUSION TECHNOLOGY.**

G.Albertini<sup>1</sup>, F.Carsughi<sup>1,3</sup>, R.Coppola<sup>2</sup>, F.Rustichelli<sup>1</sup>,  
G.Mercurio<sup>4</sup>

- 1) Università di Ancona, 60131 Ancona, Italy
- 2) Enea-Casaccia, C.P. 2400, 00100 Roma, Italy
- 3) Institut für Festkörperforschung, KFA, Jülich, Germany
- 4) J.R.C. Ispra on ENEA grant, Italy

Modified martensitic steel DIN 1.4914 (MANET) is a very promising material for the construction of first-wall in future fusion materials, mainly due to its good resistance to swelling and Helium embrittlement.

Previous results [1] have shown the usefulness of SANS to study the microstructural defects, such as those associated to radiation damage, produced in this steel during irradiation. In this contribution the continuation of this experiment is presented. The investigated samples are:

- 1) implanted with 1500 appm He + annealed at 675°C, 2 h
- 2) reference, only annealed at 675°C.

SANS data elaboration gives the size distribution for sample 1), compared to the previous results (lower dose); in the case of sample 2) the presence of carbides is shown together with magnetic inhomogeneities possibly related to fluctuations in Cr concentration [2].

- [1] G.Albertini, F.Carsughi, R.Coppola, F.Rustichelli, W.A.H.M.Vlak and C.Van Dijk. "Microstructural investigation of 12% Cr martensitic steel for NET by means of small angle neutron scattering". Journal of Nuclear Materials 176 (1990).
- [2] P.Gondi, R.Montanari and R.Coppola. J.N. Mat. 176 (1990). In press.

**A Modified Method for Two-phase-flow  
Void-fraction Determination Using  
Photon-attenuation Technique**

**HONG-MING LIU and TIEN-KO WANG**

Department of Nuclear Engineering, National Tsing Hua University,  
Hsinchu 30043, Taiwan, R.O.C.

**Abstract** — A modified one-shot method is proposed to improve the accuracy on void-fraction determination in two-phase-flow systems employing the photon-attenuation technique. The modification over the conventional method is established by the combination of the ordinary photon-counting measurements and the photon-transmission probability calculations. A series of benchmark experiments have been performed by using (1) a pack of acrylic plates modelling a plane geometry, (2) solid acrylic tubes in different sizes with various holes drilled in distributed positions modelling the two-phase flow in a cylindrical flow channel, and (3) acrylic tubes incased in stainless-steel (SS) sleeves modelling the two-phase flow in a SS flow channel. These benchmark tests show that the accuracies of void-fraction predictions are significantly improved from some ten to twenty percent by conventional method to the range of a few percent by this modified method.

Another important correction made in this work is on the effect of void fluctuation. A transmission probability ratio, defined as the probability ratio between static and dynamic void distribution, is introduced to indicate this effect and combined it with the modified method to establish a correction procedure for the void fraction determination. Results show that the effect of void fluctuation on the void-fraction determination can largely be corrected.

STRUCTURAL EVOLUTION OF THE CRYSTALLINE SILICON  
UNDER DEUTERIUM IMPLANTATION

M.V.SIDOROV, S.R.OKTYABRSKY, M.A.LOMIDZE\*, A.E.GORODETSKY\*

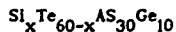
P.N. Lebedev Physical Institute, Department of Solid State  
Physics, 53 Leninsky prospect, 117924 Moscow, USSR.

\* Institute of Physical Chemistry, 31 Leninsky prospect,  
117915 Moscow, USSR.

Structural changes in (111)Si after 10keV  $D_2^+$  ion implantation with fluence in the range of  $10^{16}+10^{19}$   $D_2^+/cm^2$  at room temperature have been studied with cross-sectional transmission electron microscopy (XTEM), secondary ion mass spectroscopy (SIMS) and secondary neutral molecules spectroscopy (SNMS).

Three stages of structural as well as chemical evolution is observed. For fluence less than  $(3+4) \cdot 10^{16}$   $D_2^+/cm^2$  deuterium retains in the target through trapping on the dangling bonds with SiD-complexes formation. This process results in formation of the strongly damaged region which contains a lot of planar defects oriented in (111) directions in silicon. The strongly damaged region is centered approximately near mean projected range and followed by the buffer region which contains no deuterium but interstitial dislocation loops. As the fluence is increased the buried amorphous layer on the depth close to the maximum of the calculated damage distribution appears. Simultaneously generating of SiD<sub>2</sub>-complexes begins. The nucleation and incorporation of SiD<sub>2</sub>-complexes in the created amorphous material leads to a network of interconnected voids formation. For fluence higher than  $10^{18}$   $D_2^+/cm^2$  the erosional relief at the target surface formed due to effective sputtering of the amorphous material with voids.

## THERMOLUMINESCENCE STUDY OF SEMICONDUCTOR MATERIALS



Y.M. Amin, A.F. Maged\* and S.A. Durrani  
 School of Physics and Space Science  
 University of Birmingham  
 Birmingham B15 2TT  
 England.

## Abstract

The effect of gamma irradiation on the  $\text{Si}_x\text{Te}_{60-x}\text{As}_{30}\text{Ge}_{10}$ , where  $x=5, 12$  and  $20$  has been studied using thermoluminescence(TL). As expected in semiconductor materials, both  $x=5$  and  $x=20$  chalcogenides showed a wide TL peak ranging from  $\sim 80^\circ\text{C}$  to  $300^\circ\text{C}$ . However, these two materials also exhibited a sharp peak at temperature of  $\sim 360^\circ\text{C}$  and  $\sim 380^\circ\text{C}$  for  $x=5$  and  $x=20$  respectively. On the other hand, the  $x=12$  showed very little response to gamma radiation but if the sample was exposed to UV light (after being glowed of any TL up to  $500^\circ\text{C}$ ) and then glowed (called phototransfer-thermoluminescence), several peaks appeared at the temperature of  $\sim 80^\circ\text{C}$ ,  $180^\circ\text{C}$ ,  $300^\circ\text{C}$  and  $350^\circ\text{C}$ . The  $x=5$  and  $x=20$  samples did not show any response to UV light. Since the TL response depended on the ratio of  $\text{Te/Si}$ , it can be concluded that TL technique can also be used to characterize semiconductor materials and it would compliment other techniques such as electrical conductivity and differential thermal analysis (DTA).

---

\* On leave from:  
 National Center for Radiation Research and Technology  
 Nasr city, Cairo, Egypt.

PROGNOSTICATION OF RADIATION STABILITY OF METALLIC  
ALLOYS

A.M. Shalaev

Institute of Metal Physics, Kiev, USSR

Two questions of radiation stability are considered: radiation stability of the amorphous alloys and the void swelling of metallic alloys. The local order of amorphous alloys was investigated by NMR and electron-positron annihilation methods after irradiation by electrons and gamma-rays ( $E_e = 2-4$  MeV,  $E_\gamma = 1,2$  and 50 MeV). The void swelling for Fe-Ni-Cr alloys is considered after neutron bombardment. The analysis of radiation-induced processes in metallic materials was made in the framework of concepts on a probability of existence of both the stationary and quasistationary fluctuations of local concentration of interatomic bonding electrons. The equation which connecting stability parameters and parameters electronic structure were given. The results of calculation are in agreement with experimental data.

Ref.: A.M.Shalaev. Radiation-induced processes in metals. Moscow: Energatomizdat, 1988. - 176 p.

CHANNELING RADIATION AS AN X-RAY SOURCE FOR  
ANGIOGRAPHY AND MICROLITHOGRAPHYB.L. Berman

The George Washington University,  
Washington, DC 20052, USA  
H. Uberall\* and B.J. Faraday, SFA, Inc.,  
1401 McCormick Dr., Landover, MD 20785, USA  
X.K. Maruyama, Naval Postgraduate School,  
Monterey, CA 20943 USA

Synchrotron radiation of 33 keV ( $\lambda \approx 0.4 \text{ \AA}$ ) has been tentatively employed for coronary angiography studies; the results were successful, but so far lack clinical quality [1]. Synchrotron radiation has also been proposed as a source for microlithography and the efficient production of integrated circuits [2], using energies of 0.5 - 2.5 keV ( $\lambda \approx 5\text{-}20 \text{ \AA}$ ). This application, although not yet carried out in earnest, appears promising enough so that a number of synchrotron sources dedicated to this purpose are now being set up worldwide. These applications require storage rings for GeV electrons, costing \$20 to 60 million each. Less expensive, lower energy linacs, affordable by smaller institutions, can produce keV channeling radiation suitable for microlithography and angiography. Channeling-radiation intensities, especially for x-ray energies of some tens of keV and higher will surpass synchrotron-radiation intensities [3]. We have carried out quantitative studies confirming the above conclusions regarding the comparison of channeling radiation and synchrotron radiation. Details of these calculations will be presented. (Supported by DOE Contract No. DE-FG05-90ER81034).

\* Also at the Naval Research Laboratory, Washington, DC and Catholic University of America, Washington, DC, USA.

1. E. Rubenstein et al., Nucl. Instrum. Methods A291, 80 (1990).
2. A.R. Neureuther, in Synchrotron Radiation Research (H. Winick and S. Doniach, eds.), Plenum, New York, 1982, p. 223.
3. R.K. Klein, J.O. Kephart, R.H. Pantell, H. Park, B.L. Berman, R.L. Swent, S. Datz, and R.W. Fearick, Phys. Rev. B 31, 68 (1985).



COMPUTER SIMULATION OF COLORING CURVES IN ALKALI HALIDE  
DOPED WITH DIVALENT IMPURITIES THAT CHANGE  
THEIR VALENCE STATE BY IRRADIATION

S. Ramos Bernal and R. Soto Montiel

Departamento de Física, Facultad de Ciencias, UNAM  
Circuito exterior, C.U.  
04510, México, D.F.

We simulate coloring curves by making responsible of state I the  $S_1$  Center, stage II the  $S_2$  Center and stage III and A center.  $S_1$ ,  $S_2$  and A are dipoles with different number of trapped interstitials H. On the other hand, another way in which the number of dipoles (or  $M''$ ) changes is capturing free electrons during the irradiation process to become either  $M'$  or  $M''$ . These states have different capabilities of trapping interstitials than those of the divalent cation impurities. It is also included the possibility of hole capture by  $M'$  or  $M''$  to return to the originally divalent impurity state  $M''$ . We use ten differential equations which we solved numerically using a Runge-Kutta iteration program.

INFLUENCE OF RADIATION INTENSITY AND LEAD CONCENTRATION  
THE FIRST STAGE OF F-CENTER  
COLORING IN KCl.

S. RAMOS BERNAL, C. MEDRANO P\*. AND J.M. HERNANDEZ A\*.

DEPARTAMENTO DE FISICA, FACULTAD DE CIENCIAS, UNAM.  
CIRCUITO EXTERIOR, C.U. 04510, MEXICO D.F.  
\*INSTITUTO DE FISICA, UNAM.  
CIRCUITO EXTERIOR, C.U. 04510, MEXICO, D.F.

The first stage of F-center coloring in samples of KCl:Pb has been investigated as a function of impurity concentration and dose rate. For the range of lead concentration employed the coloring increases monotonically with concentration when samples are exposed to low radiation intensity. Moreover the amount of the first stage coloration was found to be proportional to the square root of impurity concentration. A quite different result was found to occur when the samples were irradiated at a high dose-rate. In this case the coloring increases with lead concentration only at the beginning of the irradiation and after this coloring curves of heavily doped samples crosses those of lower concentration. It is proposed that the impurity precipitation induced by irradiation may be responsible for the experimental observation that more coloring is produced in slightly doped samples than in heavily doped samples.

ROOM-TEMPERATURE F-COLORING OF LEAD DOPED  
NaCl AS A FUNCTION OF DOSE RATE AND  
IMPURITY CONCENTRATION

S. Ramos Bernal, C. Medrano P<sup>1</sup>. and J.M. Hernández A<sup>1</sup>.

Departamento de Física, Facultad de Ciencias, UNAM.  
04510, México, D.F.

<sup>1</sup>Instituto de Física, UNAM.  
Circuito Exterior, C.U.  
04510, México, D.F.

The F-coloring kinetics has been investigated at room temperature in NaCl:Pb as a function of concentration and radiation intensity. It has been found that more coloring is produced with higher concentration of impurity, in agreement with our proposed theoretical models. It is also found that this behaviour is quite dependent on the dose rate. It is interpreted as a process of annealing induced irradiation.

## A COMPARATIVE STUDY OF TOMOGRAPHIES USING GAMMA RAYS AND NEUTRONS IN NON-DESTRUCTIVE TESTING

Walsan Wagner Pereira  
Ricardo Tadeu Lopes

Nuclear Instrumentation Laboratory, Escola de Engenharia  
COPPE/UFRJ, P.O. Box 68509 - 21945 Rio de Janeiro, Brasil.

This paper aims at demonstrating the advantages, shortcomings and complementarities of a tomography development using neutrons over the one employing gamma rays in the context of their applications to non destructive testing.

A simulated experimental study was performed in order to compare the two aforementioned tomographic procedures as applied to some materials. These materials were chosen for their clear advantages and complementarities as, for instance, aluminium, iron, plastic, and aluminium hydroxide.

In our work we employed two tomographic systems, both with parallel beams. The first with a gamma radiation source (Caesium-137), with an energy of 662 KeV and an activity of  $3,9 \times 10^9$  Bq (100 mCi) and the second one employing a neutron source, the Argonaut Reactor of the Instituto de Engenharia Nuclear, IEN/CNEN, from where the thermal neutron beam of about  $10^5$  n/(cm.s) was obtained.

We may conclude from the simulated and experimental results, by means of image analysis and distortion measurements, that for a given material the adequate radiation and its energy may be chosen so as to better characterized it.

IMPURITY CONCENTRATION AND DOSE RATE DEPENDENCE  
OF THE FIRST STAGE COLORATION OF NaCl TIN DOPED SAMPLES.

S. Ramos Bernal, E. Pedrero<sup>1</sup>, M. Murrieta S.<sup>1</sup>  
and J.M. Hernandez A.<sup>1</sup>

Departamento de Fisica, Facultad de Ciencias, UNAM.  
Circuito Exterior, C.U. 04510 Mexico D.F.

<sup>1</sup>Instituto de Fisica, UNAM.  
Circuito Exterior C.U. 04510 Mexico D.F.

The amount of room temperature first stage F-center coloration in quenched samples of tin doped NaCl has been investigated as a function of impurity concentration and radiation intensity. It was ascertained that in all cases the amount of the first stage coloration is proportional to the square root of the gamma-irradiation dose rate. On the other hand this first stage is also proportional to the square root of the concentration of the impurity ions.

**Session VI**

**RADIATION IN ASTROPHYSICS AND COSMOLOGY**

## REDSHIFTS OF ATOMIC RADIATION IN FIELDS OF DIFFERING TEMPERATURES

M. Simhony

Physics 5, The Hebrew University, Jerusalem, Israel

\*\*\*

The 3 K background blackbody radiation (BBR) is due to random vibrations of electrons ( $e^-$ ) and positrons ( $e^+$ ) bound in our electromagnetic (EM) field. Thus, the temperature  $T_f$  of the field around us is  $\sim 3 \text{ K}$ .<sup>1</sup> Regions of lesser thermal activity have lower  $T_f$ , while regions of higher activity (due to, e.g., exploding nuclear stars) have higher  $T_f$ . BBR's of neighboring regions are absorbed by the bound particles at their borders. Thus, EM fields are not transparent to BBR's of their neighbors; the BBR in each region is its own, corresponding to  $T_f$  there. The 3 K radiation is not "universal"; it is identical in all directions because  $T_f$  in front of our apparatus is constant. Unlike BBR's, atomic radiation (AR) can pass through EM fields. However, with rising distance and number of border regions passed, increasing amounts of AR photons are scattered and absorbed on the randomly vibrating bound  $e^-$ ,  $e^+$ , as well as on free particles and cosmic dust. Some of these photons are reemitted at lower energies, which results in a non-linear absorption (NLA) redshift in the observed spectrum. Moreover, transition energies  $E_t$  of orbital electrons are independent of  $T_f$ . Thus, the observed transition energies are  $E' = k(T_t - T_f)$ , where  $k$  is Boltzmann's constant, and  $T_t \equiv E_t/k$ . Hence, the spectral line of a transition, occurring in a region of high  $T_f$  is redshifted from the line of such a transition, occurring in a region of low  $T_f$ . Therefore, AR entering a region of higher  $T_f$  is received blue-shifted, and in a region of lower  $T_f$  it is redshifted. In our 3 K region, blueshifts of AR from lower  $T_f$  regions are practically undetectable, so that we observe only redshifts in AR of sources in regions of  $T_f > 3 \text{ K}$ . This "field temperature redshift" (FTR), as well as the NLA, and also the gravitational (Einstein) redshifts depend directly on the distance  $l$  from the AR source, and vary with direction. They are therefore considered as the natural causes of the observed Hubble-Humason redshift.<sup>1</sup>

1. M. Simhony: The Electron Positron Lattice Space, Jerusalem 1990, (160 pp.); Abstracts of the 12th Intern. Conf. on Gen. Relativity and Gravitation, Boulder, CO 1989, p. 461.

PERPETUAL MONITORING OF THE INTEGRAL COSMIC-RAY INTENSITY  
AS AN 'EXTRA-BONUS' IN GAMMA-RAY SPECTROSCOPY

I.V. Aniĉin, A.H. Kukoĉ, P.R. Aiĉiĉ, R.B. Vukanoviĉ, G. Škoro  
and M.T. Źupanĉiĉ

The Boris Kidriĉ Institute, Vinĉa, Belgrade, Yugoslavia

The background in our gamma-ray detectors, notably in the most frequently used NaI and Ge, in the region of interest to the gamma-ray spectroscopy itself, is due to radiations from the close environment as well as to cosmic rays. Above the region of couple MeV, however, practically only cosmic-rays contribute to the background. At the sea-level, and within our usual shieldings, the energetic muons which on the average deposit some  $2 \text{ MeV/g/cm}^2$  dominate. Together with other particles from multiparticle production processes they produce the  $\Delta E$  spectrum reaching as far as couple of hundreds of MeV for an average size detector (ref.1). This offers the possibility to perpetually monitor the intensity of cosmic-rays by counting the proportional (over, say, 3 MeV) as well as all saturated pulses from the amplifier which is simultaneously performing the usual gamma-ray spectroscopy tasks. Those pulses can be either discriminated and simply counted or counted in a multiscale mode by contemporary analysers which have long dwell times. The dwelling time will be selected according to the time variation of the cosmic-ray intensity which is looked after. The high long-term stability of the spectra of germanium detectors as well as their high density make them especially suited for the purpose. The extremely wide distribution of high performance spectroscopy systems based on germanium detectors opens up the opportunity for the establishment of the global and around the clock active network of cosmic-ray intensity monitoring stations at virtually no extra cost and effort. We present some evidence supporting this idea.

- 
1. "Scint.Spec.of Gamma Rad." ed.S.Shafroth, Gordon & B. London 1967, p.33 and  
A.Kukoĉ, P.Aiĉiĉ, Proc.2nd Int.Conf.Low.Rad, Bratislava 1980, p.70



## EVALUATION OF RADIATION DOSE IN SPACE ENVIRONMENT

Shunji Takagi, Takashi Nakamura  
Cyclotron and Radioisotope Center, Tohoku University  
Sendai, Miyagi, 980, Japan

Katsumi Hayashi, Hiroyuki Handa  
Hitachi Engineering Company Ltd.  
Saiwai-cho, 3-2-1, Hitachi, Ibaraki, 317, Japan

Fumiyoshi Makino  
The Institute of Space and Astronautical Science (ISAS)  
Yoshinodai, 3-1-1, Sagami-hara, Kanagawa, 229, Japan

Tsuyoshi Kohno  
RIKEN Institute of Physical and Chemical Research  
Hirosawa, 2-1, Wako, Saitama, 350-01, Japan

### 1. Scope

The space radiation environment consist of several types of energetic charged particle : electrons, protons, helium and heavier ions. Information on the particle distribution in space are important in estimating material damage, semi-conductor soft error and biological protection.

Measurement of these particles in radiation belts have been conducted with the high energy particle monitor (HPM) aboard AKEBONO (EXOS-D) satellite of ISAS. Measured data were sorted out according to the particle type, energy and position to match wide applications.

### 2. Measurement

The AKEBONO is a aurora observatory satellite and the instruments for the measurement of electro-magnetic environment are on board. The orbit is highly eccentric with inclination of 75 degree passing through central region of the radiation belts. AKEBONO has the HPM to survey electron, proton and alpha particle. HPM is a dE/dX type counter made by four silicon semiconductor detectors and copper absorber plates so as to distinguish particle type and energy.

Measured data are received at four ground stations in Japan, Canada, Sweden and Antarctica and collected to the data base in ISAS computer.

### 3. Electrons and Protons in Radiation Belt

Efficiency of HPM detector is determined by HERMES Monte Carlo code system. Measured data are sorted by the particle type, energy, altitude, longitude and latitude to obtain spatial distribution.

### 4. Dose Evaluation

Two codes are tested for dose evaluation of inside and outside of the satellite. One is a simple dose evaluation code for design SHIELDOSE, and the another is HERMES Monte Carlo code system. HERMES is an assembled system of electromagnetic cascade Monte Carlo code EGS4 and hadron cascade Monte Carlo code HETC. Calculated dose distribution in aluminum shield by SHIELDOSE code is about 30% higher than the one by HERMES system.

### 5. Conclusion

Dose evaluation inside and outside of the satellite has been performed on the basis of measurement of radiation environment in radiation belt.

RADIATION VORTICES IN THE ELECTRON-POSITRON PLASMA  
OF THE ROTATING NEUTRON STAR

U.A. Mofiz

Institute of Nuclear Science & Technology  
Atomic Energy Research Establishment  
Savar, G.P.O. Box 3787, Dhaka, Bangladesh

We study the vortex mode of electrostatic radiation in the electron-positron plasma of the rotating neutron star. The ambient magnetic field is considered to be superstrong. Thus two fluid model of the strongly magnetized plasma is taken into account and the drift approximation is used to treat the problem. We derive a pair of coupled nonlinear equations governing the propagation of finite amplitude vortex mode in the electron-positron plasma of the rotating star. It is shown that the mode can propagate in the form of two-dimensional dipolar vortices. The latter may affect cross-field particle and energy transport in the pulsar magnetosphere.

## AUTHOR INDEX

Abdel-Wahab, M.S. II-36, II-37, II-38  
 Abdulaziz, M. II-40  
 Abdurackmanova, S. II-1  
 Abu-Zaid, H. II-49  
 Adams, L. IP-V-1  
 Adžić, P. IV-14, VI-2  
 Akkerman, A. I-18  
 Akki, T.S. IV-2  
 Albarran, G. IV-40  
 Albertini, G. IP-V-4, V-24  
 Algozini, A., Jr. IV-35  
 Allawadhi, K.L. I-34  
 Altiparmakov, D.V. IV-13  
 Amin, Y.M. II-2, IV-34, V-27  
 Amusia, M.Ya. IP-I-1, I-1,  
 Andreev, B.V. I-54  
 Andrejczuk, A. V-2  
 Anićin, I.V. I-20, II-18, II-22,  
 IV-14, IV-15, VI-2  
 Antić, D. II-7, IV-5  
 Antipas, C. II-3  
 Aoki, S. II-50, II-51  
 Appoloni, C.R. IV-35  
 Arafa, I.M. II-36, II-37  
 Arbi, S.K. IV-30, IV-31  
 Atan, H. II-5  
 Avdić, S. II-11  
 Avignone, F.T. III IP-I-3  
 Awwal, M.L. II-17  
 Ayala, A.P. I-27  
 Azorin, J. I-14  
 Babu, B.R.S. I-41, V-23  
 Bahal, B.M. IV-30, IV-31, V-22  
 Balliga, B.B. I-41  
 Ballinger, C.T. I-3  
 Baltenkov, A.S. I-1  
 Bandyopadhyay, T. II-5  
 Baraldi, C. I-17, IV-17  
 Barinov, V.Yu. V-12  
 Barna, A. II-4  
 Barnes, P. IP-V-3  
 Barroa, R.A. I-26, II-29, III-15  
 Batra, R.K. IV-3  
 Beach, A.C. II-14  
 Belyusenko, N.A. II-42, II-46, II-47  
 Benayad, S.A. IV-2  
 Beninson, D.J. IP-IV-2  
 Bento, A.C.S.M. II-10  
 Bergstrom, P.M. I-56  
 Berman, B.L. V-29  
 Bespalov, D.F. II-44  
 Bhargava, V.K. II-34  
 Chattacharjee, A. IV-37  
 Ghat, B.V. I-5  
 Shaumik, D. V-6

Bikit, I. II-15, II-16, III-11  
 Bilal, M.G. IV-32  
 Blagus, S. II-19  
 Blinov, Yu. F. V-16  
 Bogdanović, I. II-21  
 Bonzi, E.V. IV-21  
 Borisov, B.A. V-9  
 Bosch, F. IP-III-2  
 Bradley, D.A. I-9, II-5, IV-8  
 Braga Marcazzan, G.M. V-20  
 Brailovsky, E.Yu. III-4  
 Breskin, A. I-18  
 Brioschi, F. V-20  
 Brodzinski, R.L. IP-I-3  
 Brown, P.J. IP-III-4  
 Burns, R.C. II-32  
 Campbell, J.L. IP-IV-3  
 Caridi, A. V-20  
 Carsughi, F. V-24  
 Casnati, E. I-17, IV-17  
 Careda, E. IV-10, V-20  
 Cesareo, R. IV-28, IV-29  
 Changdar, S.M. III-14  
 Chatterjee, B.K. I-4, V-6  
 Chechik, R. I-18  
 Chekanov, V.A. V-9  
 Cheng Bo III-7  
 Chen, T.J. IV-1  
 Chen, Y.F. V-5  
 Chesta, M.A. II-29, IV-22  
 Cho, T. II-50, II-51  
 Chong, C.S. I-9  
 Chuang, L.S. IV-27  
 Chung, C. II-33  
 Chuwa, L.M. IV-32  
 Collar, J.L. IP-I-3  
 Conde, C.A.N. II-10, II-23  
 Conkić, Lj. II-15, II-16, III-11  
 Cooper, M.J. V-2  
 Coppola, R. IP-V-4, V-24  
 Crestana, S. IV-29  
 Csaba, E. IV-11  
 Cullen, D.E. I-3  
 Cusatis, C. I-38  
 da Silva, Abel A. II-17  
 da Silva, H.P.S. II-8  
 Darambara, D. II-14  
 Daričkova, A. V-14  
 Das, A. III-14  
 Dašić, N. IV-13  
 Davarcioglu, B. V-1  
 Davydov, Y.Yu. V-9  
 de Assis, J.T. IV-28, IV-29  
 de Barros, S.M.C. III-15  
 de Farias, R.C. I-39

de Marzo, C. IP-VI-1  
 de Oliveira, A.H. II-17  
 De Paula, E. II-27  
 de Souza, I.O. III-15  
 Demekhin, V.F. I-48  
 Demekhina, L.A. I-49  
 Demidenko, Z.A. III-4  
 Dhillon, K.S. III-9  
 Dias, T.H.V.T. II-23  
 Dillon, M.A. I-11, II-39  
 Ding Peizhu II-35  
 Dobrzynski, L. V-2  
 Donangelo, R. III-15  
 Donepudi, V. Rao I-32  
 Dos Santos, J.M.F. II-10  
 dos Santos, W.M. I-39  
 Durcik, M. III-1  
 Durrani, S.A. II-2, II-3, IV-34, V-27  
 Ehresmann, A. I-13  
 Eichler, J. I-39  
 Eissa, M.M. II-36, II-37, II-38  
 El-Adl, E.H. II-37  
 El-Bakkoush, F.A. IV-2  
 El-Daoushy, F. IV-25  
 El-Dubali, K.K. V-22  
 El-Fiki, M.A. II-36, II-37, II-38  
 El-Ghawi, U.M. IV-30, IV-31  
 Enbia, H.H. IV-30  
 Ennami, M.M. II-40  
 Ershov, N.V. III-13  
 Evseev, V.A. V-9  
 Ewan, G.T. IP-VI-2  
 Fadel, M.A. II-36, II-37  
 Fadel, M. II-40  
 Falco, A.L. II-30  
 Faraday, B.J. V-29  
 Farid, S.M. II-31  
 Fathony, M. II-2, II-3, IV-34  
 Fazinic, F. IV-18  
 Felsteiner, J. IV-17  
 Fernandez, J.E. I-21, I-22, I-23, I-24, I-25  
 Ferrari, A. IV-41  
 Florescu, V. I-55  
 Forsyth, J.B. IP-III-4  
 Gaddari, M. II-40  
 Gaev, A.C. V-19  
 Galeev, A.P. V-17, V-19  
 Garg, K.B. V-10  
 Gaspar, M.B. III-15  
 Gerndt, J. V-14  
 Gerward, L. I-43  
 Geske, G. IV-38  
 Ghani Sidek, A. II-5  
 Ghilardi, A.J.P. II-27

Ghilardi Metto, T. II-27  
 Ghose, A.M. I-9  
 Ghuman, B.S. I-6, I-7  
 Gibrakhterman, A. I-18  
 Gigante, G.E. IV-29  
 Golubev, V.S. II-43  
 Gomez, M.A. II-49  
 Goncalves, O.D. I-39  
 Gonzalez, P. I-14  
 Gordiyenko, V.P. V-12  
 Gorjunov, N.M. V-17, V-18, V-19  
 Gorodetsky, A.E. V-26  
 Grifols, J.A. IP-VI-4  
 Grigoryan, M.E. III-4  
 Grinshtein, P.M. III-3  
 Grobbelaar, J.H. II-32  
 Grosswendt, B. IV-39  
 Groza, A.A. III-2  
 Grudskii, M.Ya. I-8  
 Guaraldi, R. IV-41  
 Guchetl, R. III-3  
 Guerard, C.K. IP-I-3  
 Gulak, A.A. IV-30, V-22  
 Gulko, V.M. II-41, II-45  
 Gutierrez, A. I-14  
 Guy, L.P. I-15, I-16  
 Hamouda, J. V-2  
 Handa, H. VI-3  
 Hanumaiah, B. I-29, I-30  
 Harada, Y. IV-4  
 Harish Bahadur V-3  
 Hayashi, K. VI-3  
 Henschel, H. II-6  
 Hernandez, J.M.A. V-31, V-32, V-34  
 Hirata, M. II-50, II-51  
 Hopersky, A.N. I-46, I-47  
 Illic, R. II-26  
 Inokuti, M. I-11, I-40, II-39  
 Ishikawa, T. IV-6  
 Isozumi, Y. II-24  
 Ito, S. II-24  
 Jahagirdar, H.A. I-29  
 Jesudason, C.G. I-19  
 Johnston, P.N. V-13  
 Jojo, P.J. II-28, IV-20  
 Kaji, H. I-28  
 Kalashnikov, N.P. I-12, I-36  
 Kanno Ikuo II-9  
 Karfunkel, U. II-32  
 Kasi, S. IV-12  
 Katano, R. II-24  
 Kaučič, S. I-33  
 Keddy, R.J. II-32  
 Kekez, D. I-2  
 Kenawy, M.A. II-38

Kerur, B.R. I-30  
 Khalik Wood, A. IV-8  
 Kimura, M. I-11, I-40, II-39  
 Klapisch, R. IP-II-3  
 Knoll, G.F. IP-II-1  
 Kodra, A. II-26  
 Koehn, O. II-6  
 Kohno, T. VI-3  
 Kolomiets, N.F. II-41, II-42, II-43,  
 II-45, II-46, II-47  
 Kondoh, T. II-50, II-51  
 Kondoro, J.W.A. IV-32  
 Konopleva, R.F. V-9  
 Korol, A.V. I-1  
 Kovačević, K. I-57  
 Kozak, K. IV-11  
 Kozlovsky, K.I. II-48  
 Krajcar-Bronić, I. I-40, II-39  
 Krmpotić, Dj.M. IV-14, IV-15  
 Krmar, M. II-15, II-16, III-11  
 Krylow, D.G. V-18  
 Kuchmagra, A.A. II-41  
 Kukoč, A.H. I-20, II-18, IV-14, IV-15,  
 VI-2  
 Kulagin, N. III-5, III-10  
 Kumar, A. II-28  
 Kurakado, M. IP-II-4  
 Kuroseka, N. IV-4  
 Kuzmanović, Z. II-16, III-11  
 Kwei, C.M. V-5  
 Ladygin, E.A. V-17, V-18, V-19  
 Lagutin, B.M. I-13, I-45, I-49, I-50,  
 I-51  
 Lakosi, L. I-28  
 Latuskiewicz, J. V-2  
 Lavrentiev, S.V. I-51, I-52  
 Lebedov, A.G. II-12  
 Lee, C.-J. II-33  
 Li Xiang-dong III-6  
 Lingappa, N. IV-26  
 Little Flower, Sr. I-41  
 Liu, H.M. V-25  
 Ljubčić, A. I-33  
 Logan, B.A. I-33  
 Lomidze, M.A. V-26  
 Looi, L.M. IV-8  
 Lopes, R.T. V-33  
 Maezawa, H. II-50, II-51  
 Maged, A.F. V-27  
 Mahdawi, B.W. V-22  
 Maidanyuk, V.K. II-42  
 Mainardi, R.T. I-26, I-27, II-29,  
 II-30, IV-21, IV-22  
 Makino, F. VI-3  
 Malgrange, C. IP-I-4  
 Marinković, N. IV-16  
 Marinković, P. II-25  
 Marković, M.M. I-20, II-18  
 Martin, W.P. I-3  
 Martyanov, I.A. II-44  
 Maruyama, X.K. V-29  
 Mdebuka, A.M. I-42  
 Medrano, C. V-31, V-32  
 Megahid, R.M. IV-2  
 Megala, I.G. III-4  
 Mehta, M.K. II-34  
 Mele, I. II-13  
 Mercurio, G. V-24  
 Mikhailenko, B.V. II-41, II-45  
 Miley, H.S. IP-I-3  
 Miljanic, D. II-19  
 Mittal, R.A. I-34, V-8  
 Miyoshi, S. II-50, II-51  
 Mofiz, U.A. VI-4  
 Mohabis, A.A. V-22  
 Mohamed, F.O. V-11  
 Molinari, V.G. I-23  
 Mollah, A. S. IV-7  
 Monnin, M.M. IP-IV-1  
 Mukherjee, R.N. I-41  
 Mu Yingkui II-35  
 Muraleedharan, T.V. IV-23  
 Murrieta, M.S. V-34  
 Murti, M.V.R. I-35  
 Murty, V.R.K. I-35  
 Musalitin, A.M. V-17  
 Musilek, L. V-14  
 Mwiruki, G.M. IV-32  
 Nadolinsky, A.M. I-48  
 Nakamura, T. VI-3  
 Nam, T.L. II-32  
 Nambi, K.S.V. IV-23  
 Narayana, Y. IV-26  
 Navas, E. II-27  
 Nazarkin, I.V. V-9  
 Negron-Mendoza, A. IV-40  
 Neelakandan, K. I-41, V-23  
 Neplyuev, V.M. II-42  
 Ng, K.H. IV-8  
 Ngar, Y.K. IV-27  
 Nikitenko, S.I. V-11  
 Nikolaeva, L.G. III-2  
 Ninković, M.M. IV-33  
 Novikov, V.M. I-44  
 Ochiana, L. II-4  
 Ochiana, G. II-4  
 Ogura, K. II-51  
 Oksengondler, B. II-1  
 Oktyabrsky, S.R. V-26  
 Oliveira, C. V-21

Oncescu, M. II-4  
 Orlic, I. II-21  
 Oyarzun, C.C. IV-36  
     adoani, F. IV-41  
 Pain, G.M. V-13  
 Palathingal, J.C. I-5  
 Pan Shoufu II-35  
 Panichkin, A.V. V-17, V-18  
 Parthasaradhi, K. I-35  
 Pedrero, E. V-34  
 Pela, C.A. II-27  
 Pereira, W.W. V-33  
 Perkins, S.T. I-3  
 Pešić, M. II-7, II-11  
 Peterson, R.J. III-15  
 Petrov, I.D. I-13, I-47, I-50, I-51,  
     I-52  
 Pisk, K. I-56  
 Popov, V.A. I-45  
 Povinec, P. III-1  
 Prasad, R. II-28, III-8, IV-20  
 Prasanta Sen IP-V-2  
 Pratt, R.H. I-56  
 Primenko, G.I. II-42, II-46, II-47  
 Pritychenko, B.V. IP-VI-3  
 Proykova, A. III-12  
 Purakayastha, B. IV-37  
 Rabie, N. II-38  
 Radhakrishna, A.P. IV-26  
 Raičević, J.J. IV-33  
 Ramachandran, T.V. IV-23  
 Ramola, R.C. IV-9  
 Ramos Bernal, S. IV-40, V-30, V-31,  
     V-32, V-34  
 Rao, K.S. I-35  
 Rathkopf, J.A. I-3  
 Ravnik, M. II-13  
 Rawat, A. II-28, IV-20  
 Reeves, J.H. IP-I-3  
 Rekha, G. V-10  
 Rendić, D. II-19  
 Ristić, V.M. I-12  
 Roy, S.C. I-4, V-6  
 Rubio, M. III-16  
 Russo, S.P. V-13  
 Rustichelli, F. V-24  
 Safar, J. I-28  
 Saigusa, Y. I-31  
 Saito, H. IV-35  
 Sala, P. IV-41  
 Salgado, J. V-21  
 Sanchez, H.J. I-53, III-16  
 Sandhu, B.S. I-6  
 Santos, F.P. II-23  
 Santra, L. V-6

Sartori, R. I-24, I-25, I-53  
 Sasamoto, N. IV-4  
 Savelyev, G.I. II-40  
 Saxena, S.G. V-10  
 Sayed, A.M. II-36, II-37  
 Schechter, H. III-15  
 Schmidt, H.U. II-6  
 Schmidt, J. V-14  
 Schmoranzner, H. I-13  
 Sechenov, D.A. V-4  
 Sedov, Yu.A. II-42  
 Seeliger, D. IP-III-1  
 Sekine, T. I-28  
 Seman Mahmood, C. IV-8  
 Serba, P.V. V-16  
 Serebryakov, A.S. II-12  
 Shaban, I.S. V-11  
 Shalaev, A.M. V-28  
 Sharaf, M. II-38  
 Shevtsov, K.M. III-2  
 Shibata, T. IV-24  
 Shikanov, A.E. II-44, II-45  
 Shimizu, S. I-31  
 Shmatko, G.G. III-2  
 Short, R.C. V-13  
 Shukri, M.K.A. I-9, II-5  
 Siddappa, K. IV-26  
 Sidorov, M.V. V-26  
 Simhony, M. I-10, VI-1  
 Simović, R. IV-16  
 Singh, B. I-6, I-7, IV-19  
 Singh, B.P. III-8  
 Singh, K. III-9  
 Singh, M. IV-9  
 Singh, M. I-34, V-8  
 Singh, S. IV-9  
 Sinha, A.K. IV-37  
 Skoro, G.P. II-18, IV-14, VI-2  
 Skvarč, J. II-26  
 Slivka, J. II-15, II-16  
 Smirnov, V.V. I-8  
 Sokčić-Kostić, M. II-7  
 Solovev, S.I. V-4  
 Solov'yov, A.V. I-1  
 Somashekharappa, H.M. IV-26  
 Sood, B.S. V-8  
 Sorić, I. I-57  
 Soto Montiel, R. V-30  
 Soto Vargas, C.W. I-37  
 Spyrou, N.M. II-14  
 Stančić, V. II-20, IV-16  
 Staniček, J. III-1  
 Starchik, M.I. III-2  
 Stauffer, A.D. II-23  
 Subba Ramu, M.C. IV-23

Sud, K.K. I-37  
Sukhorukov, V.L. I-13, I-47, I-49,  
I-50, I-51, I-52  
Sumini, M. I-21  
Sur, T. I-4  
Surić, T. IP-I-2, I-56  
Svetlichny, A.M. V-4  
Sykora, I. III-1  
Tajuddin, A.A. I-9, II-5  
Takagi, S. VI-3  
Takahashi, E. II-50, II-51  
Takashi, N. IV-6  
Tan, M. II-32  
Tarakanov, V.K. II-42  
Tartari, A. I-17, IV-17  
Tawfik, A.A. II-49  
Taylor, R.B. I-15, I-16  
Telenta, B. IV-5  
Thomas, P.T. V-23  
Thontadarya, S.R. I-29, I-30  
Tomić, D. II-19  
Tonomura, A. IP-III-3  
Trkov, A. II-13  
Tsybin, A.S. II-46, II-47, II-48  
Tung, C.J. IV-1  
Tudorić-Ghemo, J. I-57  
Tustonić, T. I-33  
Tzibin, A.S. II-45  
Uberall, H. V-29  
Uchirin, G. IV-11  
Usenko, A. V-15  
Uwamino, Y. IV-24  
Valković, V. II-21, IV-10  
Varier, K.M. I-5  
Varnina, V.I. III-2  
Vasileva, M.E. I-49  
Veres, A. I-28  
Vesić, D. II-22  
Vesković, M. II-15, II-16, III-11  
Virk, H.S. IV-9, IV-19  
Viza, L.F. IV-36  
Vojnović, B. II-19  
Vranić, D. IP-II-2  
Vukanović, R. IV-14, VI-2  
Wang, Y.K. V-25  
Whittingham, I.B. I-15, I-16  
Wildberger, M. I-13  
Wilderman, S.J. I-3  
Yakovlev, K.I. II-41, II-45  
Yakovlev, K.I. II-45  
Yamaguchi, N. II-50, II-51  
Yatsu, K. II-51  
Yavna, S.A. I-45, I-46  
Yavna, S.A. I-45, I-48  
Yoshihara, K. I-28

Yunusov, M.S. II-1  
Zadro, M. II-19  
Zaikovskaya, M. II-1  
Zanzottera, E. V-20  
Zeng Ling-zhi III-6  
Zhengming Luo III-7, V-7  
Zhu Qi V-7  
Zimmerman, R.L. II-27  
Zliven, I. I-33  
Zukowski, E. V-2  
Župančić, M.T. IV-14, VI-2